

APPENDIX B

'Characteristics of Lockheed L-1011'



Lockheed SR-71A strategic reconnaissance aircraft (two Pratt & Whitney J58 turbojet engines with afterburners)

considerable camber on the wing-tip leading-edges.

Each main unit of the tri-cycle landing gear has three wheels. The main units retract inward into the fuselage, the twin nose-wheels forward. The power plant comprises two Pratt & Whitney JT11D-20B (J58) turbojet engines, each with a thrust of 32,500 lb (14,740 kg) with afterburning. A large movable centre-body shock-cone is fitted at the front of each nacelle. At the rear, aft of the four-ring afterburner flame-holder, is a ring of suck-in doors for cooling and area reduction at low speeds, and a variable-area final nozzle.

On May 1, 1965, USAF pilots set up three world records and six international class records in two YF-12A aircraft, from Edwards AFB, California. Col Robert L. Stephens and Lt Col Daniel Andre achieved 2,070-102 mph (3,331-507 kmh) over a 15.25 km course at unlimited altitude, and a sustained height of 80,257-91 ft (24,462-596 m) in horizontal flight. Major Walter F. Daniel and Major Noel T. Warner averaged 1,643-042 mph (2,644-220 kmh) over a 500-km closed circuit. Major Daniel and Capt James P. Cooney averaged 1,688-891 mph (2,718-096 kmh) over a 1,000-km closed circuit, with a 2,009 kg payload, an absolute world record, and qualifying also for records without payload and with a 1,090 kg payload. The 500-km and 1,000-km closed circuit records have since been beaten by the Soviet MiG-23.

DIMENSIONS, EXTERNAL (SR-71A):

Wing span	55 ft 7 in (16.95 m)
Length overall	107 ft 5 in (32.74 m)
Height overall	18 ft 6 in (5.64 m)

LOCKHEED L-1011 (MODEL 193) TRISTAR

In January 1966, Lockheed-California began a study of future requirements in the short/medium-haul airbus market. The design which emerged, known as the L-1011 (Lockheed Model 193 TriStar), was influenced by the published requirements of American Airlines, who specified optimum payload-range performance over the Chicago-Los Angeles route, coupled with an ability to take off from comparatively short runways with full payload.

The original design centred around a twin-turboprop configuration. Discussions which followed with American domestic carriers led to the eventual selection of a three-engined configuration, and the Rolls-Royce RB.211 high by-pass ratio turboprop was chosen as power plant.

In June 1968 the L-1011 TriStar moved to the production design stage. Construction of the first aircraft began during 1969, with roll-out scheduled for September, 1970, first flight in November 1970 and FAA certification and introduction into service in November 1971.

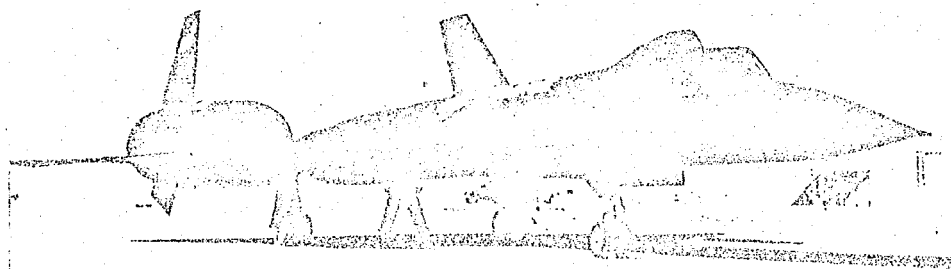
Orders and options for 181 aircraft have been received, as follows:

Eastern Air Lines	50
Delta Airlines	24
Northeast Airlines	8
Trans World Airlines	44
Air Holdings	50 (incl 10 for Air Canada, 2 for Air Jamaica)

Finance groups 5

TYPER: Three-turboprop commercial transport.

WINGS: Cantilever low-wing monoplane. Special Lockheed aerofoil sections. Aspect ratio 6.95. Chord 34 ft 4 in (10.46 m) at root, 10 ft 3 in (3.12 m) at tip. Dihedral at trailing-edge: 7° 31' on inner wings, 3° 30' outboard. Sweepback at quarter-chord 35°. The wing consists of a centre-section, passing through the lower fuselage, and an outer wing panel on each side. It is of conventional full-spar construction, with aluminium surfaces, ribs and spars, and integral fuel tanks. Hydraulically-powered aluminium ailerons of conventional two-spar box construction, with honeycomb trailing-edge, on inboard (high-speed) and outboard (low-speed) sections on each wing, operate in conjunction with aileron spoilers on the outboard sections.



Lockheed SR-71B, the tandem two-seat training version of this strategic reconnaissance aircraft

and aluminium-honeycomb. Four aluminium leading-edge slats outboard of engine pylon on each wing. Three Krueger leading-edge flaps inboard of engine pylon on each wing, made of aluminium alloy castings and sheet metal fairings. Six spoilers on the upper surface of each wing, two inboard and four outboard of the high-speed aileron, constructed from bonded sheet-metal tapered honeycomb. No trim-tabs. Flight controls fully powered. Each control surface system is controlled by a multiple redundant servo system that is powered by four independent and separate hydraulic sources. Thermal de-icing of wing leading-edge slats by engine-bleed air.

FUSELAGE: Semi-monocoque structure of aluminium alloy. Constant cross-sectional diameter of 19 ft 7 in (5.97 m) for most of the length. Bonding utilised in skin joints, for attaching skin-doublers at joints and around openings to improve fatigue life. Skins and stringers supported by frames spaced at 20-in (0.51-m) intervals. These frames, with the exception of main frames and door-edge members, are 3 in (7.62 cm) deep at the sides of the cabin, increasing progressively to a depth of 6 in (15.24 cm) at the top of the fuselage and below the floor.

TAIL UNIT: Conventional cantilever structure, consisting of variable-incidence horizontal tailplane-elevator assembly and vertical fin and rudder. Primary loads of the fin are carried by a four-spar box-beam structure, with ribs spaced at approx 20-in (0.51-m) centres. The rudder, which is in two segments, comprises forward and aft spars, honeycomb trailing-edges, hinge and actuator back-up ribs, sheet metal formers, box surface panels and leading-edge fairings. Elevators are of similar construction. Truss members for the tailplane centre-section are built up from forged and extruded sections. Outboard of the centre-section, construction is similar to that of the fin box-beam, leading- and trailing-edges. The elevators are linked mechanically to the tailplane actuation gear, to modify its camber and improve its effectiveness. No trim-tabs. Controls are fully powered. The hydraulic servo actuators receiving power from four independent hydraulic sources, under control of avionic flight control system. Control feel is provided, with the force gradient scheduled as a function of flight condition. No de-icing equipment.

LANDING GEAR: Hydraulically-retractable tri-cycle type, produced by Messner Manufacturing. Twin-wheel units in tandem on each main gear; twin-wheels on nose gear. Nose-wheels retract forward into fuselage. Main wheels retract inward into fuselage wheel-wells. Oleo-pneumatic struts in main and nose landing gear. B. F. Goodrich forged aluminium alloy wheels of split construction, with hydraulically-actuated differential brakes and antiskid

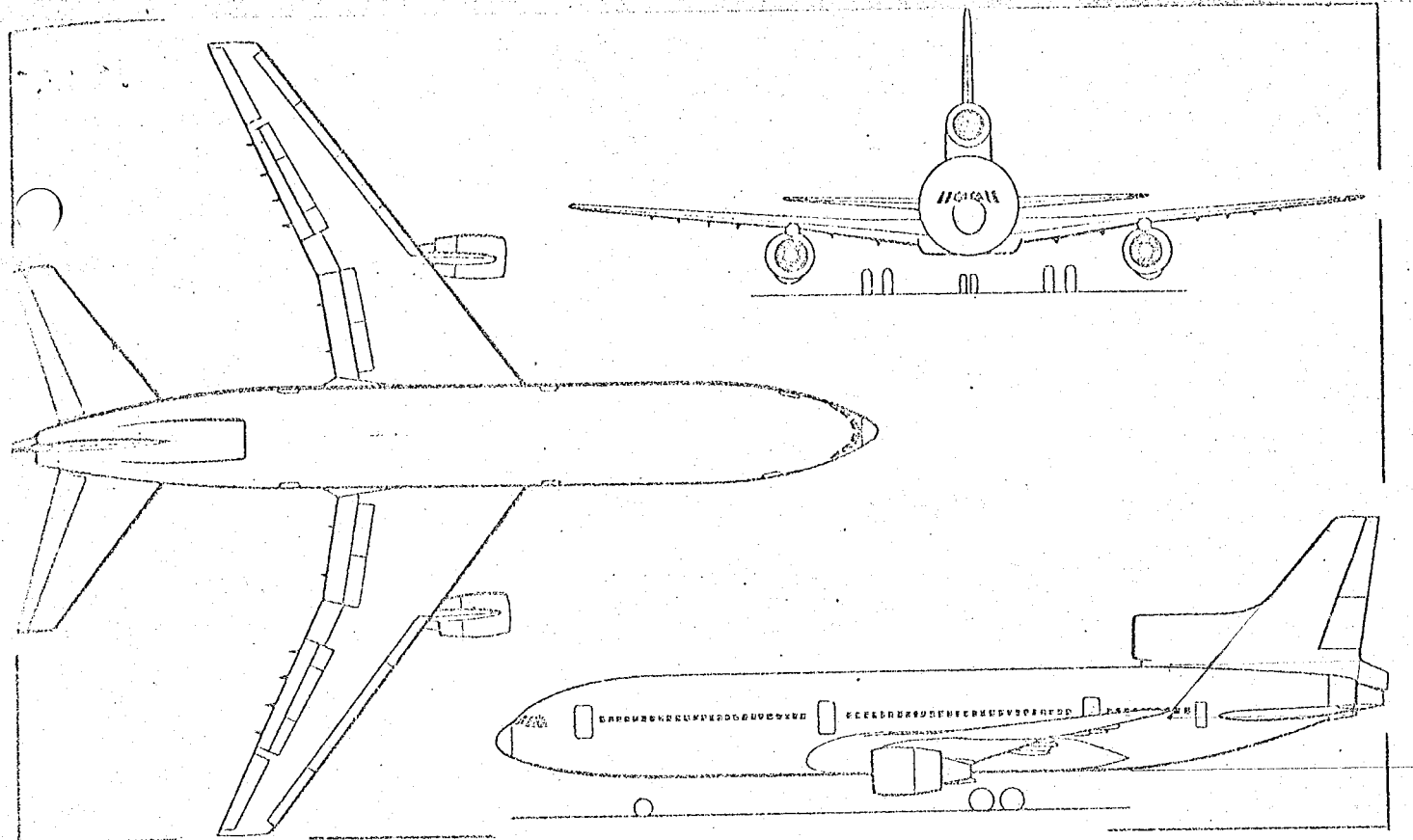
50 × 20, Type VIII, pressure 150-165 lb/sq in (10.5-11.6 kg/cm²) for short- to medium-range operational weights, 175 lb/sq in (12.3 kg/cm²) for max-range weight. Nose-wheels carry tubeless tyres size 36 × 11, Type VII, pressure 185 lb/sq in (13.0 kg/cm²). Nose-wheel unit steerable 65° each side.

POWER PLANT: Three-Rolls Royce RB.211-23-02 three-shaft turboprop engines, each rated at 28,300 hp (17,173 kg st). Two engines mounted in pods on pylons under the wings, the third mounted in the rear fuselage at the base of the fin. Two integral fuel tanks in each wing; inboard tank capacity 7,767 US gallons (29,400 litres), outboard tank capacity 3,883 US gallons (14,700 litres). Total fuel capacity 23,300 US gallons (88,200 litres). Pressure refuelling points in wing leading-edges. Oil capacity approx 14.6 US gallons (55.4 litres).

ACCOMMODATION: Crew of 13. First-class and coach mixed accommodation for 241 passengers, with a maximum of 345 in all-economy configuration. Alternative intermediate seating capacities are provided by using eight seat-trucks which permit 6, 8 or 9-abreast seating, with two full-length aisles. Underfloor galley. Seven lavatories are provided, two forward and five aft. Three passenger doors of the inward-opening plug type on each side of the fuselage, one pair immediately aft of flight deck, one pair forward of wing, one pair aft of wing. Two emergency exit doors, on each side of fuselage, at rear of cabin. Baggage and freight compartments beneath floor, able to accommodate eight containers (totalling 2,528 cu ft (71.58 m³) and 750 cu ft (21.24 m³) of bulk cargo.

SYSTEMS: Air-conditioning and pressurisation system, using engine-bleed air or APU air combined with air-cycle refrigeration. Pressurisation system maintains equivalent of 8,000 ft (2,440 m) conditions to 12,000 ft (3,658 m). Four independent 3,000 lb/sq in (210 kg/cm²) hydraulic systems provide power for the primary flight control surfaces, normal brake power, landing gear retraction and nose-wheel steering, etc. Electrical system includes four 115/200V 100 c/s generators, one on each engine and one driven by the APU, which is sited in the aft fuselage. APU provides ground and in-flight power, to an altitude of 30,000 ft (9,144 m), producing both shaft and pneumatic power for utilisation by the electric, environmental control and hydraulic systems.

ELECTRONICS AND EQUIPMENT: Standard equipment includes two ARINC 516 VHF communication transceivers, two ARINC 547 VHF navigation systems, two ARINC 568 intercom or mics, an ARINC 561 weather radar system, two ARINC 532D air traffic control transponders, partial provision for a dual collision avoidance system, three vertical gyroscopes, and full blind-



Lockheed Model L-1011 TriStar high-density transport (three Rolls-Royce RB.211 turbofan engines)

Dimensions, External:

Wing span	155 ft 4 in (47.34 m)
Length overall	177 ft 8 in (54.16 m)
Height overall	55 ft 4 in (16.87 m)
Wing span	71 ft 7 in (21.82 m)
Wing track	36 ft 0 in (10.97 m)
Wing base	70 ft 0 in (21.34 m)

Passenger doors (6):

Height	6 ft 4 in (1.93 m)
Width	3 ft 6 in (1.07 m)
Height to sill	15 ft 1 in (4.60 m)

Emergency passenger doors (2):

Height	5 ft 0 in (1.52 m)
Width	2 ft 0 in (0.61 m)
Height to sill	15 ft 1 in (4.60 m)

Baggage and freight compartment doors (forward and centre):

Height	5 ft 8 in (1.73 m)
Width	5 ft 10 in (1.78 m)
Height to sill	8 ft 7 in (2.62 m)

Baggage and freight compartment doors (aft):

Height	4 ft 0 in (1.22 m)
Width	3 ft 8 in (1.12 m)
Height to sill	9 ft 7 in (2.92 m)

Dimensions, Internal:

Length, excluding flight deck and underfloor	135 ft 5 in (41.28 m)
--	-----------------------

Max width	18 ft 11 in (5.77 m)
Max height	8 ft 2 in (2.49 m)
Floor area	2,337 sq ft (217.12 m ²)
Volume	16,000 cu ft (453 m ³)
Baggage holds, underfloor, containerised:	
Volume	2,528 cu ft (71.58 m ³)
Freight hold, underfloor, bulk cargo:	
Volume	750 cu ft (21.24 m ³)

Areas:

Wings, gross	3,755 sq ft (348.85 m ²)
Alirons (total)	80 sq ft (7.43 m ²)
Trailing-edge flaps (total)	268 sq ft (24.90 m ²)
Leading-edge flaps (total):	
Inboard Krueger	70 sq ft (6.50 m ²)
Outboard slats	118 sq ft (10.96 m ²)
Spoilers (total)	122 sq ft (11.33 m ²)
Fins	550 sq ft (51.10 m ²)
Rudder	128 sq ft (11.89 m ²)
Tailplane	1,282 sq ft (119.10 m ²)

Weights and Loadings:

Manufacturer's empty weight	268,782 lb (94,763 kg)
Operating empty weight	225,491 lb (102,280 kg)
Max payload	87,811 lb (39,839 kg)
Max T-O weight	409,000 lb (185,552 kg)
Max ramp weight	411,000 lb (186,423 kg)

Max "zero fuel" weight	308,500 lb (139,935 kg)
Max landing weight	348,000 lb (157,848 kg)
Max wing loading	118.5 lb/sq ft (578.5 kg/m ²)

Performance (estimated, at max T-O weight):

Max level speed at 30,000 ft (9,145 m)	582 mph (936 km/h)
--	--------------------

Max diving speed (structural limitations)	Mach 0.95 or 500 mph (806 km/h) CAS
---	-------------------------------------

Max cruising speed at 35,000 ft (10,670 m)	Mach 0.85
--	-----------

Econ cruising speed at 35,000 ft (10,670 m)	Mach 0.80
---	-----------

Stalling speed (take-off configuration)	148 mph (238 km/h) EAS
---	------------------------

Stalling speed (cruise configuration)	190 mph (306 km/h) EAS
---------------------------------------	------------------------

Rate of climb at S/L	2,300 ft (853 m) min
----------------------	----------------------

Service ceiling	35,000 ft (10,670 m)
-----------------	----------------------

T-O run	8,394 ft (2,558 m)
---------	--------------------

T-O to 35 ft (10.7 m)	9,835 ft (2,997 m)
-----------------------	--------------------

Landing from 50 ft (15 m)	3,895 ft (1,187 m)
---------------------------	--------------------

Landing run	2,594 ft (790 m)
-------------	------------------

Range with max fuel and 40,000 lb (18,145 kg) payload at Mach 0.85	3,915 miles (6,300 km)
--	------------------------

Range with max payload (256 passengers, 5,000 lb = 2,270 kg cargo)	3,287 miles (5,290 km)
--	------------------------

LOCKHEED-GEORGIA COMPANY

100 South Cobb Drive, Marietta, Georgia 30060
Lockheed-Georgia's main building at Marietta covers 76 acres and is believed to be the largest aircraft production plant under one roof in the world. Aircraft in current production on its assembly lines are the C-130 Hercules turboprop transport, the JetStar light jet transport and the C-130A heavy logistics transport, the largest transport ever ordered into production anywhere in the world.

LOCKHEED MODEL 352 HERCULES

USAF designations: C-130, HC-130, JC-130, EC-130 and WC-130.

Other designations: C-130, EC-130 and LC-130
Marine Corps designation: KC-130

US Coast Guard designations: EC-130 and HC-130

The Hercules was designed to a specification issued by the USAF Tactical Air Command in 1951.

It was awarded its first production contract for the C-130A in September 1952, and the first C-130A and C-130B was manufactured.

Details of these basic versions and many other variants for special duties can be found in the 1967/68 *Jane's*. Later versions of

esp T56-A-7A turboprop engines and two 1,360 US gallon (5,145 litre) underwing fuel tanks. Normal max T-O weight is 155,000 lb (70,310 kg). Take-off at overload gross weight of 175,000 lb (79,380 kg) increases the range and endurance capabilities, with certain operating restrictions at this higher weight. Total of 485 ordered for USAF Military Airlift Command (130), Tactical Air Command (215), US Navy (12), US Coast Guard (1), Canadian Armed Forces (24), Iranian Air Force (17), Turkish Air Force (5), Brazilian Air Force (11), Swedish Air Force (2), Saudi Arabian Air Force (9), Royal Australian Air Force (12), Argentine Air Force (3), USAF Aerospace Rescue and Recovery Service (14) and Norwegian Air Force (6). First C-130E flew on 25 August 1961. Deliveries began in April 1962.

EC-130E. Special version of C-130E for US Coast Guard.

C-130F (formerly GV-1U). Seven for transport duties with US Navy. Similar to KC-130F, but without underwing pylons and internal refuelling equipment. AWW 135,000 lb (61,235 kg).

WC-130E. Weather reconnaissance version operated by the USAF.

A-7 turboprops. Equipped for in-flight refuelling to service two jet aircraft simultaneously. Entire refuelling equipment can be quickly and easily installed and removed. Two C-130A's loaned to USMC in the Summer of 1957 for flight refuelling tests. The production tanker version, first flown on January 22, 1960, has a tankage capacity of 3,600 US gallons (13,620 litres) in its cargo compartment. Able to fly 1,600 miles (1,600 km) at cruise ceiling at 340 mph (547 km/h), and transfer 31,000 lb (14,060 kg) of fuel at 25,000 ft (7,620 m) at a refuelling speed of 355 mph (571 km/h) with normal military reserves. Normal crew of five to seven.

C-130H. Basically a C-130E with more powerful engines, T56-A-15 turboprops rated at 4,910 eshp for take-off, but limited to 4,500 eshp. Five delivered to Royal New Zealand Air Force.

HC-130H. Lockheed was awarded two initial contracts in September 1963 for this extended-range air search, rescue and recovery version to be utilised by the Aerospace Rescue and Recovery Service of the USAF for aerial recovery of personnel or equipment and other duties. The US Coast Guard subsequently ordered three. New folding nose-mounted recovery system makes possible repeated pick-ups from ground of

1000

1000

1000

1000

APPENDIX C

'Engine Charts'

○

○

○

GUARANTEED CALIBRATION STAND PERFORMANCE

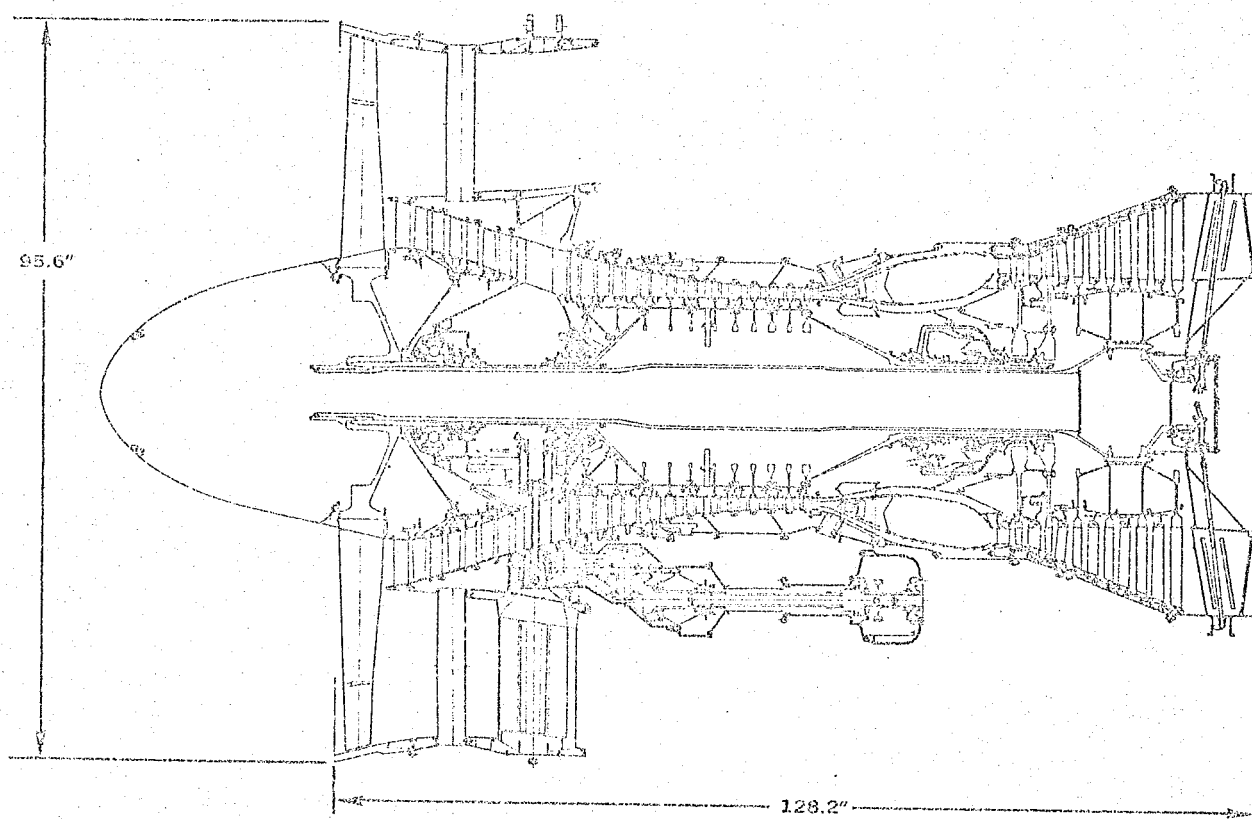
PRATT & WHITNEY JT 9D1

RATING	SEA LEVEL STATIC OUTPUT	
	THRUST-lbs.	TSFC lb/hr/lb
TAKE-OFF	42,000	.339
MAXIMUM CONTINUOUS	37,300	.329
MAXIMUM CLIMB	37,300	.329
MAXIMUM CRUISE	33,100	.322

GUARANTEED DRY WEIGHT

Including standard equipment

8330 lbs.



STANDARD EQUIPMENT

(Included in engine price and dry weight)

- Fuel Control System Including Fuel Pumps, Altitude Compensated Thrust and Speed Control Unit
- Engine Ignition System Without Power Source
- Fuel Heater, Fuel Oil Cooler and Oil Tank Assembly
- Acoustic Treatment in Fan Discharge Air Passage Walls
- Firesail
- Exhaust Thermocouples and Pressure Probes
- Rotating Spinner
- Provisions for Driving the Following Accessories:
 - Low Pressure Rotor — Tachometer
 - High Pressure Rotor — Tachometer, Two Fluid Pumps, Starter and Constant Speed Drive Unit
- Provision for Mounting an Alternator on the High Pressure Rotor Gearbox

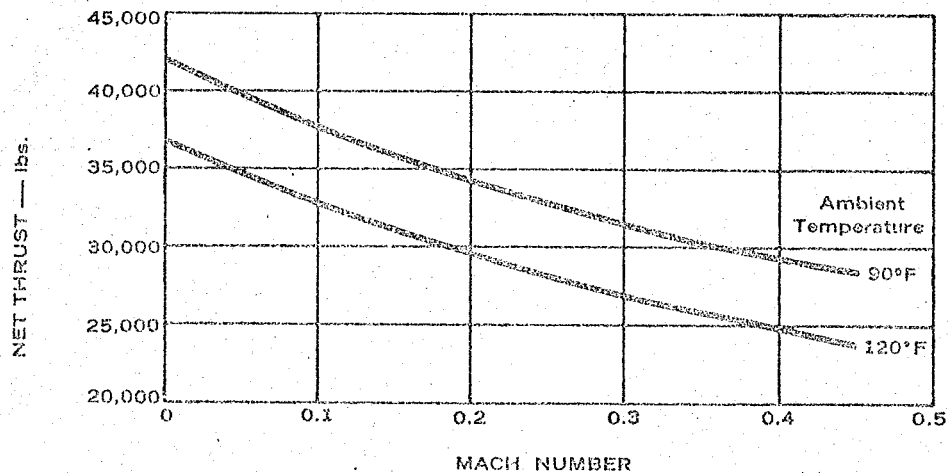
ESTIMATED PERFORMANCE DATA

STANDARD ATMOSPHERIC CONDITIONS

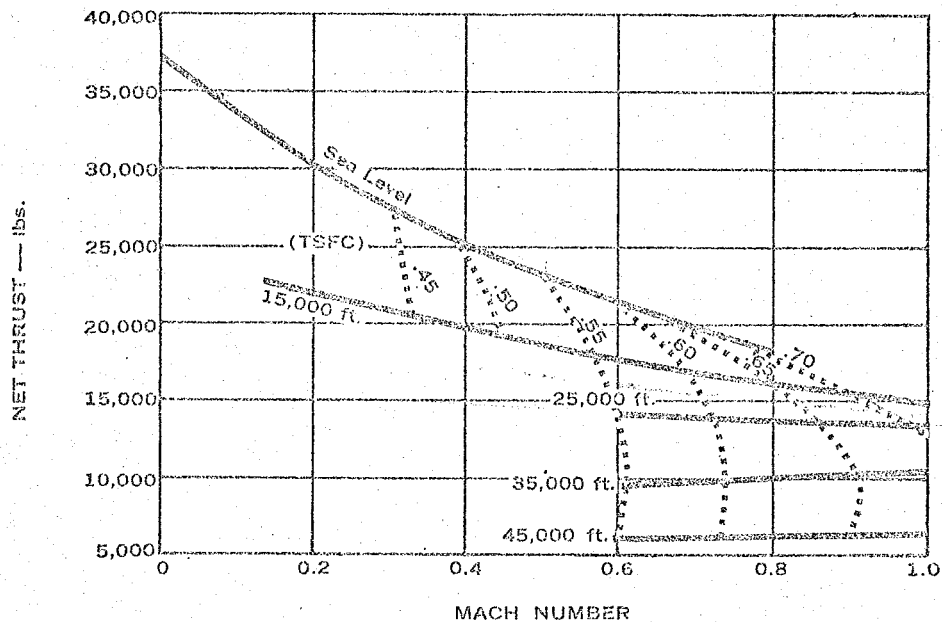
FIXED AREA JET NOZZLES

100% RAM RECOVERY

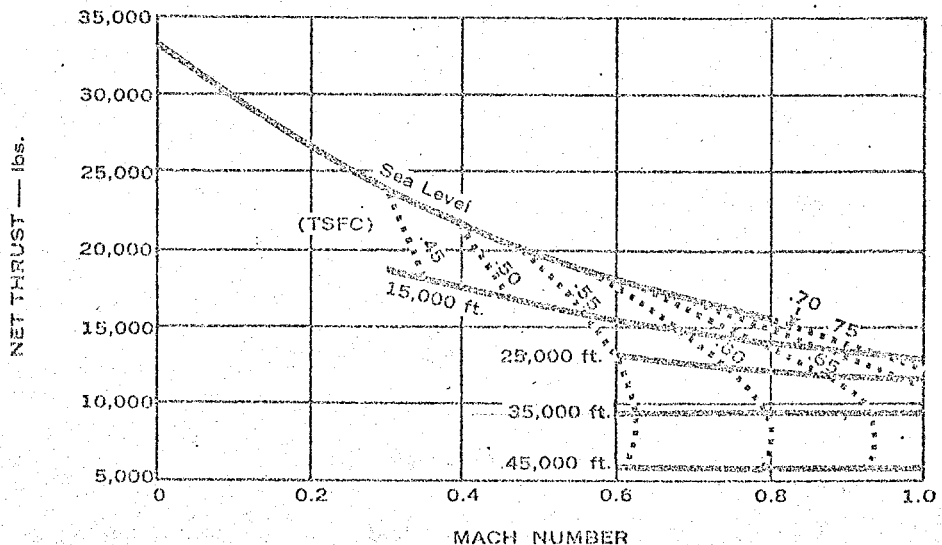
TAKE-OFF PERFORMANCE
SEA LEVEL



MAXIMUM CONTINUOUS AND
MAXIMUM CLIMB RATINGS



MAXIMUM CRUISE RATINGS



GUARANTEED CALIBRATION STAND PERFORMANCE

PRATT & WHITNEY JT 907

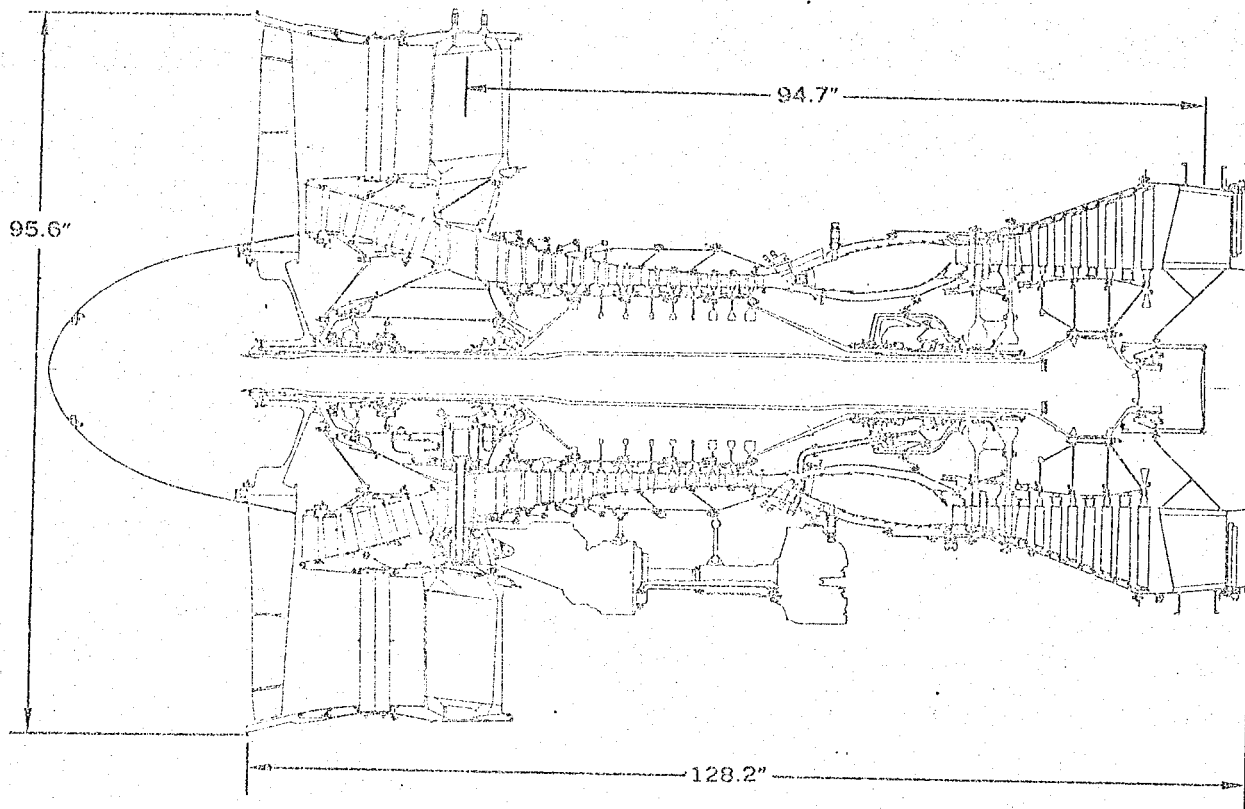
RATING	SEA LEVEL STATIC OUTPUT	
	THRUST-lbs.	TSFC lb/hr/lb
TAKE-OFF *	45,500	0.355
MAXIMUM CONTINUOUS	38,500	0.337
MAXIMUM CLIMB	38,500	0.337
MAXIMUM CRUISE	35,500	0.332

* T. O. Thrust of 47,000 lbs. available to 36° F with water injection (40 lb. increase in weight for water injection equipment).

GUARANTEED DRY WEIGHT

Including standard equipment

8770 lbs.



STANDARD EQUIPMENT

(Included in engine price and dry weight)

- Fuel Control System Including Fuel Pump, Altitude Compensated Thrust and Speed Control Unit
- Engine Ignition System Without Power Source
- Fuel Heater, Fuel Oil Cooler and Oil Tank Assemble
- Acoustic Treatment in Fan Discharge Air Passage Walls
- Fireseal
- Exhaust Thermocouples and Pressure Probes
- Rotating Spinner

Provisions for Driving the Following Accessories:

- High Pressure Rotor — Tachometer, Two Fluid Pumps, Starter and Constant Speed Drive Unit

Provision for Mounting an Alternator on the High Pressure Rotor Gearbox and Low Pressure Rotor Tachometer

ADDITIONAL EQUIPMENT

(Available at increased price and increased dry weight)

Water Injection Equipment Including:

- Water Regulator
- Piping
- Water Spray Nozzles

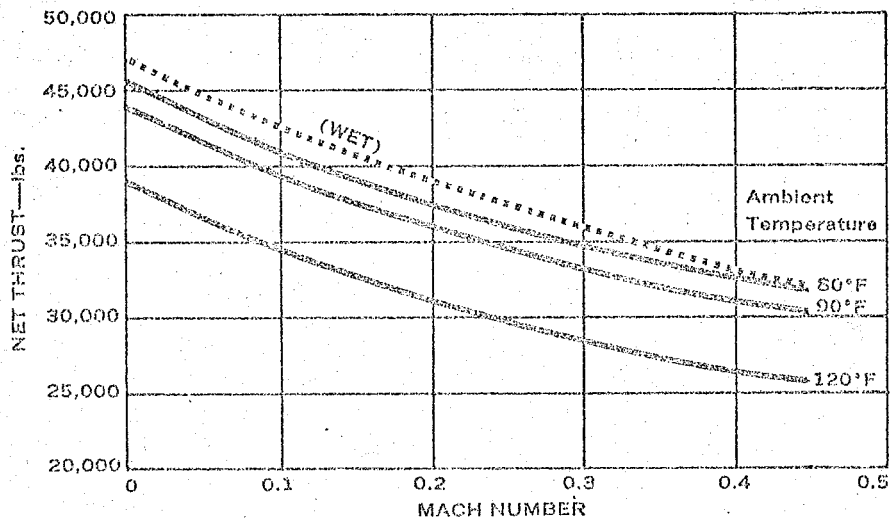
ESTIMATED PERFORMANCE DATA

STANDARD ATMOSPHERIC CONDITIONS

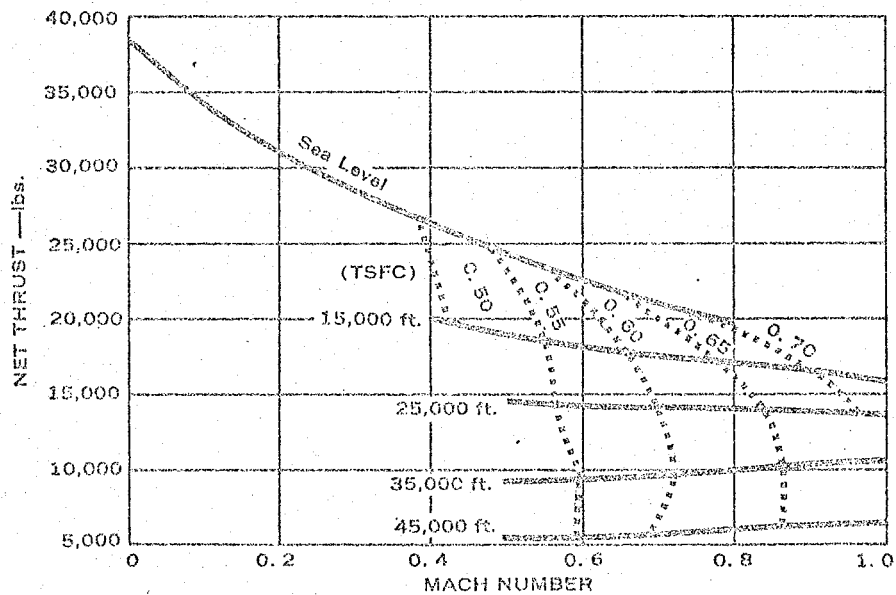
FIXED AREA JET NOZZLES

100% RAM RECOVERY

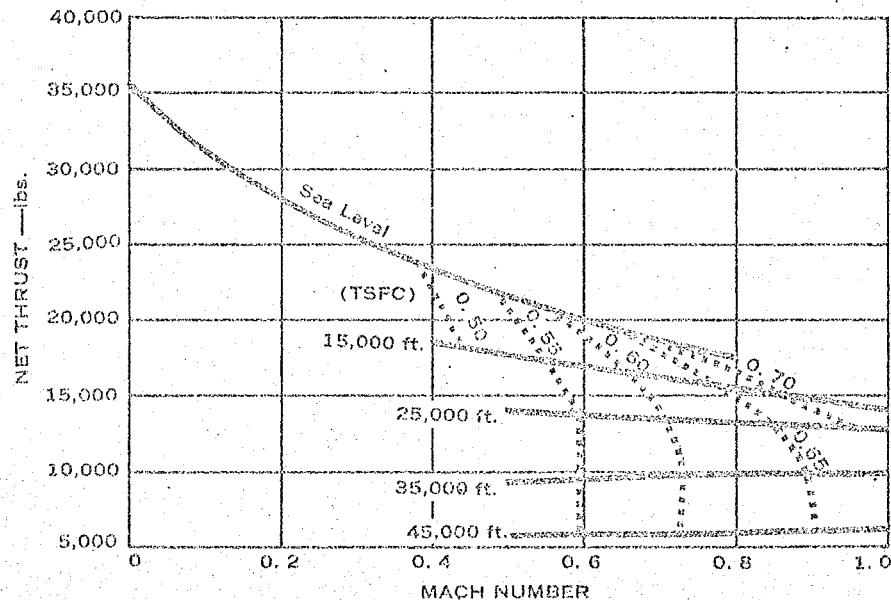
TAKE-OFF PERFORMANCE
SEA LEVEL



MAXIMUM CONTINUOUS
AND
MAXIMUM CLIMB RATINGS



MAXIMUM CRUISE RATINGS





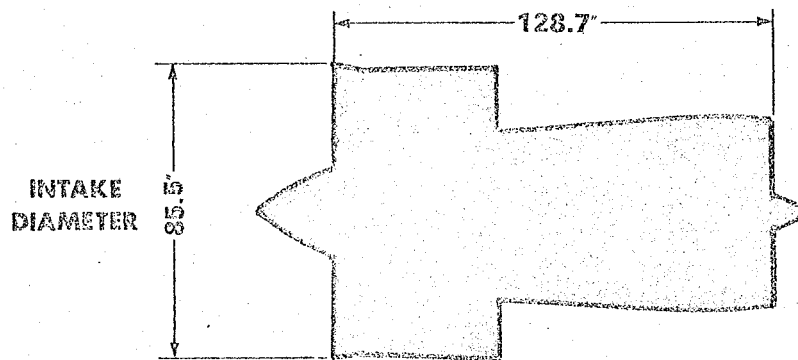


Leading particulars

RB 211-22

Overall Compression Ratio	27:1
By-Pass Ratio	5:1
Max. Take-off Thrust (Maintained to 84°F.)	40,600 lb.
Max. Cruise Thrust 35,000 ft. 0.85 Mn.	9,267 lb.
Specific Fuel Consumption (at above condition)	0.628 lb./hr./lb.
Max. Basic Dry Weight	6,353 lb.
Associated Equipment	<ul style="list-style-type: none">— Fan Reverser— Hot Stream Spoiler— Pod Cowlings and Systems— Noise Reduction Nozzle

DIMENSIONS — BASIC ENGINE

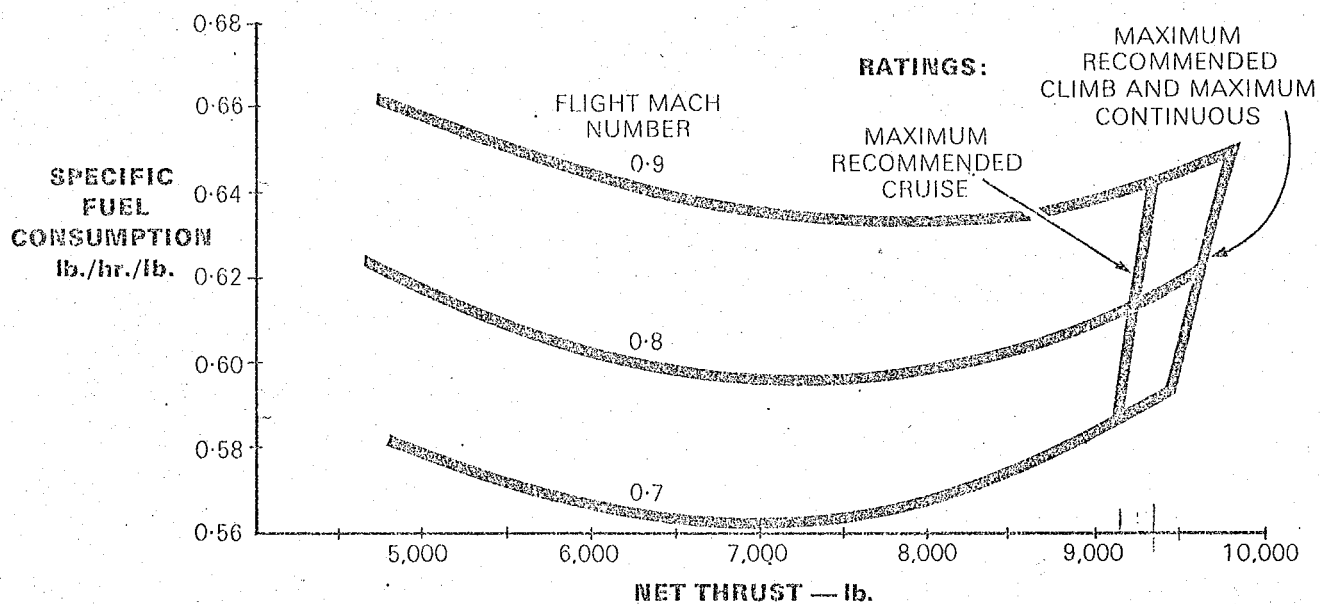


N.B. No allowance has been made in the performance quoted on this sheet for the effect of air off-takes or duct losses.



RB 211-22

PERFORMANCE AT 35,000 FT. PRESSURE
ALTITUDE, ISA CONDITIONS, NO LOSSES.



NOTE:

This performance does not include internal losses of the by-pass stream downstream of the fan outlet guide vane exit

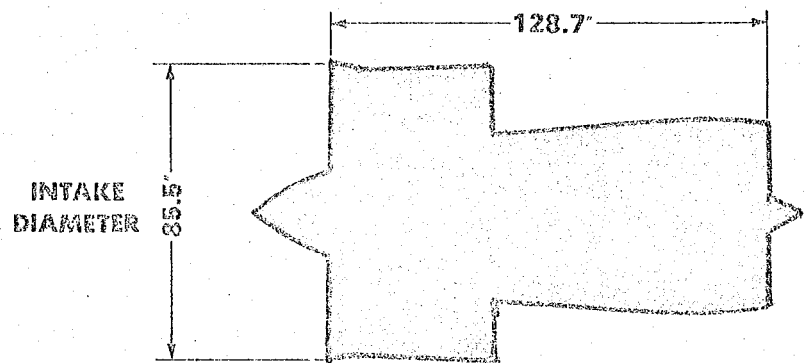


Leading particulars

RB 211-23

OVERALL COMPRESSION RATIO	27:1
BY-PASS RATIO	5:1
MAX. TAKE-OFF THRUST (Maintained to 90°F.)	38,400 lb.
MAX. CRUISE THRUST 35,000 ft. 0.85 Mn.	8,970 lb.
SPECIFIC FUEL CONSUMPTION (at above condition)	0.624 lb./hr./lb.
MAX. BASIC DRY WEIGHT	6,353 lb.
ASSOCIATED EQUIPMENT	<ul style="list-style-type: none">-- Fan Reverser-- Hot Stream Spoiler-- Pod Cowlings and Systems-- Noise Reduction Nozzle

DIMENSIONS - BASIC ENGINE



N.B. No allowance has been made in the performance quoted on this sheet for the effect of air off-takes or duct losses.

Brochure T.S.D. 1664

11.11.11

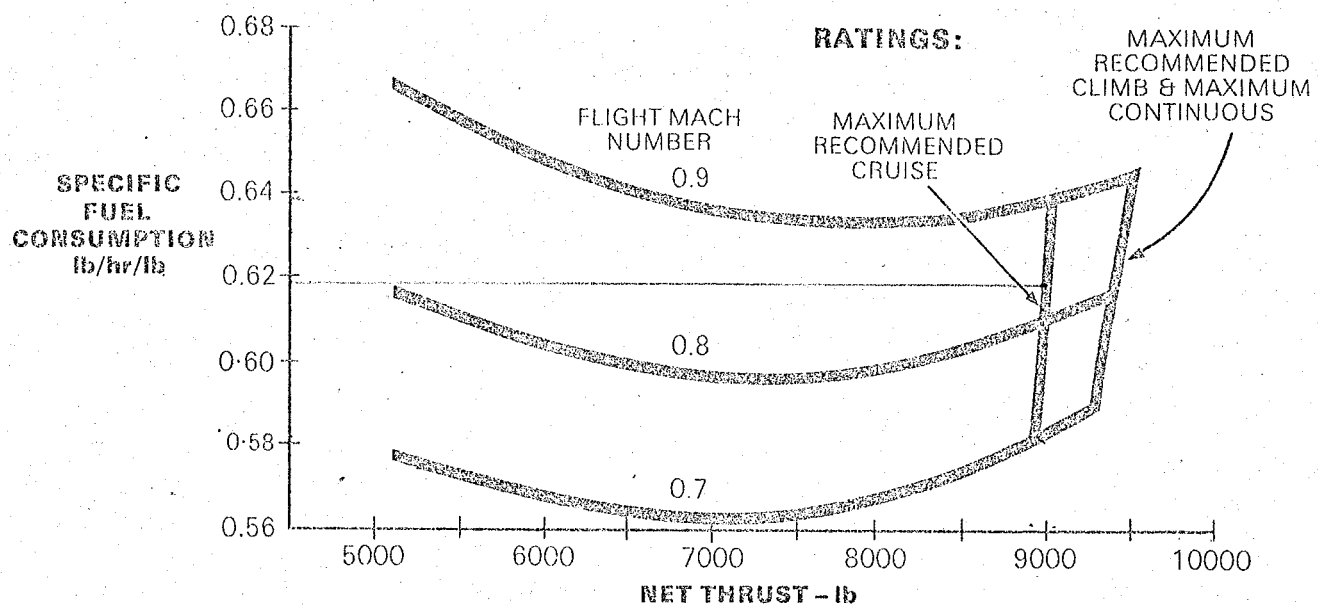
11.11.11

11.11.11

11.11.11

RB 211-23

PERFORMANCE AT 35,000 FT. PRESSURE
ALTITUDE, ISA CONDITIONS, NO LOSSES.



NOTE:

This performance does not include internal losses of the bypass stream downstream of the fan outlet guide vane exit.



APPENDIX D

'Preliminary Design Calculation
Techniques'



PRELIMINARY DESIGN

AIR BUS

Specifications :

- | | | |
|----|----------------------|----------|
| a) | Cruise Mach Number | M_{cr} |
| b) | Number of Passengers | N_P |
| c) | Range | R |
| d) | Field length | X |

First Estimates :

Given above specifications, the first estimates of the proposed design are arrived at based on comparative studies. One would expect the range of values for the following parameters to be:

- | | | |
|--|---------------------------------|--------------------------------|
| Cruise Altitude | h_{cr} | 30,000 to 35,000 ft. |
| Take off Wing Loading | $\left(\frac{W}{S}\right)_{TO}$ | 95 to 125 lbs/ft. ² |
| Ratio of take off weight to payload weight | $\frac{W_{TO}}{W_{PL}}$ | 3 to 8 depending on range |

As a first approximation, to be evaluated subsequently, the fuel consumption during take off and subsequent climb to the cruise altitude is assumed as $0.03 W_{TO}$.

The ratio of the thrust available from the engine during cruise at the cruise altitude, to the maximum static thrust at sea level may be estimated from engine performance charts.

For example for the RB 211-23 engines

Lapse Ratio, $\left(\frac{T_{cr}}{T_{SSL}}\right) = \frac{8970}{38,400} = 0.2336$
 at $M = 0.85$,
 $h = 35,000$

First estimate of the ratio $\left(\frac{W}{T}\right)_{TO}$ at take off

Since $\left(\frac{L}{D}\right)_{cr} = \left(\frac{W}{T}\right)_{cr}$

$$\left(\frac{L}{D}\right)_{cr} = \frac{0.97 W_{TO}}{0.2336 T_{SSL}} = 4.1524 \left(\frac{W}{T}\right)_{TO}$$

$$\left(\frac{W}{T}\right)_{TO} = \frac{1}{4.1524} \left(\frac{L}{D}\right)_{cr}$$

Based on a study of existing aircraft the ratio $\left(\frac{L}{D}\right)_{cr}$ ranges from 14 to 15. This value depends, amongst others, on the aerodynamic cleanliness of the aircraft, the optimum design of the wing to reduce induced drag and compressibility drag, the size of the fusilage etc.

Assuming $\left(\frac{L}{D}\right)_{cr} = 14$, which figure will be arrived at accurately later on during the design,

$$\left(\frac{W}{T}\right)_{T0} = \frac{14}{4.1524} = 3.3715$$

$$\left(\frac{T}{W}\right)_{T0} = 0.2966$$

This value is seen to compare favorably with that for the present generation aircraft.

The payload, which is that part of the aircraft weight associated with its earnings, is related to the number of passengers and the cargo. It is taken that,

$$W_{PL} = 240 N_p$$

The figure 240, consists of 160 lbs. as the weight of each passenger, 40 lbs. as his baggage and 40 lbs. as cargo per passenger.

$$\text{Assuming } \left(\frac{W_{T0}}{W_{PL}}\right) = 5$$

$$W_{T0} = 5(240N_p)$$

$$T_{SSL} = 0.2966 W_{T0}$$

The ratio $\frac{T_{SSL}}{T_{SSL/Eng}}$ would give an indication of the number of engines required on the aircraft.

WING GEOMETRY

The following parameters are chosen as contributing to an optimum wing design

Aspect Ratio

$$AR = 7$$

Wing Sweepback on the 1/4 chord line

$$\Lambda_{1/4 c} = 35^\circ$$

Taper Ratio (Ratio of tip chord to root chord)

$$\lambda = \frac{C_T}{C_R} = 1/3$$

The NACA 65 series airfoil is selected for its design C_L value, low profile drag and fairly high Critical Mach number.

The wing thickness ratio $\left(\frac{t}{c}\right)$ is to be selected. We proceed as follows.

Selecting $\left(W/S\right)$ at beginning of cruise as 100.

and the induced drag efficiency factor as ~~1.0~~ 0.85 to 0.9 calculate C_L and C_{D_i}

Assume C_{D_0} (The zero lift drag of the aircraft without effects of compressibility) as $C_{D_0} = 0.015$. This is a representative

figure for this type of aircraft. We will arrive at this figure accurately later in the design.

$$C_D = C_{D_0} + C_{D_i} + \Delta C_{D_{Comp.}}$$

$$\left(\frac{C_D}{C_L}\right) = \frac{1}{14} \quad \text{knowing } C_L \text{ calculate } C_D$$

$$\text{and hence } \Delta C_{D_{Comp.}}$$

Using the charts and explanations supplied for compressibility (wave) drag rise one calculates the $\left(\frac{t}{c}\right)$ permissible at the cruise Mach number under consideration.

- 4 -

ESTIMATION OF DRAG RISE BEYOND THE CRITICAL
MACH NUMBER M_{CR}

The following procedure, using the accompanying charts based on wind tunnel tests, may be adopted for the prediction of drag rise beyond the critical Mach Number.

From the wing geometry the following quantities are known:

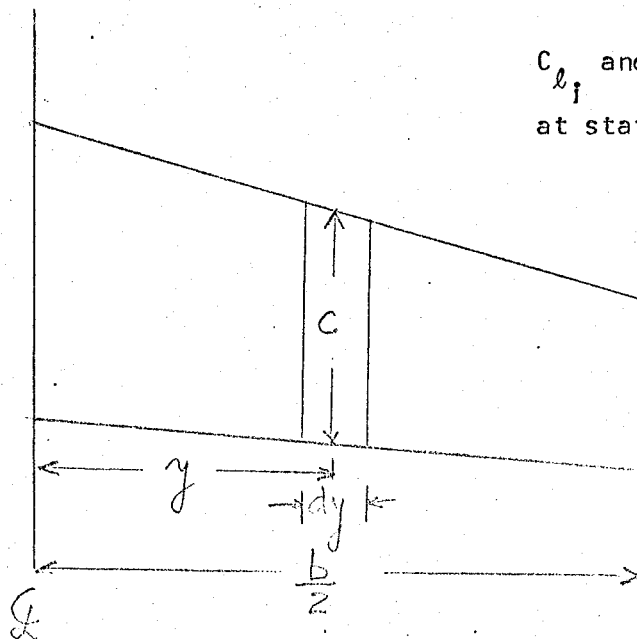
- a) Sweepback angle of the $\frac{1}{4}c$ line, $\Lambda \frac{1}{4}c$.
- b) Aspect Ratio, AR.
- c) Average streamwise thickness ratio, $(\frac{t}{c})_{av.}$

$$(\frac{t}{c})_{av.}^2 = \frac{\int (\frac{t}{c})^2 c dy}{\int c dy}$$

- d) Wing design lift coefficient, C_{L_i}

$$C_{L_i}^2 = \frac{\int (C_{L_i})^2 c dy}{\int c dy}$$

C_{L_i} and $(\frac{t}{c})_l$ are local values
at station y



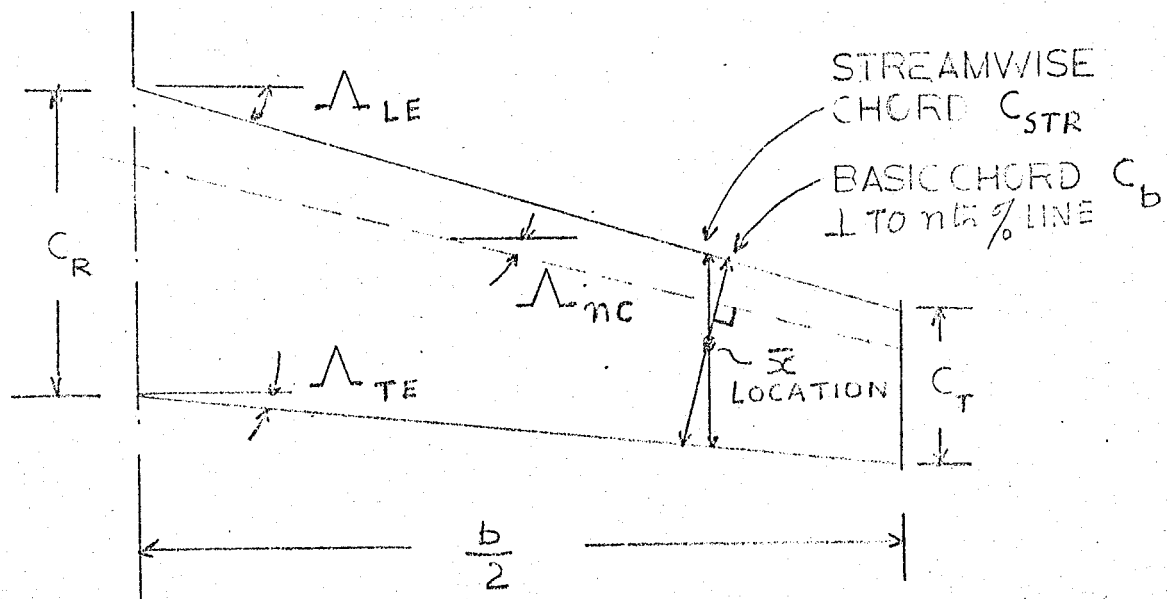
- 1) At the values of wing $(\frac{t}{c})_{av.}$ and $\Lambda \frac{1}{4}c$ read from Figs. 1 and 2 the values of M_{DD} at flight C_L values of 0.2 and 0.4 .
- 2) Corresponding to the wing design lift coefficient C_{L_i} read from Fig. 3 the values of $(\Delta M_{DD})_{camber}$ at flight C_L values of 0.2 and 0.4 .
- 3) For the given aspect ratio AR of the wing, read from Fig.3, the values of $(\Delta M_{DD})_{AR}$ at flight C_L values of 0.2 and 0.4 .
- 4) The corrected M_{DD} value is then obtained , at flight C_L values of 0.2 and 0.4 as the sum of quantities from above.

$$M_{DD_{corrected}} = M_{DD} + (\Delta M_{DD})_{camber} + (\Delta M_{DD})_{AR}$$

- 5) Use drag rise shapes of Fig.5 for given sweep angle and find ΔC_D corresponding to $\Delta M = M_{cruise} - M_{DD_{corrected}}$ at flight C_L values of 0.2 and 0.4 .
- 6) M_{DD} values at flight C_L values other than 0.2 and 0.4 may be estimated by interpolation using Fig. 4 . At these other values of C_L , $\Delta M_{DD_{camber}}$ and $\Delta M_{DD_{AR}}$ may be obtained from Fig.3, interpolating if necessary. The drag rise ΔC_D at $\Delta M_{cruise} - M_{DD_{corrected}}$ at C_L value other than 0.2 and 0.4 may be obtained by inetrpolation of ΔC_D values from Fig. 5

Note: Tailored Wing - represents wing with camber and twist distribution representative of present wing planforms.

RELATIONSHIPS BASED ON WING GEOMETRY



- AR — ASPECT RATIO
 Λ — SWEEP ANGLE
 LE — LEADING EDGE
 TE — TRAILING EDGE
 nc — n th PERCENT CHORD LINE
 C_R — ROOT CHORD, C_T — TIP CHORD
 λ — TAPER RATIO C_T/C_R
 $\frac{t}{c}$ — THICKNESS RATIO

$$AR \cdot \tan \Lambda_{LE} = AR \cdot \tan \Lambda_{nc} + 4n \frac{1-\lambda}{1+\lambda}$$

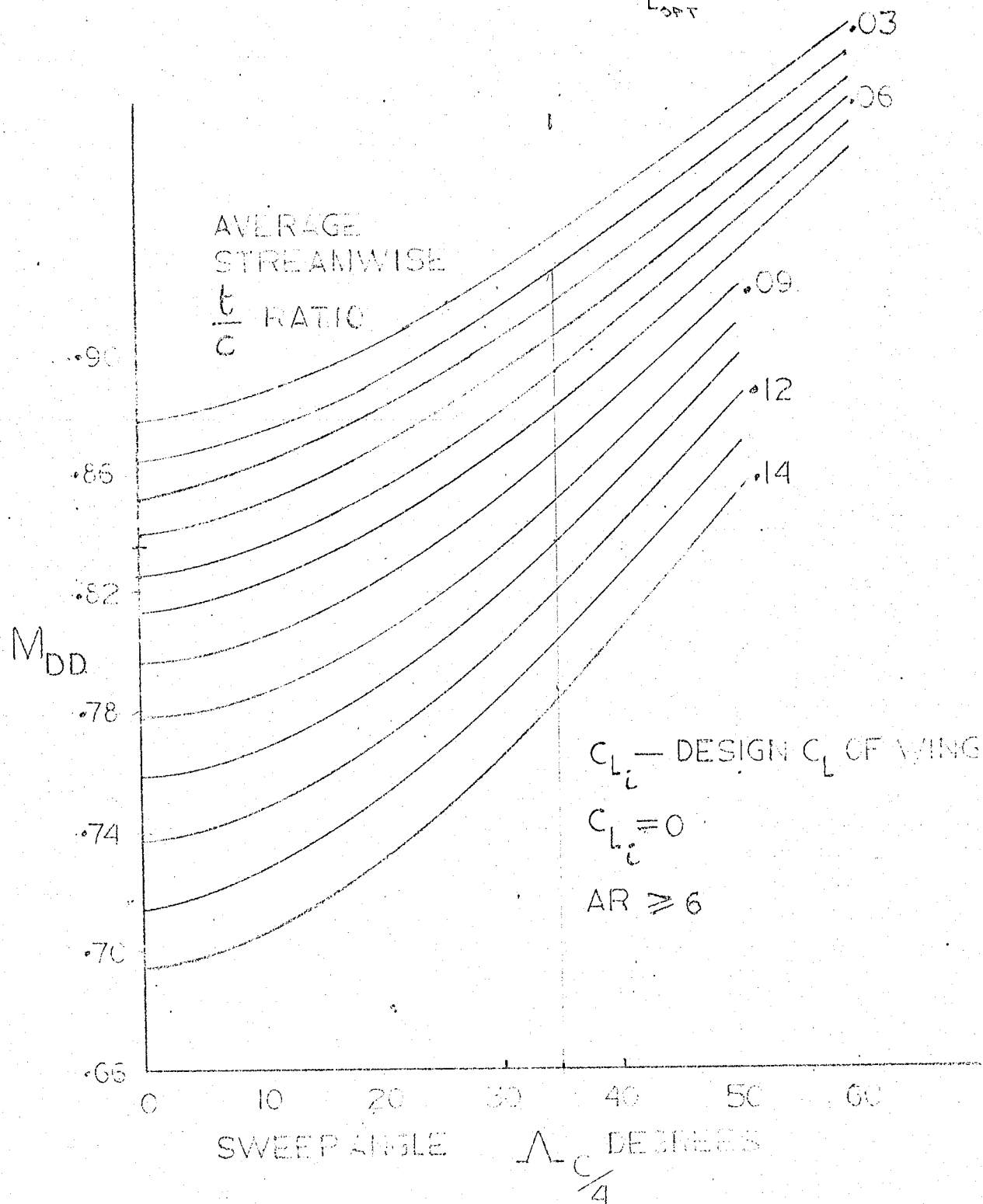
$$\left(\frac{t}{c} \right)_{STR} = \left(\frac{t}{c} \right)_b \cdot \frac{C_b}{C_{STR}}, \text{ AND } \frac{C_{STR}}{C_b} = \bar{x} \frac{\sin(90 + \Lambda_{LE} - \Lambda_{nc})}{\sin(90 - \Lambda_{LE})} + (1 - \bar{x}) \frac{\sin(90 + \Lambda_{TE} - \Lambda_{nc})}{\sin(90 - \Lambda_{TE})}$$

- \bar{x} — MAX THICKNESS LOCATION ON BASIC CHORD AS A FRACTION OF BASIC CHORD
 n — FRACTION OF C_{STR} THROUGH WHICH n th PERCENT CHORD LINE PASSES

DRAG DIVERGENT MACH NUMBER

FIG 1

AT 0.002 DRAG RISE AND $C_L = 0.2$



○

○

7

○

DRAG DIVERGENT MACH NUMBER

Fig 2

AT 0.002 DRAG RISE AND $C_{L_{OPT}} = 0.4$

AVERAGE STREAMWISE

$\frac{t}{c}$ RATIO

M_{DD}

0.90

0.85

0.80

0.75

0.70

0.65

0.60

10°

20°

30°

40°

50°

60°

SWEEP ANGLE $\Delta \frac{c}{4}$ DEGREES

0.03

0.06

0.09

0.12

0.14

$C_{L_i} = 0$

$AR_i \geq 6$

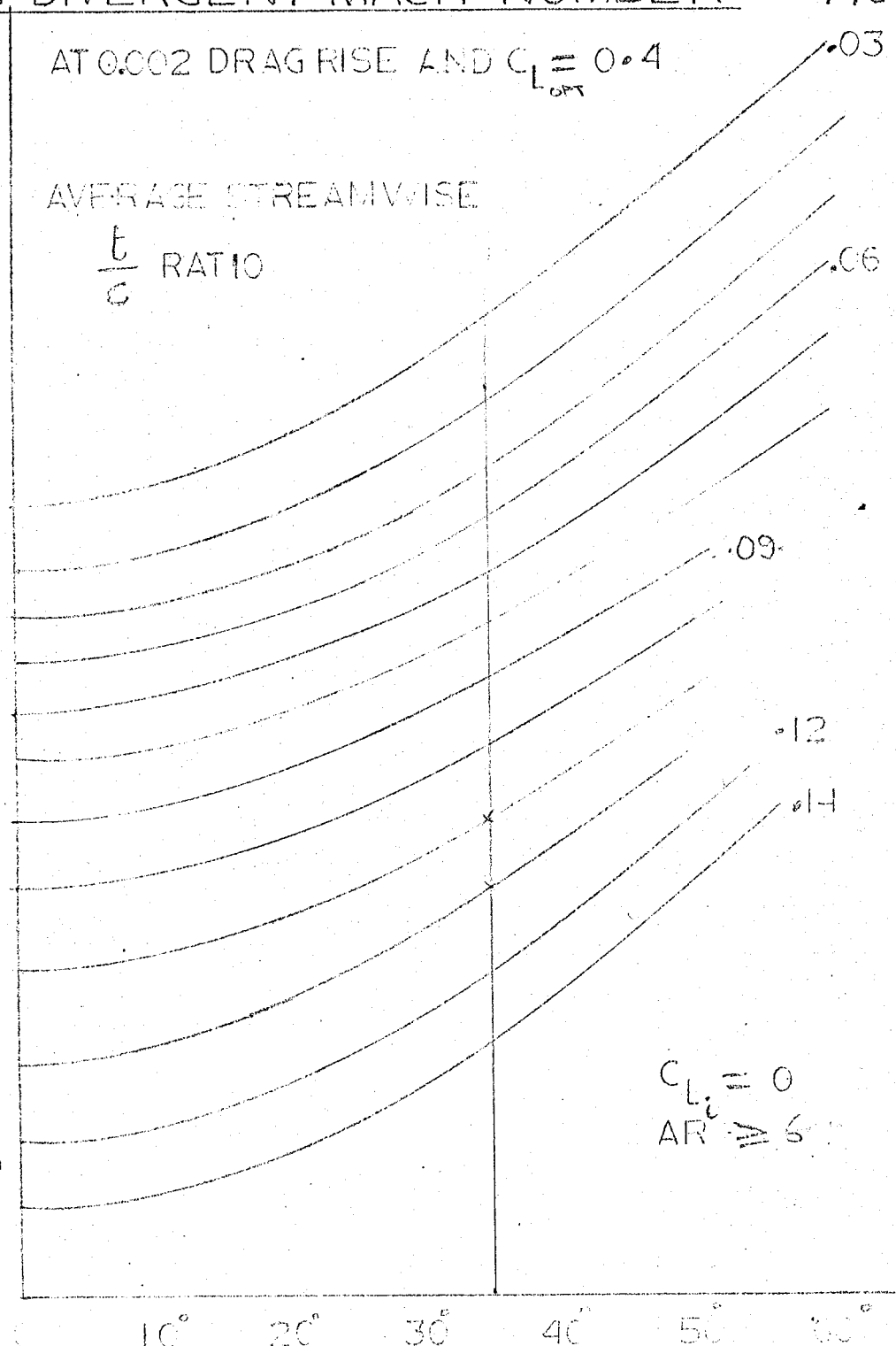
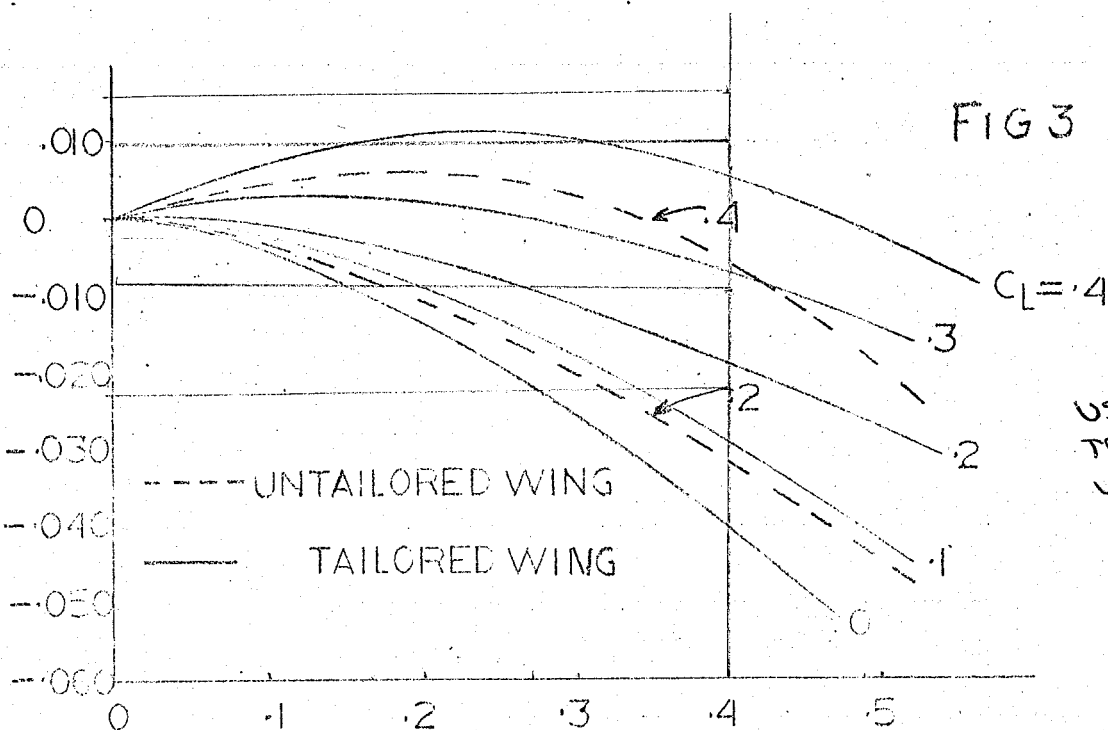


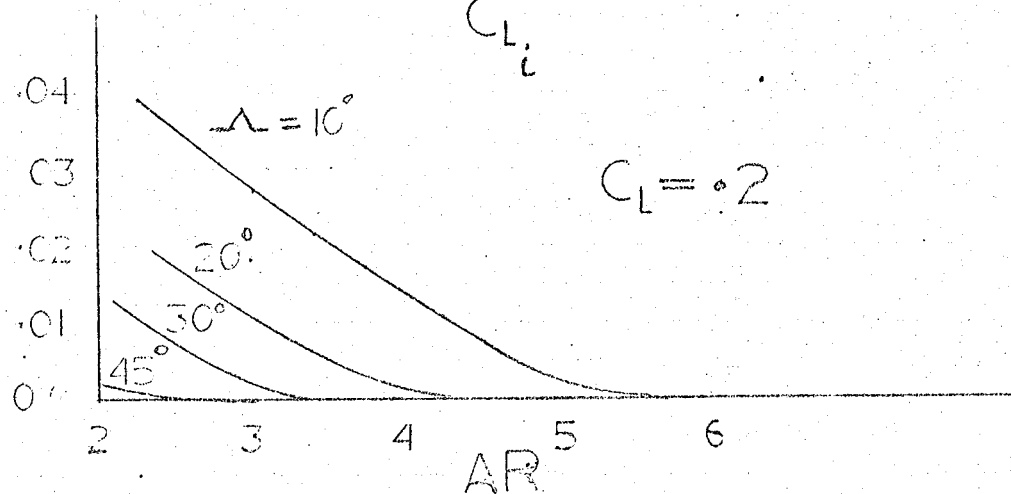
FIG 3

ΔM_{DD}
DUE TO
CAMBER

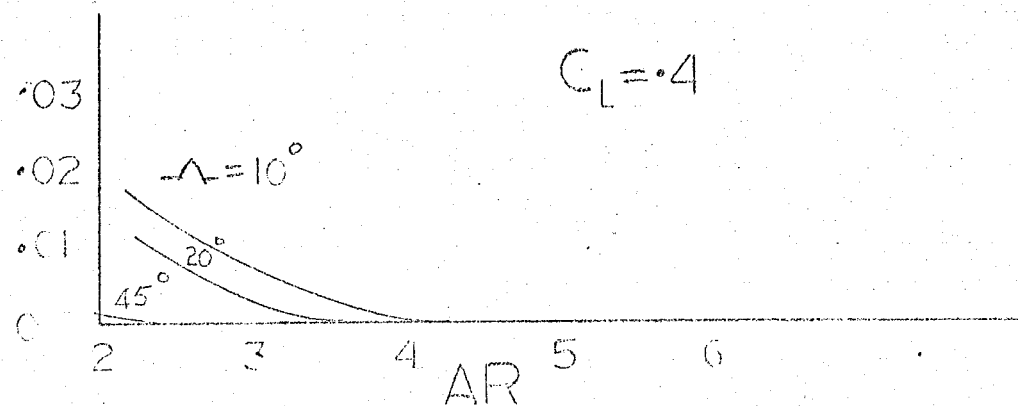


USE
TAILORED
WING
DATA

ΔM_{DD}
DUE TO
ASPECT
RATIO

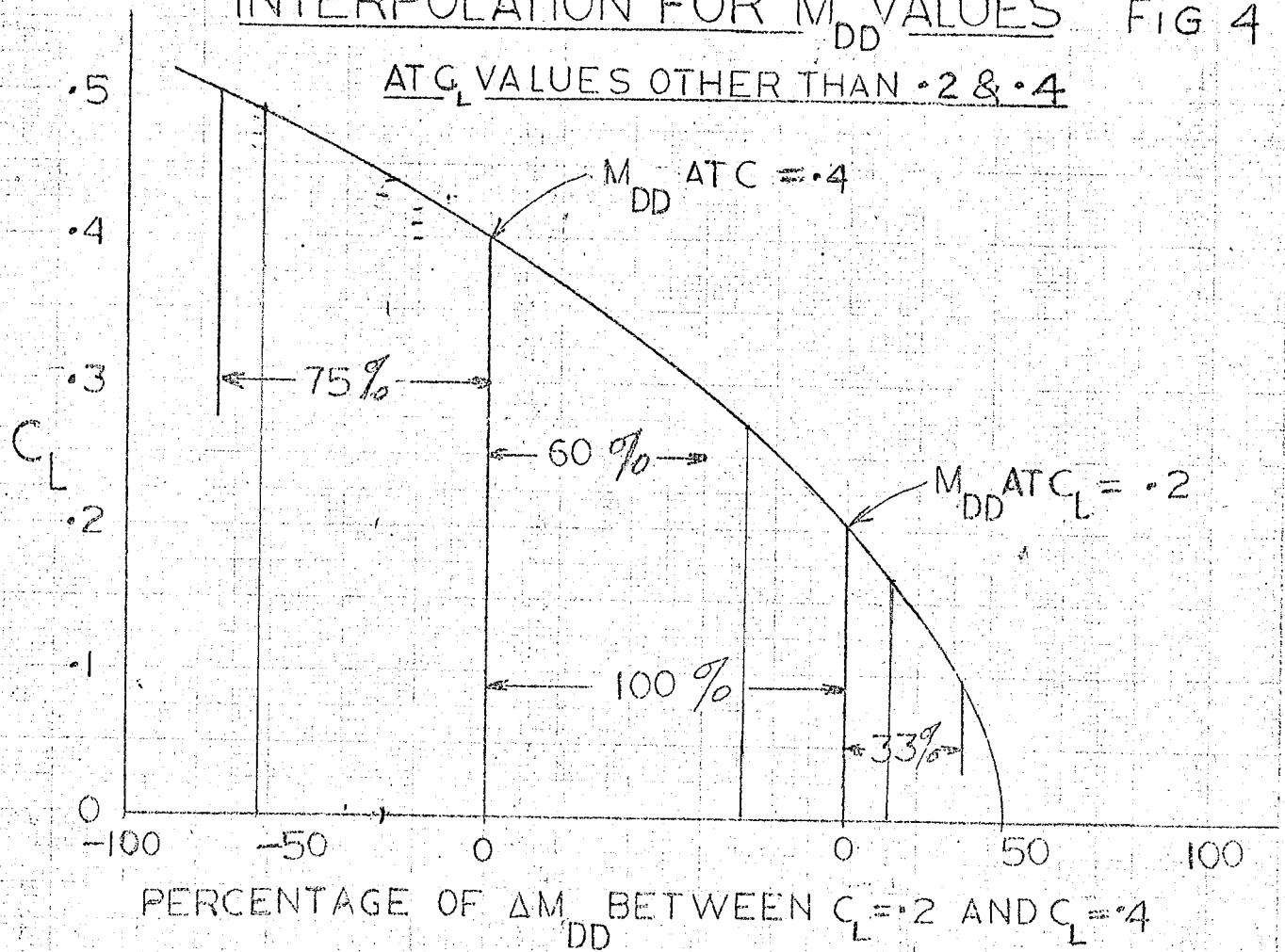


ΔM_{DD}
DUE TO
ASPECT
RATIO



INTERPOLATION FOR M_{DD} VALUES FIG 4

AT C_L VALUES OTHER THAN .2 & .4



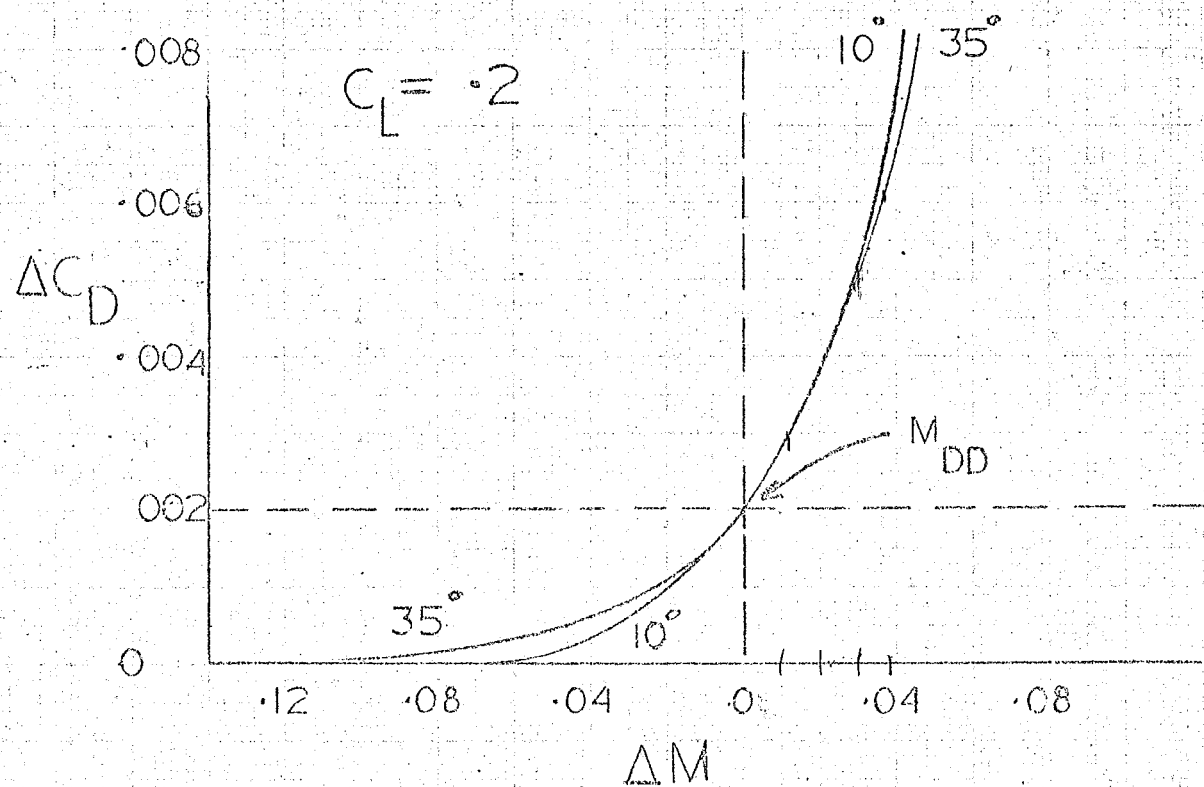
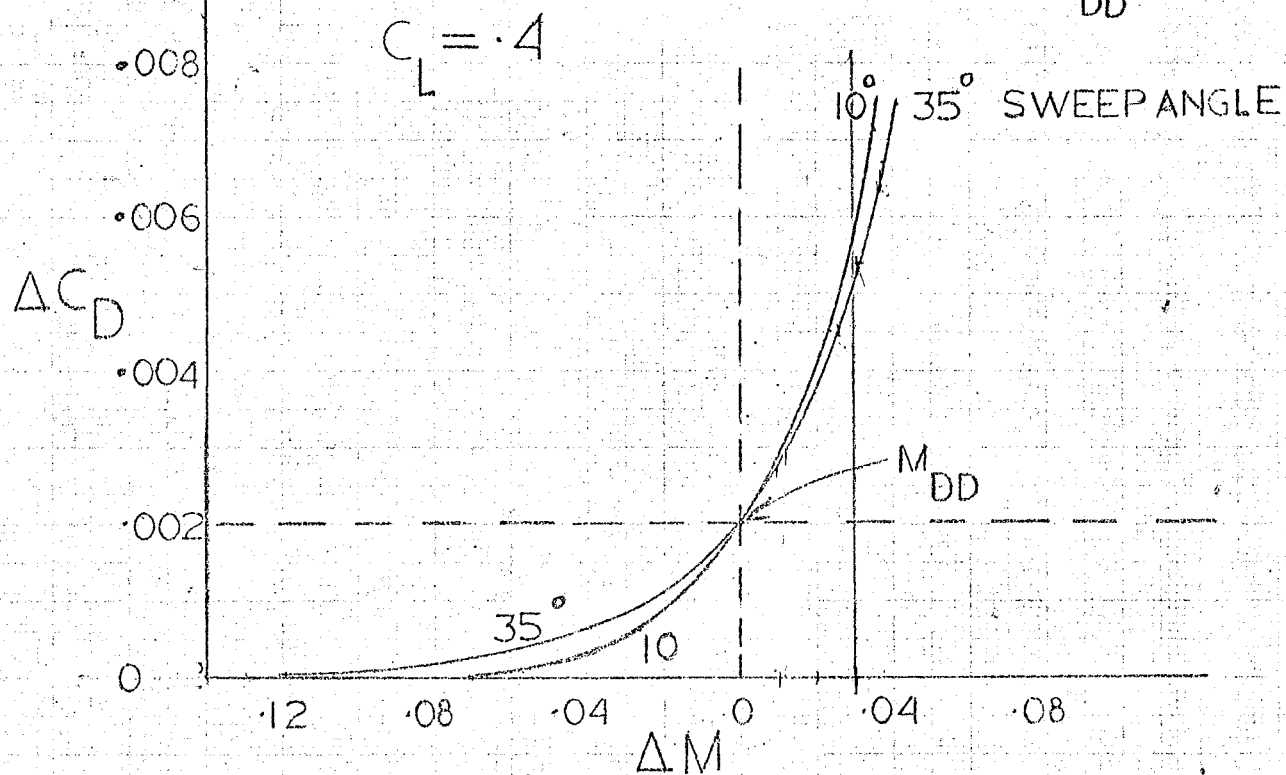
EXAMPLE

$$\begin{array}{rcl}
 M_{DD} \text{ AT } C_L = 0.4 & = & 0.750 \\
 M_{DD} \text{ AT } C_L = 0.2 & = & 0.800 \\
 \hline
 \Delta M_{DD} & = & 0.050
 \end{array}
 \left. \vphantom{\begin{array}{rcl} M_{DD} \text{ AT } C_L = 0.4 \\ M_{DD} \text{ AT } C_L = 0.2 \\ \Delta M_{DD} \end{array}} \right\} \text{FROM FIGS}$$

$$\text{AT } C_L = 0.5 \quad M_{DD} = 0.750 + (-0.75)(0.050) = 0.712$$

$$\text{AT } C_L = 0.1 \quad M_{DD} = 0.800 + (-0.33)(0.050) = 0.817$$

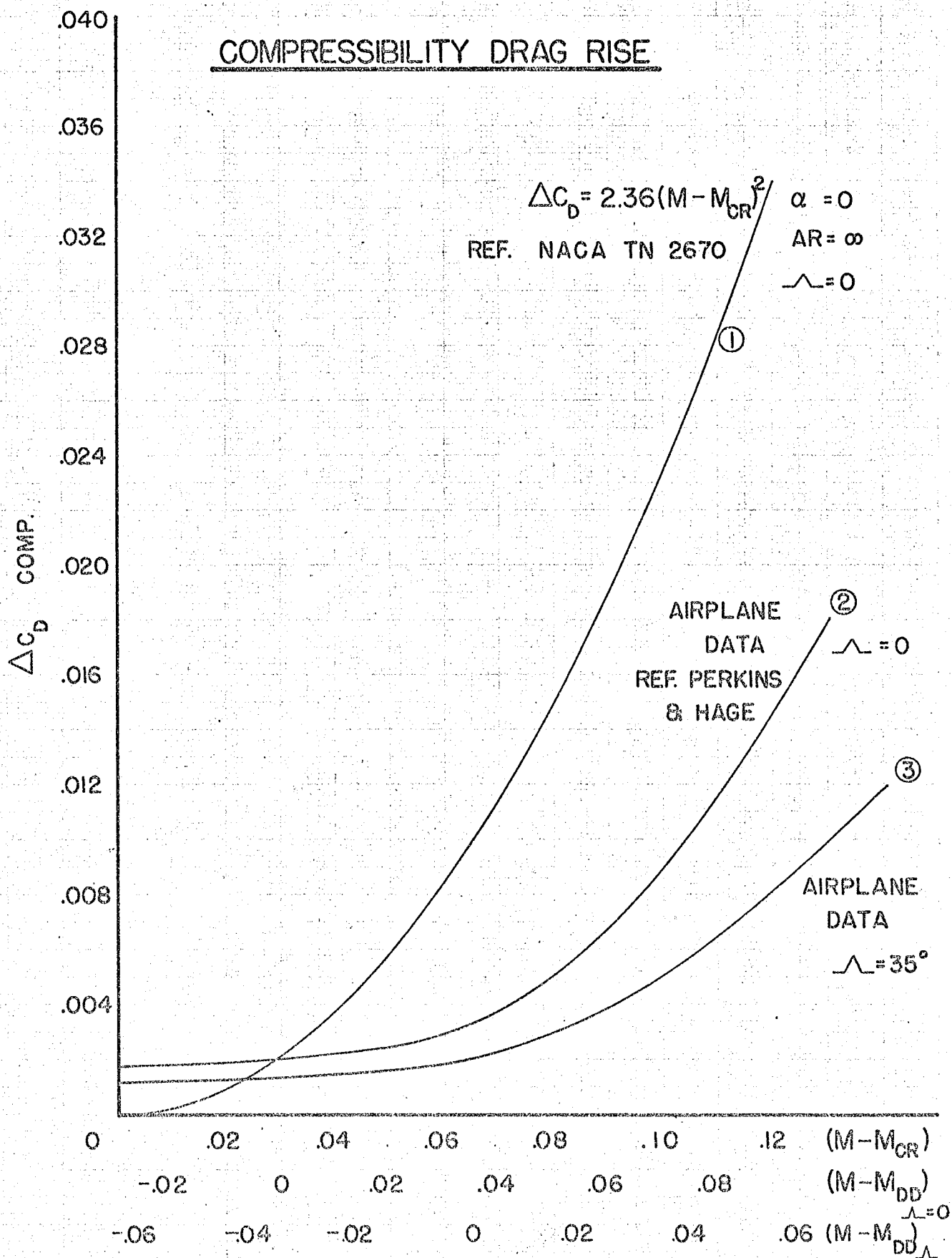
DRAG RISE BEYOND M_{DD} FIG. 5



4444



COMPRESSIBILITY DRAG RISE

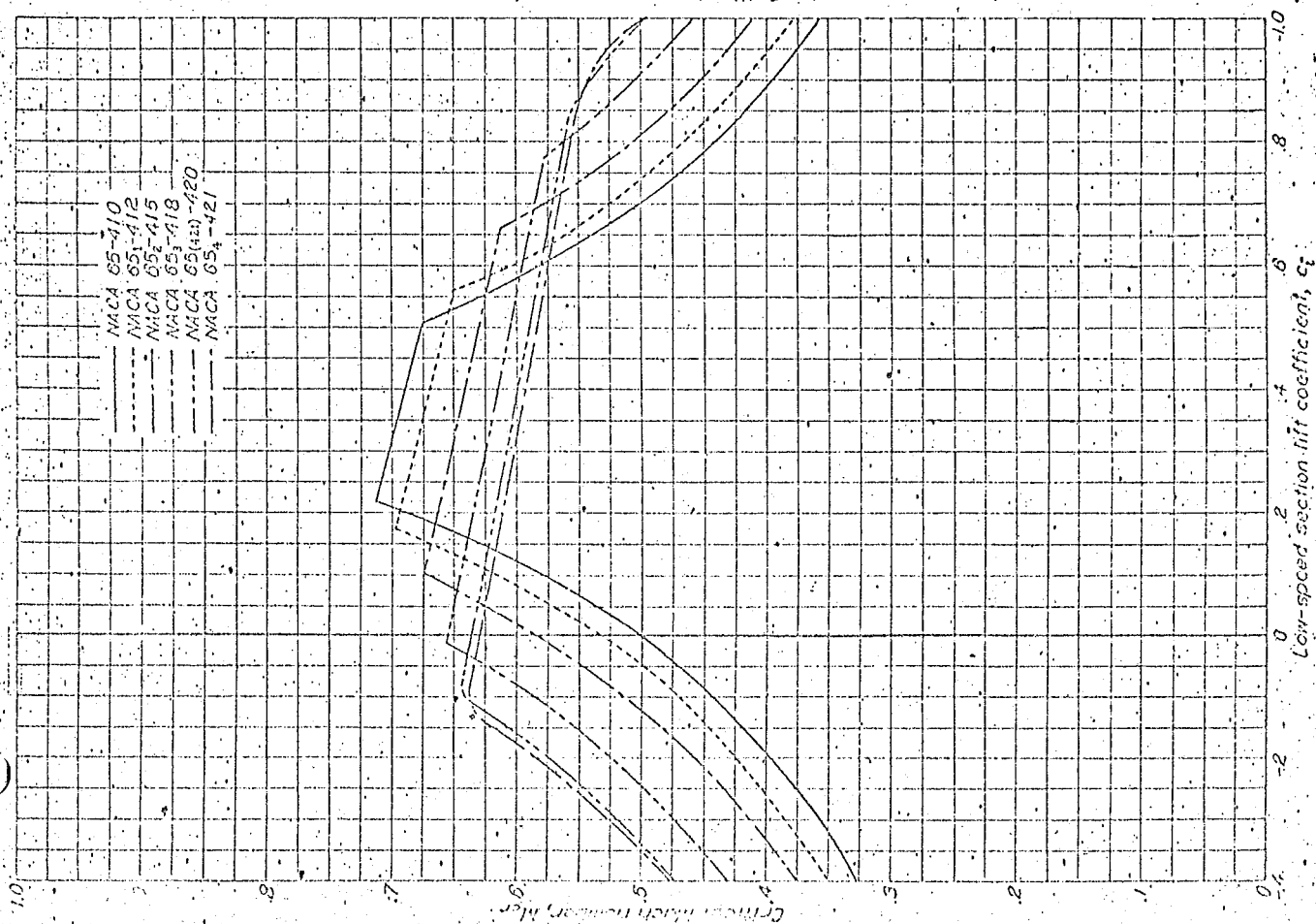


11

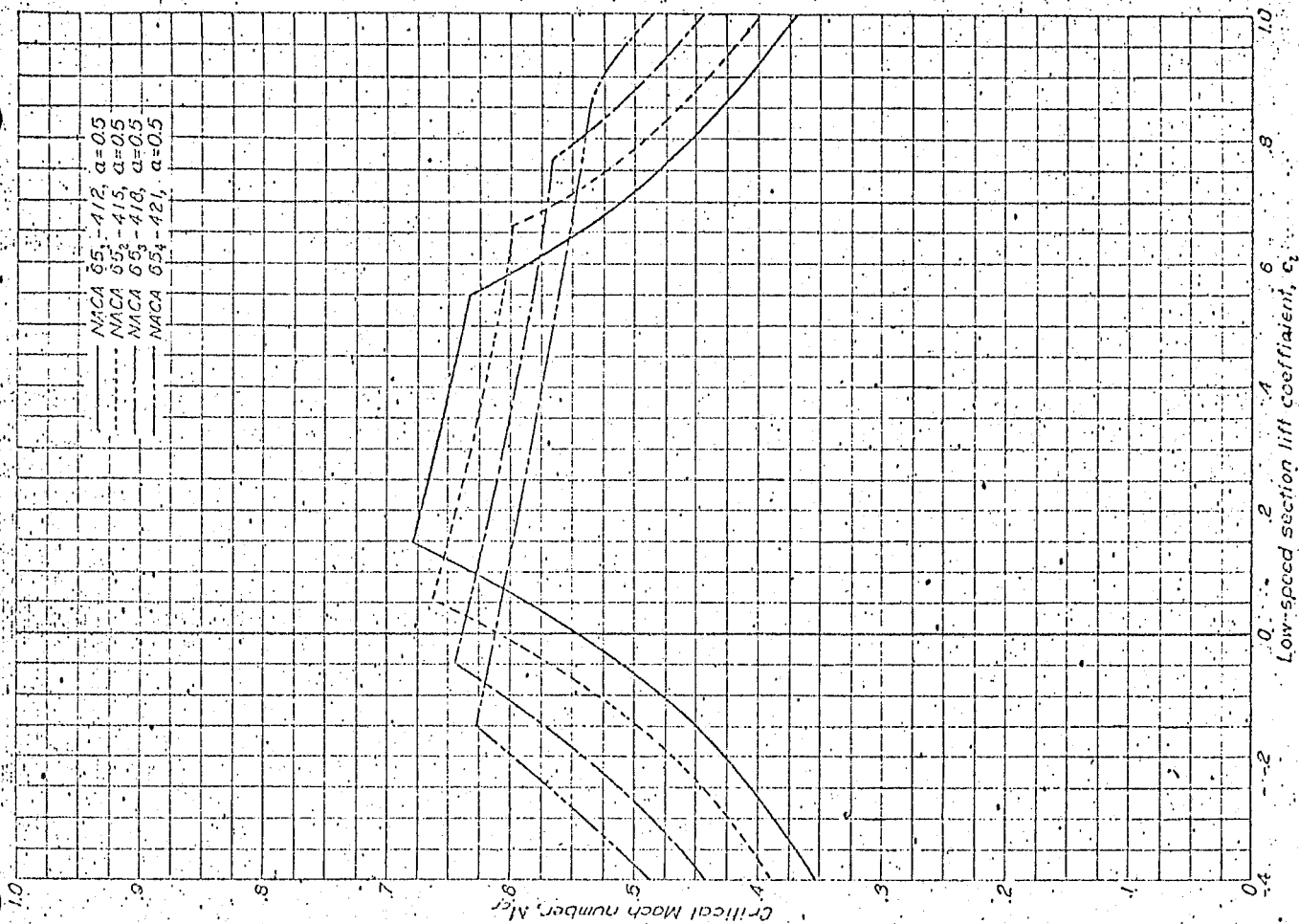
12

13

14



Variation of critical Mach number with low-speed section lift coefficient for several NACA 45-series airfoil sections of various thicknesses, equipped for a design lift coefficient of 0.4.



Variation of critical Mach number with low-speed section lift coefficient for several NACA 65-series airfoil sections with mean line of the type $a=0.5$ and cambered for a design lift coefficient of 0.4.



APPENDIX E

'Estimation of Parameters based on Generalized
Design Charts'

ESTIMATION OF PARAMETERS BASED ON GENERALISED DESIGN CHARTS :

One can arrive at the values of the various parameters, such as, $(\frac{W}{S})_{T0}$, $(\frac{T}{W})_{T0}$, h_{cr} , AR , $\Lambda_{1/4c}$, λ , $(\frac{t}{c})$, etc., based on comparative studies and empirical relations. It is evident that these values have been tentatively fixed and are subject to variations.

However, these values significantly influence the performance of an aircraft such as take off, landing, climb, cruise, range, and cost.

If at this stage, a study is made of the influence of these parameters on the performance requirements, one could confirm the choice of these parameters, or alter them suitably.

This task is performed with the help of generalized design charts.

GENERALIZED DESIGN CHARTS:

These charts may be constructed to study the influence of various parameters on performance.

The parameters used to set up functional relationships, depend on the discretion of the designer. It is suggested that design charts be set up using $(\frac{W}{S})_{T0}$ and $(\frac{T}{W})_{T0}$ as the basic parametric variables to set up the functional relationships.

Consider now the various performance requirements.

1. Landing:

While the major airports may have landing fields 9000 ft. or longer, it would be necessary to use smaller fields in covering the range in stages. Hence a landing field length of 6000 ft. is chosen.

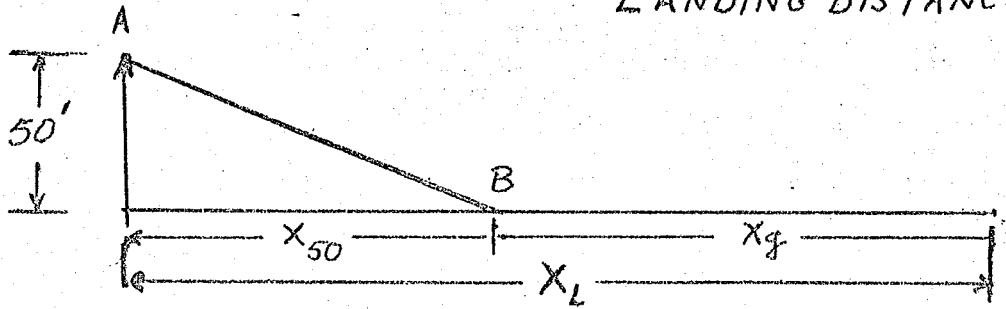
The landing distance specified by the F.A.R. is the horizontal distance on the ground required to glide over a 50 ft. obstacle, touch down and roll to a stop.

C

O

C

LANDING DISTANCE



Assuming the glide angle to be small, the change in the total mechanical energy of the particle from positions A to B is equal to the work done in moving through the distance AB.

Length AB $\sim X_{50}$

$$\frac{W}{2g} (V_A^2 - V_B^2) + 50 W = F \cdot X_{50}$$

$$\frac{V_B^2}{2a} = X_g$$

Let $V_A = 1.30 V_S$ and $V_B = 1.15 V_S$, where V_S is the stalling speed of the aircraft with full flaps.

$$V_S^2 = \frac{841 \left(\frac{W}{S}\right)_L}{\sigma C_{LMAX}}$$

C_{LMAX} - Maximum lift coefft. with full flaps

σ - Density ratio.

a - Deceleration on the ground

$\left(\frac{W}{S}\right)_L$ - Wing loading during landing.

Also $F=D$ and $\frac{W}{F} \sim \frac{L}{D}$

The total landing distance $X_L = X_{50} + X_g$

$$X_L = \frac{L}{D} \left[4.8 \frac{\left(\frac{W}{S}\right)_L}{\sigma C_{LMAX}} + 50 \right] + 556 \frac{\left(\frac{W}{S}\right)_L}{a \sigma C_{LMAX}}$$

Using a safety factor of $\frac{1}{0.6}$ as recommended by F.A.R. ,

$$X_L = \frac{L}{D} \left[8 \frac{\left(\frac{W}{S}\right)_L}{\sigma C_{LMAX}} + 83.3 \right] + 927 \frac{\left(\frac{W}{S}\right)_L}{a \sigma C_{LMAX}} \quad \text{----- (1)}$$

Knowing $X_L = 6000$, and assigning values for $\left(\frac{L}{D}\right)$, σ , a , C_{LMAX} , the landing wing loading $\left(\frac{W}{S}\right)_L$ can be calculated.

The ground deceleration $a = 7$ to 12 ft. / sec^2 depending on the landing surface and the effectiveness of reverse thrust mechanism.

A value of 10 for ground deceleration seems both feasible and not too large for passenger comfort. $(\frac{L}{D})$ for landing may be taken as 5.5

The maximum lift coefficient for the swept wing without flaps can be had from figure, for given sweep and $(\frac{t}{c})_{\frac{1}{4}c}$ ratio.

This value is increased by 15% by the leading edge flaps and slots.

The trailing edge flaps (triple slotted) further augments this figure by a factor of 1.82 for a flap deflection of 45° .

However a $C_{L_{MAX}}$ not in excess of 2.57 may be used in above calculations.

$(\frac{W}{S})_L$ is the maximum permissible design landing wing loading and is obtained from above relationship (Eq. 1)

If one assumes, as is the recommended practice, that this $(\frac{W}{S})_L$ is reached when $\frac{1}{3}$ of the total fuel is used up (or jettisoned for emergency landing),

$$W_L = W_{T0} - \frac{1}{3} W_f = W_{T0} (1 - \frac{1}{3} \frac{W_f}{W_{T0}})$$

$$(\frac{W}{S})_L = (\frac{W}{S})_{T0} (1 - \frac{1}{3} \frac{W_f}{W_{T0}})$$

$$(\frac{W}{S})_{T0} = \frac{(\frac{W}{S})_L}{1 - \frac{1}{3} \frac{W_f}{W_{T0}}} \quad \text{----- (2)}$$

To calculate $\frac{W_f}{W_{T0}}$, consider the Breguet range formula.

$$R = \frac{V}{C} \frac{C_L}{C_D} \ln \left(\frac{W_1}{W_2} \right)$$

R - miles

V - m.p.h.

$$(\frac{W}{S}) = \frac{1}{391} C_L \sigma V^2$$

C - lbs./lb./hr. (T.S.F.C.)

$$(\frac{W}{S}) = 1481 \delta M^2 C_L$$

$$V^2 = 1481 \times 391 M^2 \left(\frac{\delta}{\sigma} \right)^{.5}$$

$$V = 761 M \left(\frac{\delta}{\sigma} \right)^{.5}$$

$$R = 761 \frac{M}{C} \frac{C_L}{C_D} \left(\frac{\delta}{\sigma} \right)^{.5} \ln \left(\frac{W_1}{W_2} \right)$$

R - miles

$$R = 661 \frac{M}{C} \frac{C_L}{C_D} \left(\frac{\delta}{\sigma} \right)^{.5} \ln \left(\frac{W_1}{W_2} \right)$$

R - nautical miles

$$\left(\frac{W_1}{W_2}\right) = e^{-\frac{R}{661} \frac{C}{M} \frac{C_D}{C_L} \left(\frac{\sigma}{\delta}\right)^{.5}} \quad \text{----- (3)}$$

W_1 - Weight at beginning of cruise

W_2 - Weight at end of cruise is taken as when 75% of fuel has been used up.

$$W_1 = .97 W_{T0}$$

$$W_2 = W_{T0} - .75 W_f$$

$$\left(\frac{W_1}{W_2}\right) = \frac{.97}{1 - .75 \frac{W_f}{W_{T0}}} \quad \text{----- (4)}$$

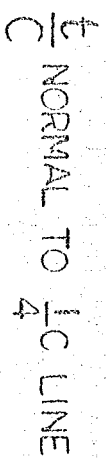
From (3) and (4) we have,

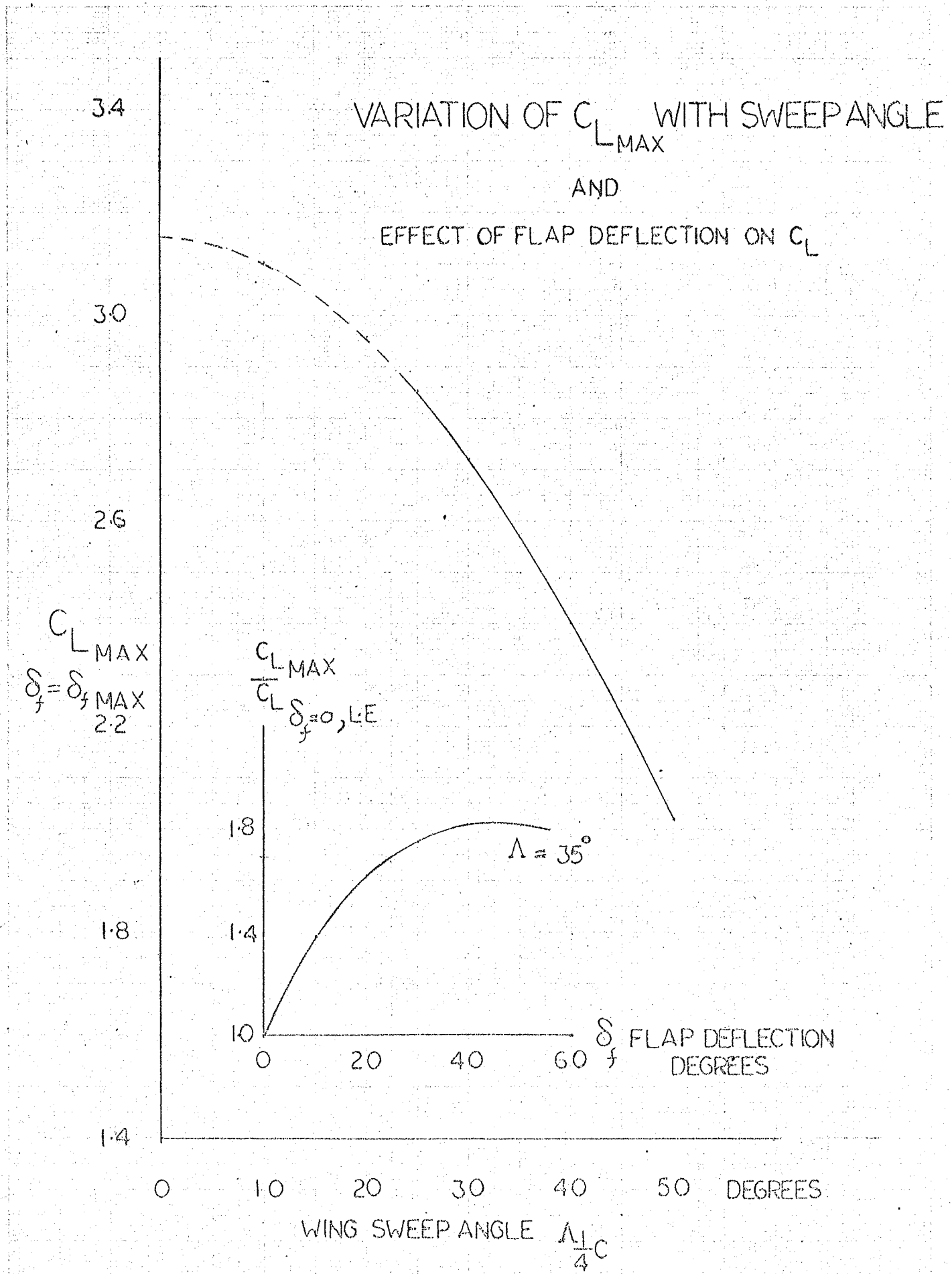
$$\left(\frac{W_f}{W_{T0}}\right) = 1.333 - 1.293 e^{-\frac{R}{661} \frac{C}{M} \left(\frac{C_D}{C_L}\right) \left(\frac{\sigma}{\delta}\right)^{.5}} \quad \text{----- (5)}$$

$\left(\frac{W_f}{W_{T0}}\right)$ can be evaluated from (5) and used in (2) to find $\left(\frac{W}{S}\right)_{T0}$

This $\left(\frac{W}{S}\right)_{T0}$ is the maximum design take off wing loading permissible.

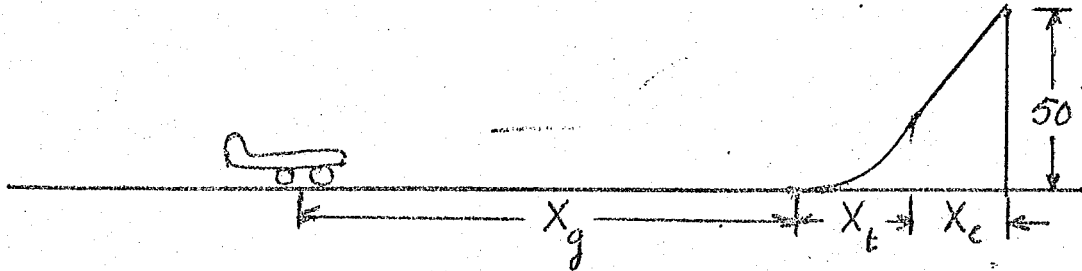
WITHOUT HIGH LEFT DEVICES





2. Take-off :

A functional relationship between the parametric variables, $(\frac{W}{S})_{T0}$ and $(\frac{T}{W})_{T0}$ can be established for take-off performance of the aircraft.



The take-off distance consists of the ground run X_g , the transition distance X_t , and the distance to clear the 50 ft. obstacle X_c .

$$X_{T0} = X_g + X_t + X_c$$

The accuracy of predictions of the take-off distance by analytical methods, depends on the validity of the assumptions made in the calculations. This, and the fact that piloting technique plays a part in the actual distance required for take-off, makes analytical predictions suspect.

For preliminary design purposes, use of Take-off charts based on a study of commercial turbojet aircraft is recommended.

For the present design the take-off field length of 6000 ft. is multiplied by a factor of 0.75 to account for failure of one engine during take-off. Corresponding to this length, from the take-off chart read value of $K = \frac{W}{S} \frac{W}{T} \frac{1}{C_{L_{T0}}} \frac{1}{\sigma}$

σ , the density ratio is taken as 0.926, to account for a hot day condition.

$C_{L_{T0}}$ is taken as $0.75 C_{L_{MAX_{T0}}}$. $C_{L_{MAX_{T0}}}$ is the maximum or stalling

value of lift coefficient, with L.E. devices and flaps taken to be set at 25° . In addition "Ground Effect" could augment the value by about 10%.

For the value of K from the take-off chart, knowing σ and $C_{L_{T0}}$, and assigning values for $(\frac{W}{S})_{T0}$, values of $(\frac{T}{W})_{T0}$ can be calculated.

These values of $(\frac{T}{W})_{T0}$ are increased by 10% to account for reduction of thrust on a hot day. A plot of the parameters $(\frac{W}{S})_{T0}$ vs $(\frac{T}{W})_{T0}$ is drawn for the take-off performance of the aircraft.

3. Weight:

A functional relationship may also be established based on the limitations imposed by considering the weight of the aircraft.

The weight of the aircraft consists of the following breakdown.

i) Structural Weight	-----	W_{ST}	lbs.
ii) Pay Load	-----	W_{PL}	"
iii) Fuel Weight, system	-----	W_{fs}	"
iv) PowerPlant Weight	-----	W_{pp}	"
v) Fixed equipment	-----	W_{FE}	"
vi) Miscellaneous.	-----	W_{Misc}	" $0.045 W_{T0}$

$$\text{Hence, } W_{T0} = W_{ST} + W_{PL} + W_f + W_{pp} + W_{FE} + W_{Misc}.$$

$$W_{ST} = W_{T0} \left[0.16 + 0.538 \left(\frac{W}{S} \right)^{-0.37} \right] K_{AR} K_{\frac{t}{c}} K_{\lambda}$$

The above is an empirical relationship for the structural weight, based on a study of current jet transports. (Ref: Corning, p.2.29). The correction factors, K_{AR} , $K_{\frac{t}{c}}$, and K_{λ} may be read off the charts provided.

$W_{PL} = 240 N_p$. This is based on the number of passengers N_p , with 160 lbs. as passenger weight, 40 lbs. as his baggage, and 40 lbs. per passenger as cargo.

$W_{fs} = 1.0175 W_f$. The fuel and system is estimated at 1.0175 times the weight of fuel W_f .

$$W_{fs} = 1.0175 \left(\frac{W_f}{W_{T0}} \right) W_{T0} \quad \text{and} \quad \frac{W_f}{W_{T0}} = 1.333 - 1.293 e^{-\frac{R}{661} \frac{C}{M} \frac{C_D}{C_L} \left(\frac{\sigma}{\delta} \right)^5}$$

If the engines operate at their rated thrust at the cruising altitude,

$$\frac{C_D}{C_L} = \frac{L}{.97} \left(\frac{T}{W} \right)_{T0}, \quad \text{where } L \text{ is the lapse ratio of the engines.}$$

$$\text{Hence, } W_{fs} = 1.0175 W_{T0} \left[1.333 - 1.293 e^{-\frac{R}{661} \frac{C}{M} \frac{L}{.97} \left(\frac{T}{W} \right)_{T0} \left(\frac{\sigma}{\delta} \right)^5} \right]$$

$$W_{pp} = 1.3385 N_e W_{\text{Eng-Dry}}$$

The power plant consists of the engines, controls and starter, tail pipe, thrust reverser and other accessories. The factor of 1.3385 is used to account for these items.

The fixed equipment includes furnishings and service items for the passengers, which is estimated at 160 lbs. per passenger, the flight crew members and stewardesses. They may be rated, on an average, at 200 lbs/ member.

$$W_{FE} = 160 N_p + 200 N_c$$

Addition of the above items, after rearrangement, gives the following expression.

$$W_{T0} \left[-0.401 - 0.16 K - 0.538 K \left(\frac{W}{S} \right)^{.37} + 1.316 e^{-\frac{R}{661} \frac{C}{M} \frac{L}{.97} \left(\frac{T}{W} \right)_{T0} \left(\frac{\sigma}{\delta} \right)^{.5}} \right] = 400 N_p + 200 N_c + W_{pp}$$

For each $\left(\frac{T}{W} \right)_{T0}$, knowing thrust of the engines T_{SSL} , calculate W_{T0} and solve for $\left(\frac{W}{S} \right)_{T0}$, substituting values for $R, C, M, L, \sigma, \delta, N_p, N_c, W_{pp}$ and K .

$$\text{Note } K = K_{AR} K_t K_\lambda$$

A plot of the parameters $\left(\frac{W}{S} \right)_{T0}$ and $\left(\frac{T}{W} \right)_{T0}$ based on the weight of the aircraft gives a limiting boundary, on the generalized design chart.

For each wing loading then, the corresponding thrust loading is the maximum attainable for the aircraft under consideration, If the engines have been selected, for a given $\left(\frac{T}{W} \right)_{T0}$, W_{T0} is known, hence the wing area and geometry are known at the corresponding $\left(\frac{W}{S} \right)_{T0}$.

It is now possible to lay out the aircraft and from the lay out one can estimate the profile drag of the configuration.

4. Cruise performance;

To establish the relationship between $(\frac{W}{S})_{T0}$ and $(\frac{T}{W})_{T0}$ during cruise, $(\frac{C_L}{C_D})$ ratio during cruise must be known. Then from the relationship

$\frac{C_D}{C_L} = \frac{L}{0.97} (\frac{T}{W})_{T0}$, $(\frac{T}{W})_{T0}$ can be calculated. The ratio $\frac{C_D}{C_L}$ is dependent on the aerodynamic characteristics of the aircraft.

At the beginning of cruise when the aircraft weighs $0.97 W_{T0}$, $0.97 (\frac{W}{S})_{T0} = 1481.8 M^2 C_L$, from which for a given $(\frac{W}{S})_{T0}$, C_L can be calculated.

$$C_{Di} = \pi \frac{C_L^2}{AR e}$$

ΔC_{D0} the compressibility drag rise can be calculated at this C_L ,

Mach No, for the particular wing $(\frac{t}{c})$ ratio.

$$C_D = C_{D0} + C_{Di} + \Delta C_{D0}$$

However C_{D0} is dependent on the wetted area of the aircraft (skin friction and form drag dependent on the Mach No and Reynolds No.)

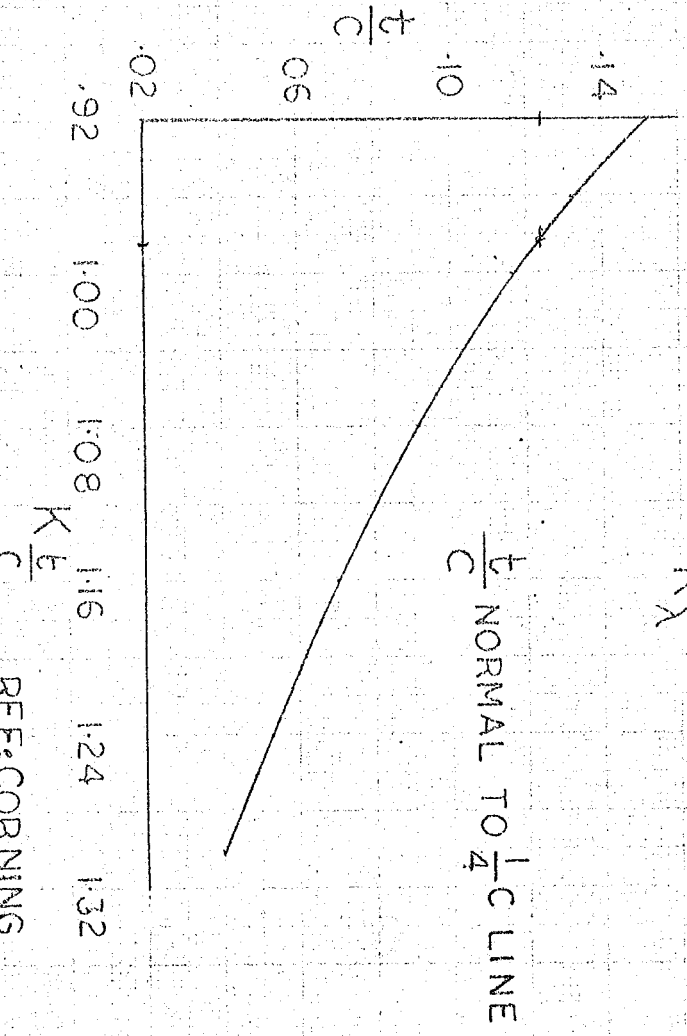
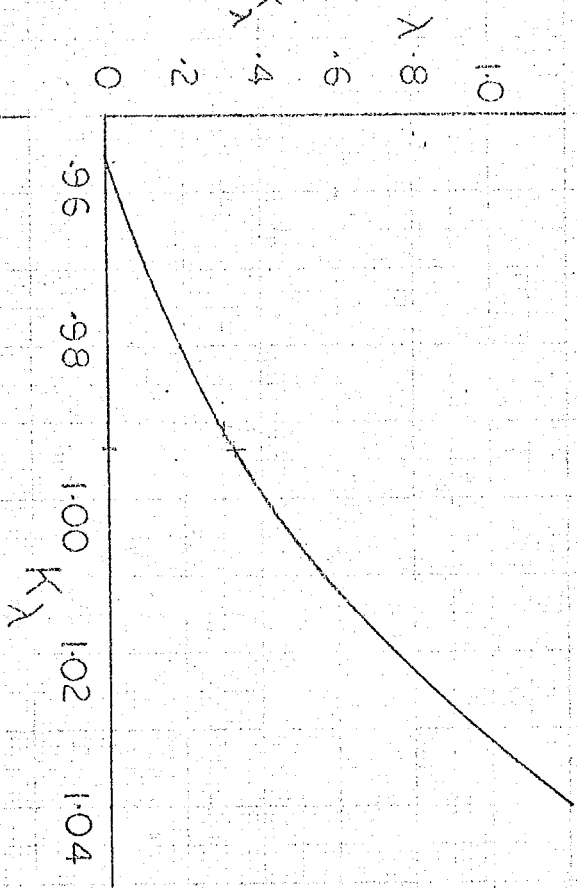
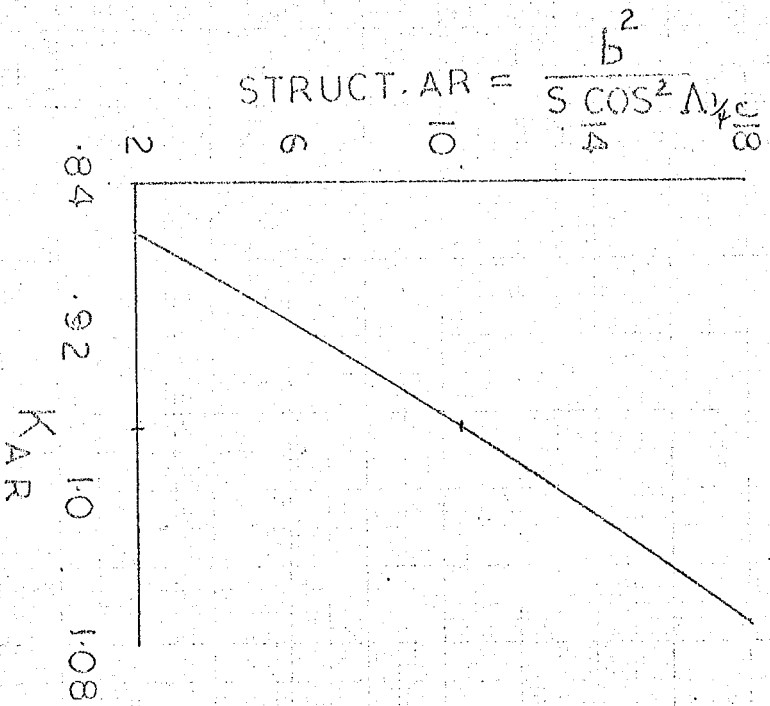
C_{D0} values of 0.013, 0.015, and 0.017 are selected and using these successively, one can calculate the relationship between $(\frac{W}{S})_{T0}$ and $(\frac{T}{W})_{T0}$. The plot of this relationship on the generalized chart indicates the $(\frac{T}{W})_{T0}$ necessary at each $(\frac{W}{S})_{T0}$ to sustain cruise at each of these C_{D0} values. As the wing loading varies, the physical characteristics of the aircraft varies giving different values of C_{D0} , and the particular wing loading with its characteristic C_{D0} value that absorbs the rated thrust is the desired wing loading.

To select this wing loading C_{D0} values have to be computed based on wetted areas from the aircraft lay out.

WEIGHT CORRECTION

FACTORS

$$W_{STR} = W_{T0} \left[0.16 + 0.538 \left(\frac{W}{S} \right)^{-0.37} \right] K_{AR} K_{\lambda} K_{\frac{t}{C}}$$



$\frac{t}{C}$ NORMAL TO $\frac{1}{4}C$ LINE

1

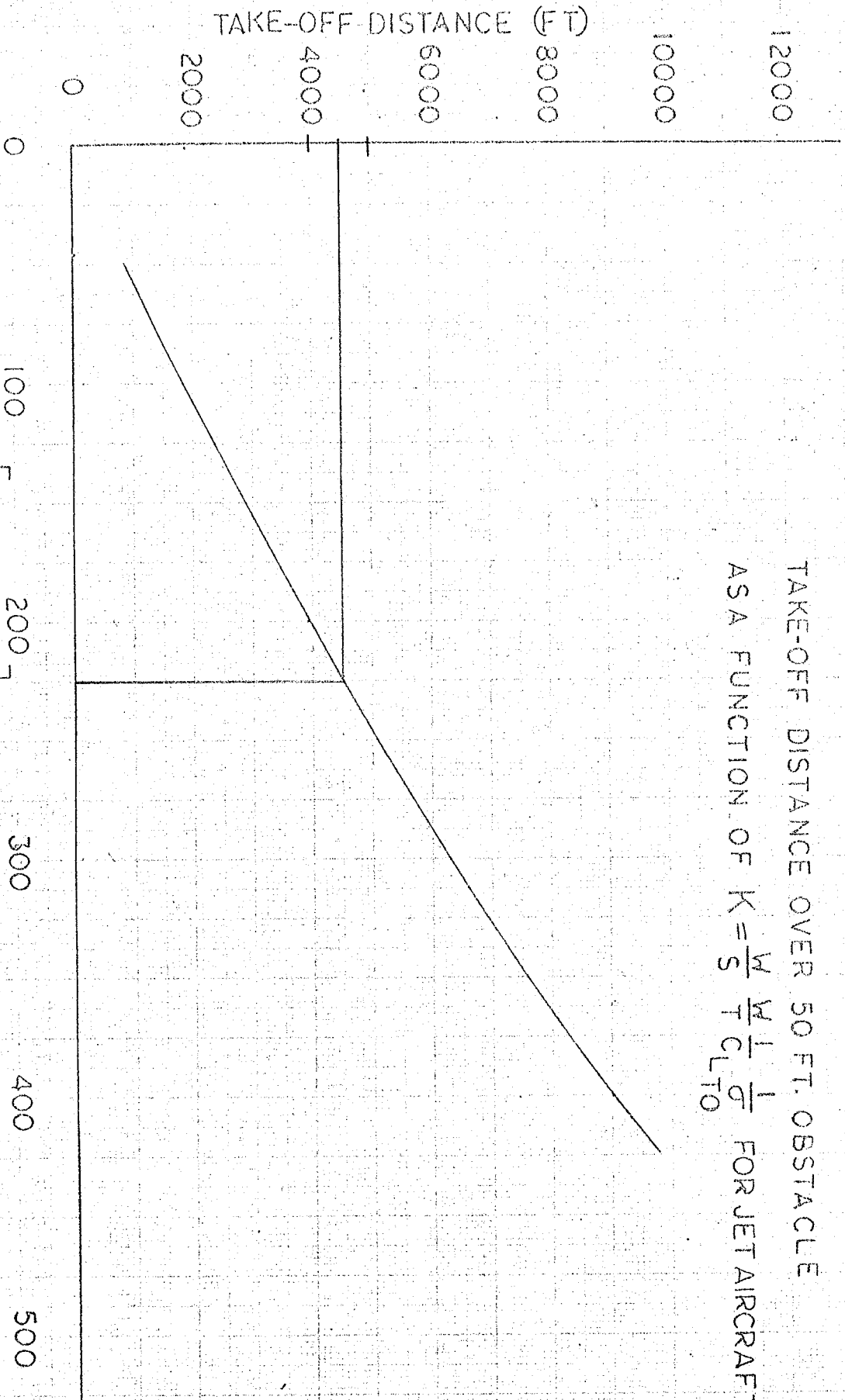
2

3

TAKE-OFF CHART

TAKE-OFF DISTANCE OVER 50 FT. OBSTACLE

ASA FUNCTION OF $K = \frac{W}{S} \frac{W}{T} \frac{1}{C} \frac{1}{C_{LTO}}$ FOR JET AIRCRAFT



$$\left[\frac{W}{S} \frac{W}{T} \frac{1}{C} \frac{1}{C_{LTO}} \right] = K$$

REF: PERKINS & HASE
FIG:4-27, P197

Estimation of the profile drag coefficient C_{D_0} :

The profile drag, or the zero lift drag of the components, wing, fuselage, empennage, etc., may be summed up to obtain the total C_{D_0} of the aircraft. Interference effects must in addition be taken into account. The profile drag consists of both skin friction and form drag. Use of turbulent boundary layer skin friction coefficients effectively accounts for both these .

The estimation of the profile drag, based on the wetted areas or the exposed areas of the aircraft, requires a layout of the aircraft in three views. The wing geometry being known, the wing planform can be drawn. The length and diameter of the fuselage are dependent on the payload (passengers and cargo). The horizontal tail area is about $\frac{1}{5}$ of the wing area. The vertical tail area is about $\frac{1}{6}$ of the wing area. These values are representative of transport category aircraft. Nacelle dimensions can be arrived at from the engine size.

Having estimated the wetted areas for the aircraft, the profile drag coefficient may be computed. The procedure indicated in the following pages is fundamental. The nomenclature and graphical data are from a report on drag evaluation by North American Aviation Inc.

Drag Estimation

The total drag of an airplane consists of mainly-

- 1) The zero lift drag
- 2) The induced drag
- 3) Wave drag or the drag increment due to compressibility of air in the transonic region

The zero lift drag or the parasite drag consists of skin friction drag and form drag. These quantities are functions of R.N. and M.NO. Form drag for wings, empennage and the fuselage is considerably small, a result obtained by streamlining. However, nacelles and forebodies with base areas given rise to considerable base drag.

In different flight attitudes, drag due to deflected control surfaces must be taken into account. Eq: "Trimmed drag" due to elevator deflection in steady cruise and in landing the drag of the landing gear.

Zero Lift Drag: Sum of zero lift drag of various components, wing, fuselage, tailplane, nacelles, etc.

$$C_{D0} = \sum K C_f \frac{S_{\pi}}{S_{W_{ref}}}$$

K = Form factor

C_f = Skin friction drag coefficient at the R.NO. and M.NO. under consideration

S_{π} = Wetted area

$S_{W_{ref}}$ = Wing reference area

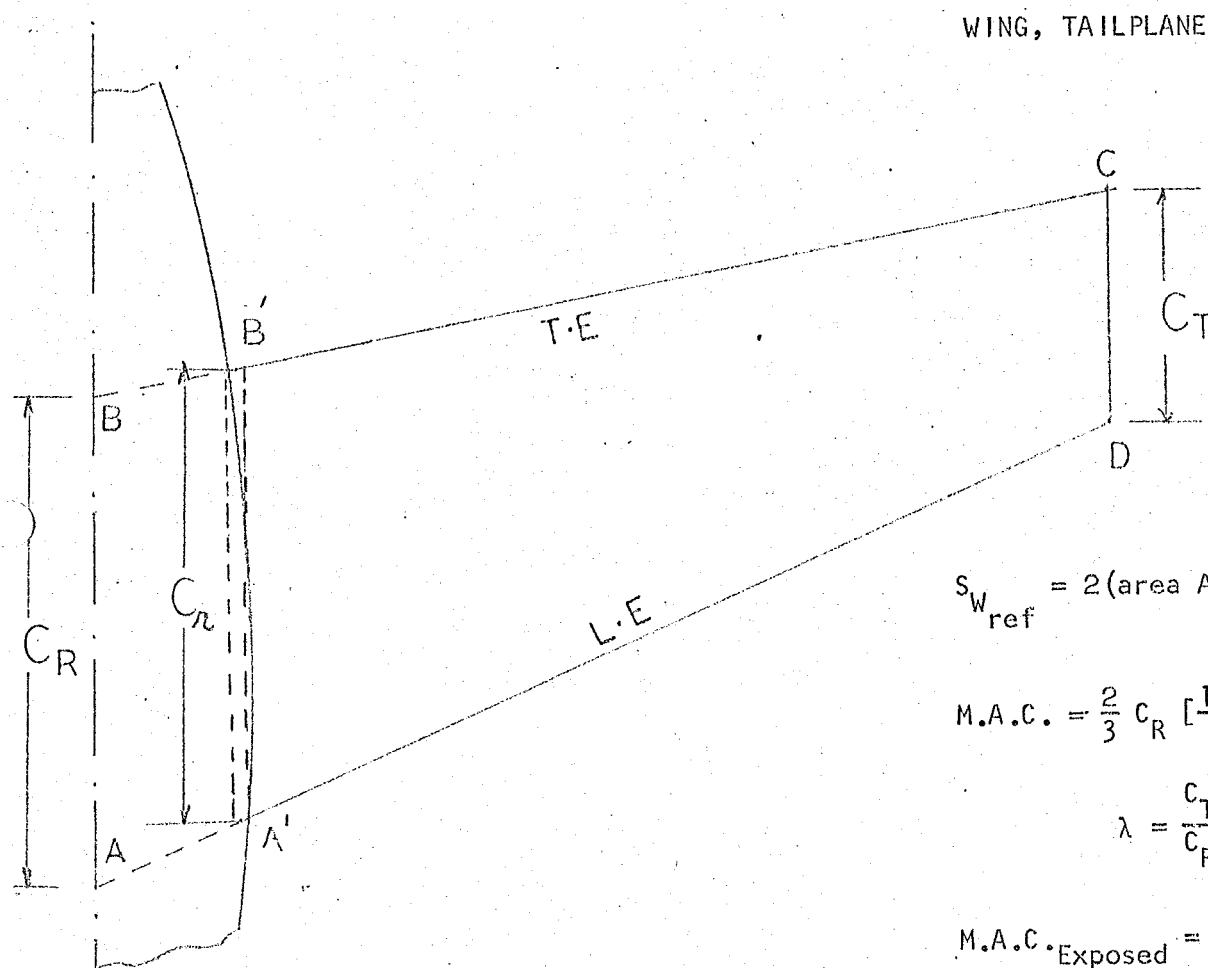
The value of C_{D0} at one significant R.N. and M.NO. is calculated (say cruise condition) = $C_{D0_{ref}}$

At any other flight condition

$$C'_{D0} = C_{D0_{ref}} \frac{C_{f_{wing}}}{C_{f_{wing_{ref}}}}$$

In the estimation of the zero lift drag, it is here proposed to consider the "three view diagram" of the aircraft from which the wetted areas of the various components may be estimated.

At the relevant R.NO. and M.NO. the skin friction drag coefficient may be read from figure. A suitable form factor is taken for each component which would account for surface irregularities and roughness of the body and interference effects. The form drag of streamlined bodies is effectively included by considering skin friction coefficients with turbulent boundary layer.



WING, TAILPLANE

$$S_{W_{ref}} = 2(\text{area } ABCD)$$

$$M.A.C. = \frac{2}{3} C_R \left[\frac{1+\lambda+\lambda^2}{1+\lambda} \right]$$

$$\lambda = \frac{C_T}{C_R}$$

$$M.A.C._{Exposed} = \frac{2}{3} C_r \left[\frac{1+\lambda'+\lambda'^2}{1+\lambda'} \right]$$

$$\lambda' = \frac{C_T}{C_r}$$

$$S_{W_{Exposed}} = 2(A'B'CD)$$

$$S_{W_{wetted}} = 2 S_{W_{Exposed}}$$

$$C_{D0_{wing}} = K_{wing} C_{f_{wing}} \frac{S_{W_{wetted}}}{S_{W_{reference}}}$$

FUSELAGE
CENTRE LINE

C_R - length AB

C_T - length CD

C_r - length A'B'

K_{wing} is given as a function of $\left(\frac{c}{c_{wing}}\right)$

$c_{f_{wing}}$ = skin function drag coeff is based on

M.NO and R.NO (based on M.A.C. exposed)

The zero lift drag of empennage is found in the same way as for the wing

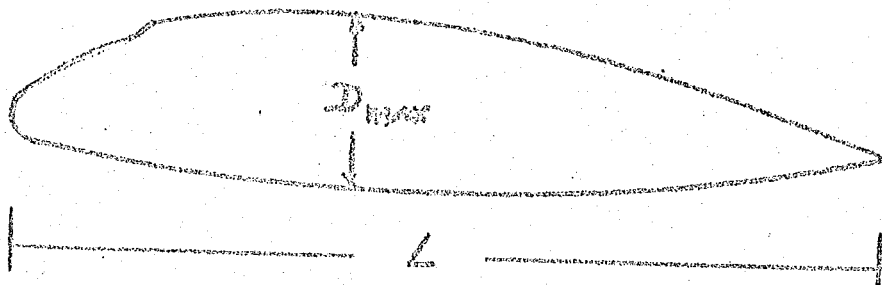
FUSELAGE

Fineness ratio F.R. = $\frac{l}{D_{max}}$

If cross-section is other than circular

$D_{max_{equiv}} = 1.128 \sqrt{A_{fus_{max}}}$

where $A_{fus_{max}}$ = max fuselage cross sectional area.



C

O

C

$$S_{F_{\text{wetted}}} = \int_0^L \pi D dl = \pi (\text{area of side view of fuselage})$$

$$\approx 0.9 \pi D_{\text{max}} L$$

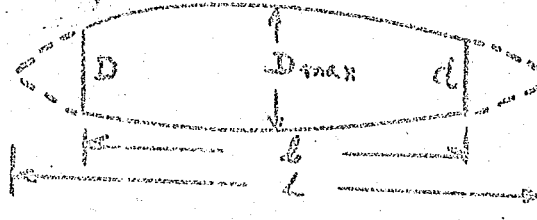
The factor 0.9 takes into account the departure of the shape of fuselage from a circular cylinder

$$C_{D_{\text{fus}}} = K_{\text{fus}} D_{\text{fus}} S_{F_{\text{wetted fuselage}}}$$

K_{fus} : form factor based on fineness ratio

$C_{f_{\text{fus}}}$: based on M.NO $R.NO \left(\frac{VL}{V}, L = \text{length of fuselage.} \right)$

Nacelles



The faired fineness ratio is calculated

If body does not fair to a point

$$F.R. = \frac{L}{D_{\text{max}}}$$

$$F.R. = \frac{L}{D} \sqrt{1 - \frac{d^2}{D^2}}$$

The wetted surface area and form factor are found from graphs and the zero lift drag coefficient may be calculated

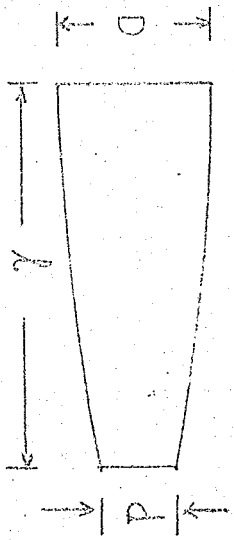
$$C_{D_{\text{nacelles}}} = K_{\text{nac}} C_{f_{\text{nac}}} \frac{S_{\text{wetted}}}{V_{\text{ref}}}$$

$$F.R. = \frac{L}{D} \left[\frac{1}{1 - \frac{d^2}{D^2}} \right]$$

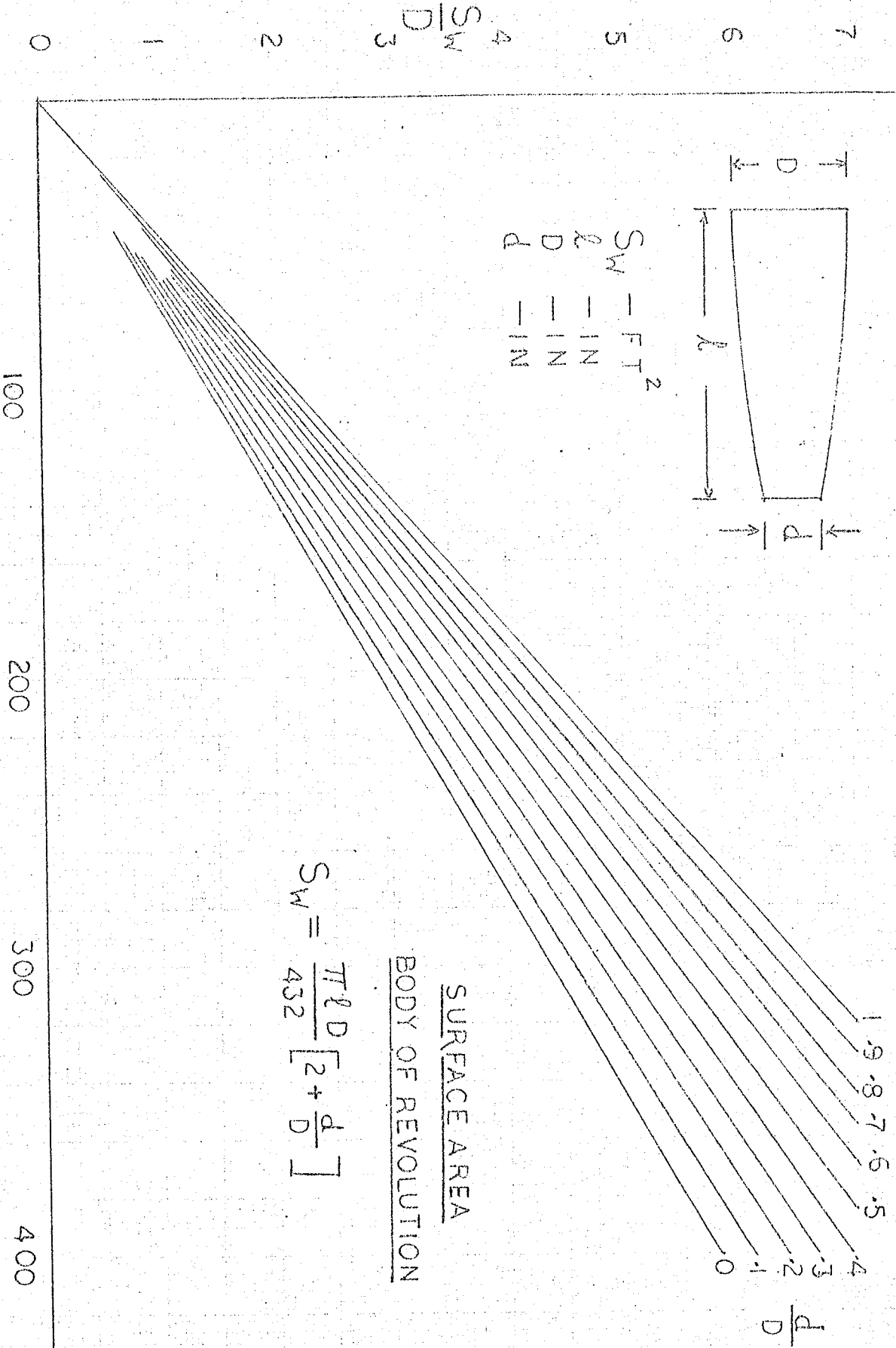
for a conical body

$C_{f_{\text{nac}}}$: based on M.NO $R.NO \left(\frac{VL}{V}, L = \text{faired length} \right)$

PARABOLIC BODY OF REVOLUTION



$S_W - FT^2$
 λ — IN
 D — IN
 d — IN



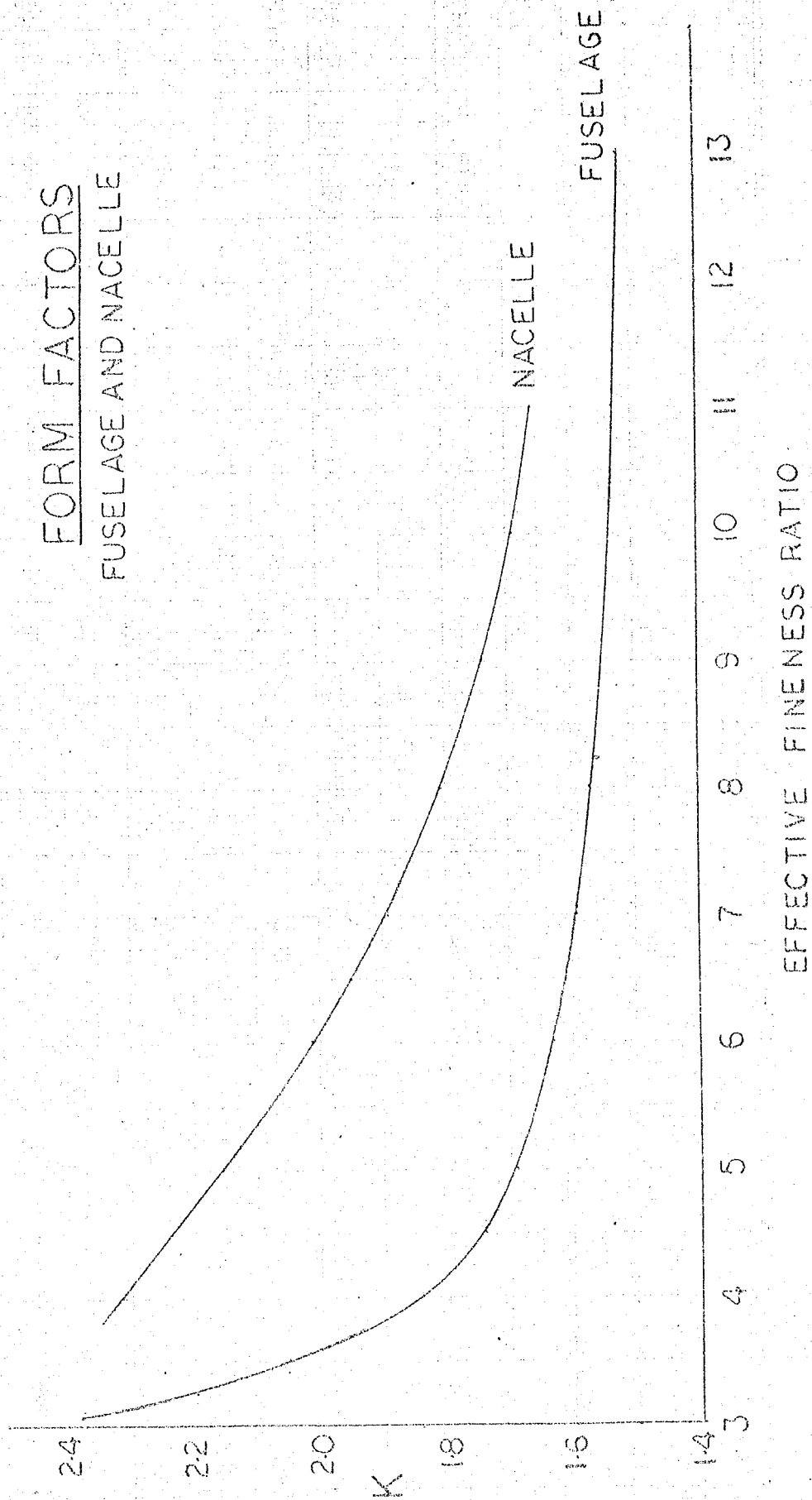
SURFACE AREA

BODY OF REVOLUTION

$$S_W = \frac{\pi \lambda D}{432} \left[2 + \frac{d}{D} \right]$$

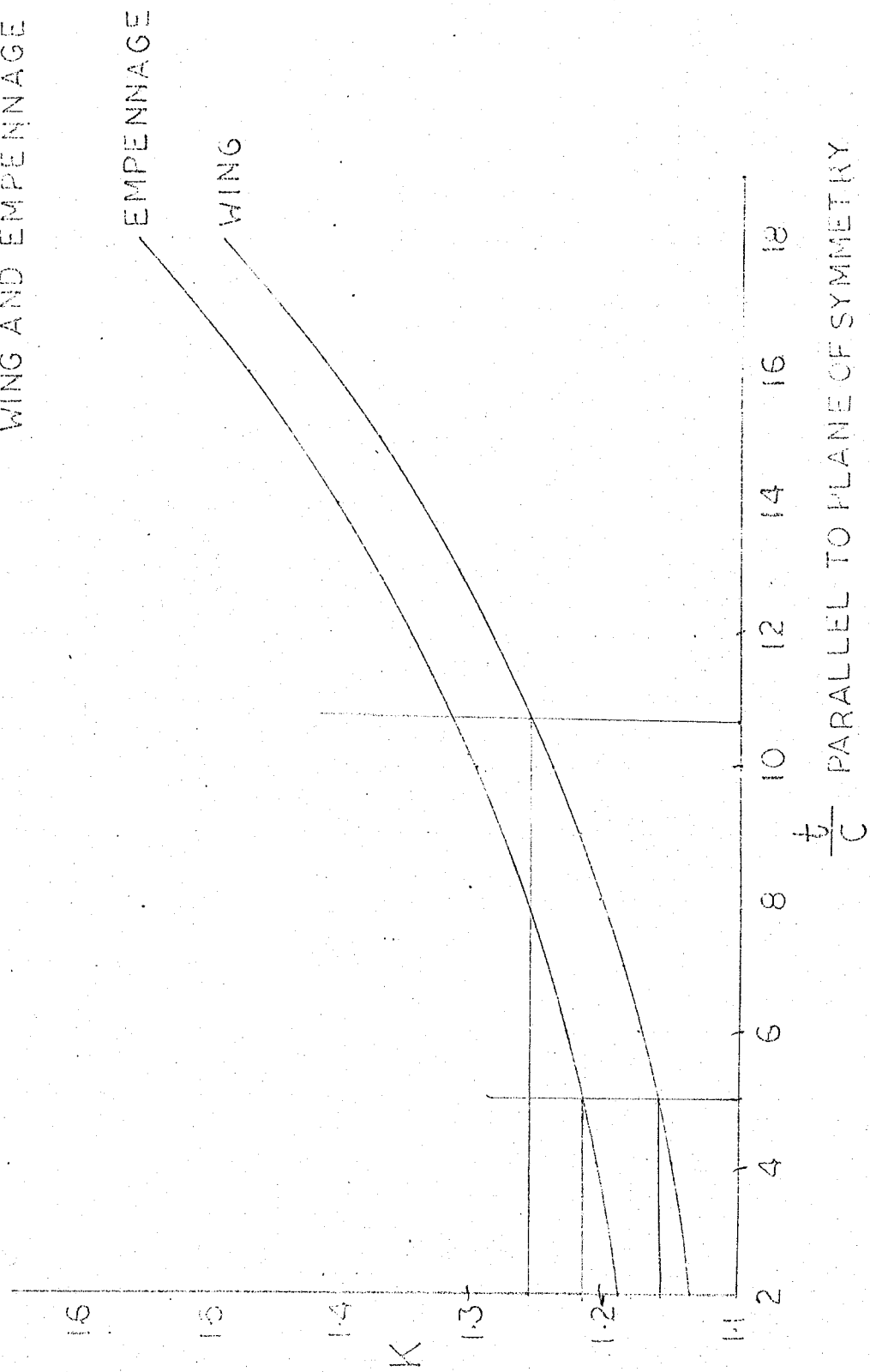
λ INCHES

FORM FACTORS
FUSELAGE AND NACELLE



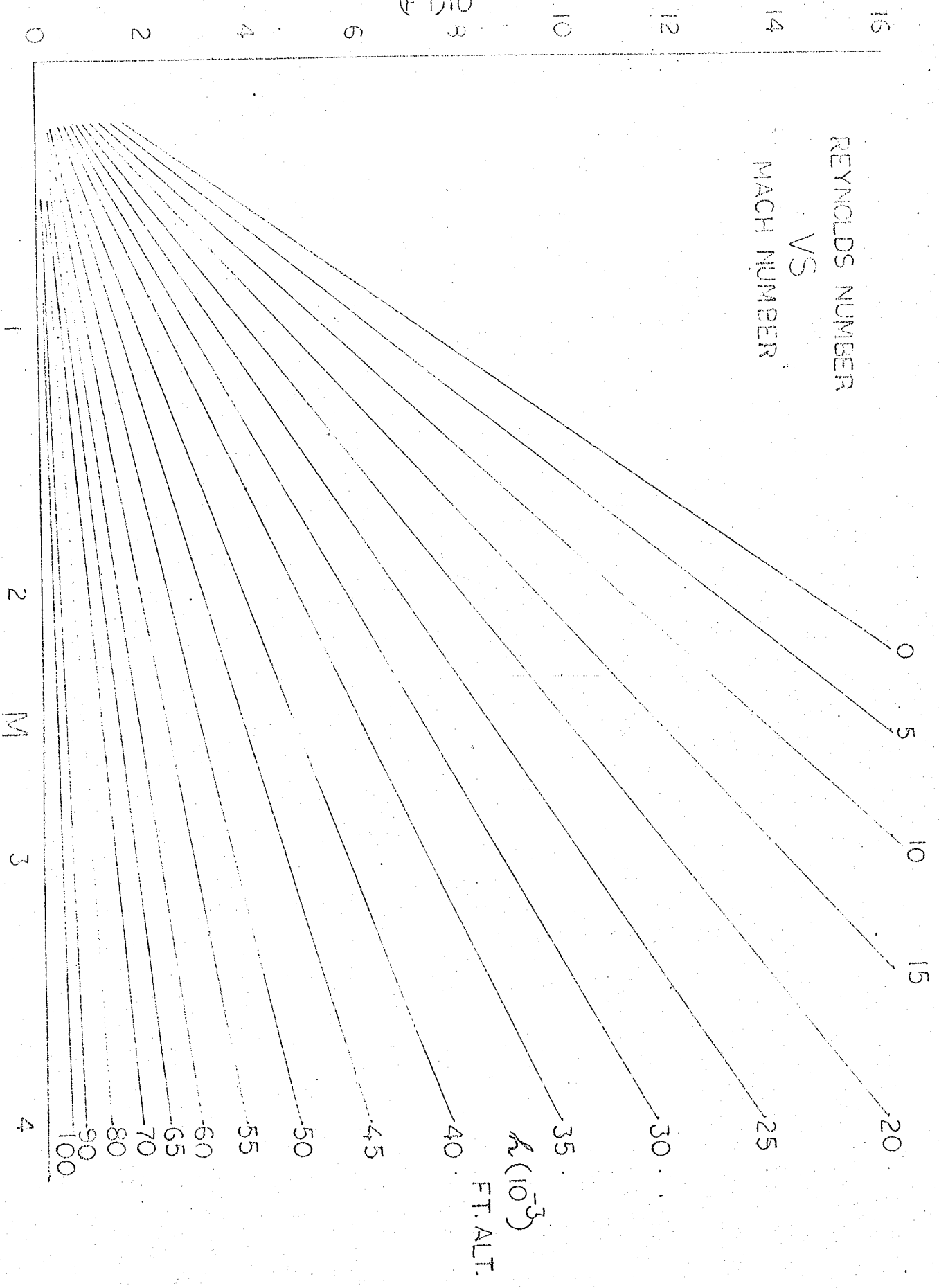
FORM FACTORS

WING AND EMPENNAGE

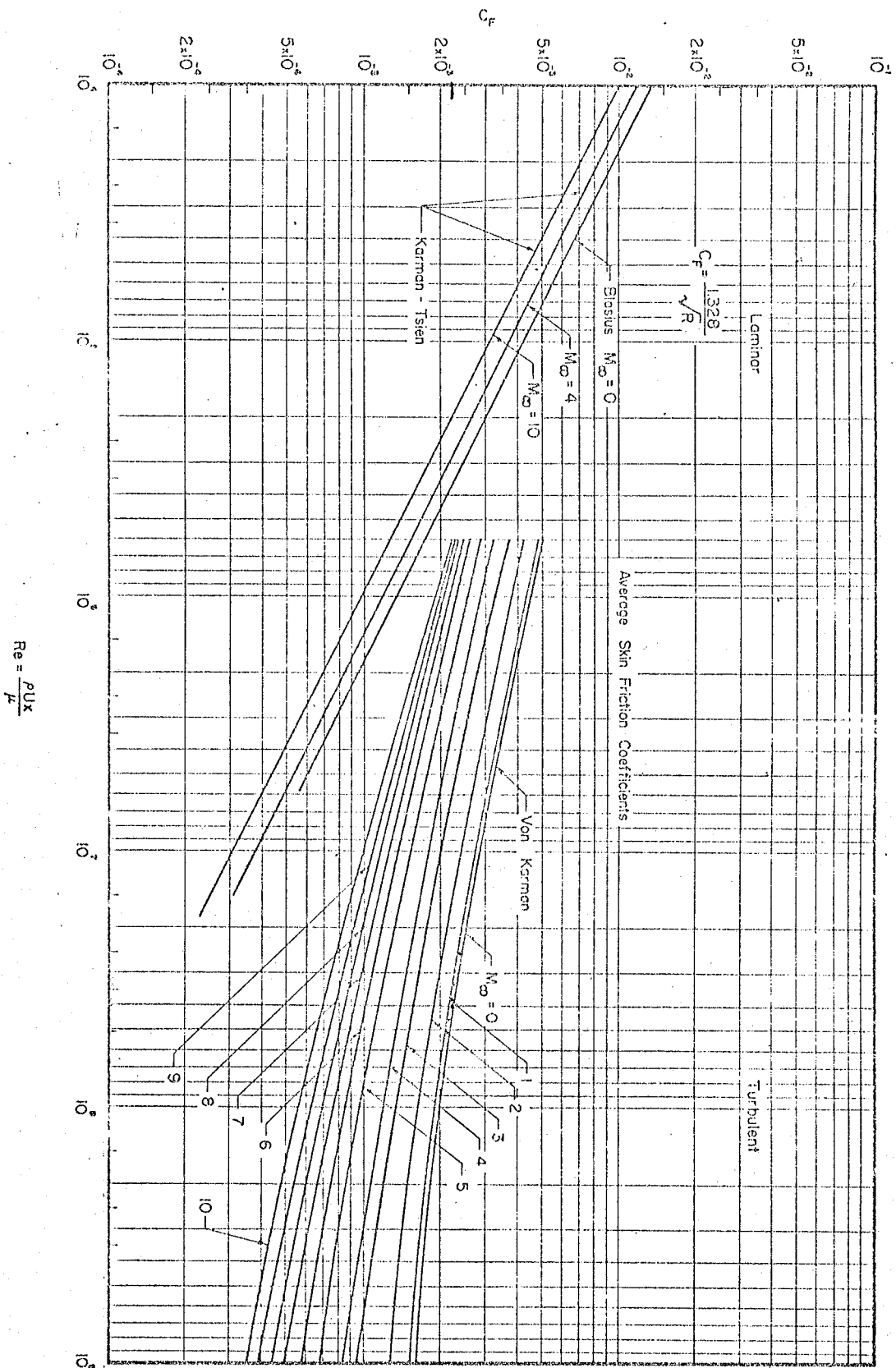


REYNOLDS NUMBER VS MACH NUMBER

$\frac{RN}{(FT)10^6}$







Flat Plate Skin Friction Coefficients for Extended Mach Numbers.

C

O

O

APPENDIX F

'Center of Gravity Determination Techniques'

C

O

C

Center of gravity calculations and Layout of the Airplane.

The center of gravity location for various loading conditions must be determined in order to ascertain the c.g. travel and to establish limits thereof.

For locating the c.g. position, the weight is considered in five categories.

- | | |
|---------------------------|----------|
| 1. Structural weight | W_S |
| 2. Fuel weight | W_F |
| 3. Power Plant weight | W_{PP} |
| 4. Fixed Equipment Weight | W_{FE} |
| 5. Pay load weight | W_{PL} |

1. Structural Weight:

The weight of the structure is evaluated by an empirical relation as:

$$W_S = W_{TO} [.16 + .538 \left(\frac{W}{S} \right)^{-.37}] K_{AR} K_{t/c} K_{\lambda}$$

The total weight of the structure is further subdivided into five component categories as:

<u>Component</u>	Weight of Component/Weight of Structure	Component c.g. location
Wing	.40	.22 MAC for $\lambda = 35^\circ$
Fuselage	.31	.45 length of Fuselage
Empenage	.08	.25 MAC of tail surfaces
Nacelles	.05	.40 length of nacelle
Landing Gear	.16	.10 MAC behind most aft airplane c.g. location

2. Fuel Weight plus associated piping and accessories:

$$W_f = 1.0175 \left(\frac{W_f}{W_{T0}} \right) W_{T0}$$

The c.g. of the fuel system weight may be taken at the c.g. of the fuel tanks.

3. Power Plant Weight:

$$W_{PP} = 1.3385 W_{ENG \text{ dry}} N_{ENG}$$

The c.g. of the power plant is located at the c.g. of the engines.

4. Fixed Equipment Weight:

$$W_{FE} = 160 N_P + 200 N_C + .045 W_{T0}$$

This equipment is used to service the passengers and the crew. It consists of items such as seats, coat racks, air vents, air conditioning, etc. The c.g. of passenger associated equipment is located at the passenger seat. The c.g. of crew equipment is located at the crew seat and attendant equipment is located at the attendant's station.

Miscellaneous items such as instruments, radio, radar, etc. not covered under other categories are estimated as $.045 W_{T0}$. These may be assumed to have a c.g. location at the instrument panel in the cockpit.

5. Payload Weight:

$$W_{PL} = 240 N_P$$

The payload weight is subdivided into three categories:

<u>Category</u>	<u>Weight</u>	<u>c.g. location</u>
Passenger	160 N_p	at passenger seat
Baggage	40 N_p	at c.g. of baggage compartments
Cargo	40 N_p	at c.g. of cargo compartments

The airplane c.g. location is determined by the relation

$$x_{cg} = \frac{\sum W_i \cdot x_i}{\sum W_i}$$

The distances x_i and x_{cg} are measured with respect to some datum line (usually the nose of the airplane). Location of the airplane c.g. for any loading condition and arrangement may be determined in tabular form.

<u>Item</u>	<u>Weight (W_i)</u>	<u>Distance from datum (x_i) inches</u>	<u>$M_i = W_i \cdot x_i$</u>
A	W_A	x_A	$W_A \cdot x_A$
B	W_B	x_B	$W_B \cdot x_B$
.	.	.	.
.	.	.	.
.	.	.	.
Wing	W_{Wing}	$(x_{cg} + a \text{ MAC})$	$W_{Wing} (x_{cg} + a \text{ MAC})^*$
Landing gear	W_{LG}	$(x_{cg} + .10 \text{ MAC})$	$W_{LG} (x_{cg} + .10 \text{ MAC})$
Nacelle	W_{NAC}	$(x_{cg} - \delta \text{ NAC})$	$W_{NAC} (x_{cg} - \delta \text{ NAC})$
Z	W_Z	x_Z	$W_Z \cdot x_Z$
<hr/>			<hr/>
	$\sum W_i$		$\sum W_i \cdot x_i + W_{Wing} (x_{cg} + a \text{ MAC})$ $+ W_{LG} (x_{cg} + .10 \text{ MAC}) + W_{NAC}$ $(x_{cg} - \delta \text{ NAC})$

*a = distance from cg location to Wing cg location in decimal fraction of MAC

From this table

$$x_{cg} = \frac{\sum W_i x_i + a \text{ MAC } \bar{W}_{wing} + .10 \text{ MAC } W_{LG} - \delta_{NAC} W_{NAC}}{\sum W_i - W_{wing} - W_{LG} - W_{NAC}}$$

This establishes the location of the airplane c.g. with respect to the datum line and may also establish the location of the wing with respect to the fuselage.

For longitudinal stability of the airplane, the most rearward position of the c.g. must not exceed .30 MAC under any condition of loading and arrangement. For longitudinal control, the allowable c.g. travel must be restricted to the limits $.20\text{MAC} < \text{c.g.} < .30\text{MAC}$.

① To fix the wing with respect to the fuselage, consider the condition in which the airplane is empty of all payload, i.e., passengers, baggage, and cargo, but is otherwise completely loaded, i.e., full fuel load and full complement of crew. Find the c.g. location for this condition as explained above. Set the wing with respect to the fuselage by locating the c.g. for this configuration at .20 MAC of the wing.

Now investigate the c.g. location for the fully loaded airplane, i.e. full fuel load, full passenger load, full baggage, and full cargo load. Determine the c.g. location for this fully loaded condition without specifying the baggage and cargo stowage location i.e., without specifying $x_{\text{baggage} + \text{cargo}}$. In this condition, the c.g. location for the baggage and cargo arrangement necessary to equilibrate the remainder of the distributed weight and result in a c.g. location for the airplane which lies within the limits $.20 \text{ MAC} < \text{c.g.} < .30 \text{ MAC}$ can be easily determined

as

$$x_{cg} = \frac{W_{T0} x_{cg} - W_{T0-\text{baggage-cargo}} x_{T0-\text{baggage-cargo}}}{W_{\text{baggage} + \text{cargo}}}$$



By distributing the baggage and cargo stowage compartments with respect to the station $x_{cg \text{ baggage + cargo}}$ the desired location of the airplane c.g. in the fully loaded configuration can be achieved.

As a check, the c.g. location for the empty plane with only the crew and 25% fuel load should be determined. This must be within the limit $.20 \text{ MAC} < \text{c.g.} < .30 \text{ MAC}$.

A layout of the airplane is made to facilitate the weight and balance calculations. If this layout is made to scale, the distance of the various items from the datum line, x_i , can be determined by measurement on the drawing.

In this layout the general arrangement of passenger seats, aisles, attendants' stations, crew stations, galleys, lavatories, coat racks and overhead racks is specified for the high density configuration. The fuselage is made to enclose this arrangement as a circular cylinder with a rounded nose section and a tapered aft section supporting the tail.

Since the tail has not been sized at this time, an estimate of its size and configuration is required. This estimate will be refined when stability and control of the airplane is evaluated.

The wing planform has already been established. Location of the wing position with respect to the fuselage is made during this weight and balance evaluation as described.

Location of the fuel tanks in the wings is approximate at this time. More specific establishment of this item will be made when the wing loading is considered. The main criterion for fuel tank location is that it should be as close to the airplane c.g. as possible



since fuel is consumed during flight and an off c.g. location would cause continuous movement of the airplane center of gravity.

Nacelles and engines are set in approximate location at this time. Wind tunnel studies of interference effects of thrust and drag are required to establish the final location of these items.

In the tricycle configurations, the main landing gear must be located behind the most aft airplane c.g. position. This location can be taken as 10% of the wing MAC behind the most aft airplane c.g. position.



APPENDIX G

'Estimation of Downwash Techniques'

ESTIMATION OF DOWNWASH AT THE TAIL.

$$AR = 7$$

$$\angle \frac{L}{4} C = 35^\circ$$

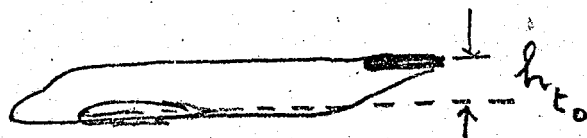
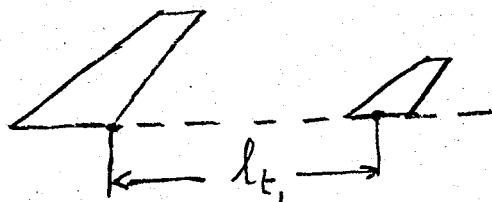
$$\lambda = \frac{1}{3}$$

l_t = DISTANCE FROM TRAILING EDGE OF
ROOT CHORD TO (A.C) OF TAIL.

h_{t0} = HEIGHT OF (A.C) OF TAIL ABOVE
WING CHORD PLANE

b_v = SPAN OF TRAILING VORTEX SHEET
AT TAIL

a = HEIGHT OF (A.C) OF TAIL ABOVE
TRAILING VORTEX SHEET PLANE AT TAIL.



$$\left(\frac{\partial \epsilon}{\partial \alpha} \right)_t = \left(\frac{\partial \bar{\epsilon}}{\partial \alpha} \right) \frac{\epsilon_t}{\bar{\epsilon}}$$

$\left(\frac{\partial \epsilon}{\partial \alpha} \right)_t$ - average over tail

$\left(\frac{\partial \bar{\epsilon}}{\partial \alpha} \right)$ - value at plane of Symmetry.

REF: DOWNWASH PREDICTION.

JAMES L. DECKER

AERO ENGG. REVIEW

1956.

DOWNWASH CHARACTERISTICS

WING AR: 7
 $\Lambda_{ic} = 35^\circ$
 $\frac{A}{\lambda} = \frac{1}{3}$

$\left(\frac{\partial \epsilon}{\partial \alpha}\right)$

$\frac{2 h_{L_0}}{b}$

$\frac{2 h_{L_0}}{b}$

1.6

1.2

0.8

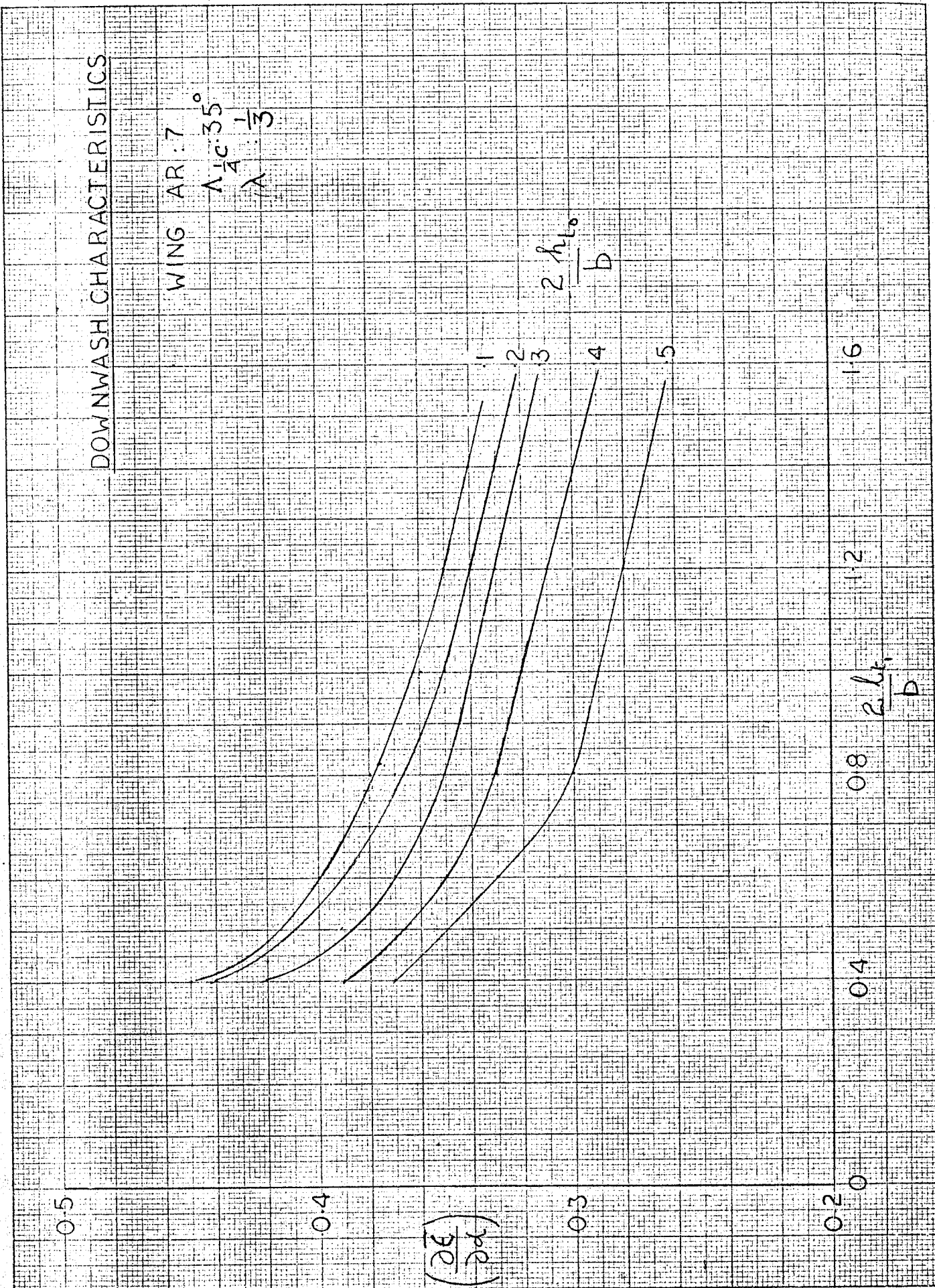
0.4

0.2

0.5

0.4

0.3



FACTORS FOR ESTIMATION

OF

AVERAGE DOWNWASH

OVER TAIL SPAN

$$\frac{b_v}{b} \frac{2a}{b_v}$$

$$\frac{2a}{b_v}$$

$$\frac{b_v}{b}$$

WING

AR: 7

$\Lambda_{tc}: 35^\circ$

$\lambda: \frac{1}{3}$

75

95-50

25

90-0

0

0.4

0.8

1.2

1.6

$$\frac{2b_v}{b}$$

$$\frac{2b_v}{b}$$

0.5

0.4

0.3

0.2

0.1



$\frac{2a}{b_v}$

0

± 0.2

± 0.6

± 1.0

$\frac{C_p}{E}$

EFFECT OF TAIL SPAN AND

TAIL HEIGHT ON DOWNWASH

ANGLE AT THE TAIL

FIG. 6

16

1.4

12

10

8

6

4

2

0

$\frac{b_t}{b_v}$

APPENDIX H

'Velocity-Load Factor Diagram Construction Techniques'

[illegible]

Velocity-Load-factor diagram [(V-n) diagram]

The various loading conditions for an airplane are usually represented on a graph of the limit load factor, n , plotted against the indicated airspeed, V_i . This diagram is often called a V-n diagram, or a V-g diagram, since the load factor, n , is related to the acceleration of gravity, g . In such diagrams, the indicated airspeed is used, since all airloads are proportional to q . The value of q is the same for the air density, ρ , and the actual airspeed at altitude, as it is for the standard sea level density, ρ_0 and the indicated airspeed i.e.

$$q = \frac{1}{2} \rho V^2 = \frac{1}{2} \rho_0 V_i^2$$

where

$$V_i = V \sqrt{\sigma}$$

The V-n diagram is, therefore, the same for all altitudes if the indicated airspeed is used.

The aerodynamic forces acting on an airplane are in equilibrium with the forces of gravity and inertia. In symmetric maneuvers, if the airplane has no angular acceleration, both the gravity and inertia forces will be distributed in the same manner as the weight of the various items of the airplane and will have resultants acting through the center of gravity of the airplane. The vertical component of the resultant gravity and inertia force is the force nW acting at the center of gravity of the airplane. The load factor n is obtained from a summation of vertical forces

$$C_{L_a} q S_w = n W$$

whence

$$n = \frac{C_{L_a \max} \rho_o S_w}{2W} \frac{V_i^2}{V_{i \text{ stall}}^2}$$

The maximum value of the lift force coefficient $C_{L_a \max}$ may be attained at various airplane speeds. For level flight at a unit load factor, ($n = 1$), the value of V_i corresponding to $C_{L_a \max}$ would be the stalling speed of the airplane. In accelerated flight, the maximum lift coefficient might be obtained at higher speeds. For $C_{L_a \max}$ obtained at twice the stalling speed, a load factor of four ($n = 4$) would be developed. this follows from the condition

$$V_{i \text{ stall}}^2 = \frac{2W}{C_{L_a \max} \rho_o S_w}$$

and

$$\begin{aligned} n &= \frac{C_{L_a \max} \rho_o S_w}{2W} \frac{V_i^2}{V_{i \text{ stall}}^2} \\ &= \left(\frac{V_i}{V_{i \text{ stall}}} \right)^2 \end{aligned}$$

for

$$V_i = 2V_{i \text{ stall}}$$

$$n = \left(\frac{2V_{i \text{ stall}}}{V_{i \text{ stall}}} \right)^2 = 4$$

Since it is possible to obtain high angle of attack and high lift coefficients momentarily in a pull up, a force coefficient of 1.25 $C_{L_a \max}$ represents the highest angle of attack for which the wing is analyzed.

The value of the load factor, n , may be plotted against the airplane velocity V_i as the line OA in Fig. 10-1. This plot represents a limiting condition for symmetric maneuvers of the airplane since it is possible to maneuver the air plane at speeds and load factors corresponding to points below or to the right of this line, but it is impossible to maneuver at speeds and load factors corresponding to points above or to the left of the line, because this would represent angles of attack greater than the stalling angle.

The line AC in the figure represents the limit maximum maneuvering load factor for which the airplane is designed. This load factor is determined from the specifications for which the airplane is designed. (It is not practical to design the airplane structure so that it could not be overstressed by violent maneuvers in this range, therefore, the pilot must restrict maneuvers so that he does not exceed this load factor.)

The line CD in the figure represents the limit permissible diving speed for the airplane. This value is set as the maximum permissible speed for safety and controlability of the airplane. For transport airplanes this is the compressibility limit for controllable flight taken as $M_c + .05$ or any demonstrable safe velocity beyond V_c .

Line OB corresponds to line OA except that the wing is at a negative stalling angle of attack and the air load is down on the wing. The relation for line OB is:

$$n = \frac{-C_{L_{a \max}} \rho_o S_w V_i^2}{2W}$$

where $C_{L_{a \max}}$ is the maximum negative lift coefficient for the airplane.

No momentary excess of $-C_{L_{a \max}}$ is anticipated in this case.

The line BE corresponds to the line AC, except that the limit load factor specified for negative maneuvers is considerably less than that

for positive maneuvers and terminates at the velocity V_c .

The line ED is drawn from the cruise velocity V_c linearly to the dive velocity point at $n = 0$ to complete the envelope.

The airplane may, therefore, be maneuvered in such a manner that velocities and load factors corresponding to points within the area O A C D E B may be attained. The most severe structural loading conditions are represented by the corners of the diagram, points A B C D E. Points A and B represent the positive high angle of attack (+HAA) and negative high angle of attack (-HAA) conditions. Point C represents the positive low angle of attack (+LAA) condition and Point E the negative low angle of attack (-LAA) condition. The high velocity zero angle of attack condition occurs at point D.

Gust Loads

a) The airplane is assumed to be subjected to symmetrical vertical gusts in level flight. The resulting limit load factors must correspond to the conditions determined as follows:

(1) Positive (up) and negative (down) rough air gusts of 66 fps at V_B must be considered at altitudes between sea level and 20,000 feet. The gust velocity may be reduced linearly from 66 fps at 20,000 feet to 38 fps at 50,000 feet.

(2) Positive and negative gusts of 50 fps at V_C must be considered at altitudes between sea level and 20,000 feet. The gust velocity may be reduced linearly from 50 fps at 20,000 feet to 25 fps at 50,000 feet.

(3) Positive and negative gusts of 25 fps at V_D must be considered at altitudes between sea level and 20,000 feet. The gust velocity may be reduced linearly from 25 fps at 20,000 feet to 12.5 fps at 50,000 feet.

(b) The following assumptions must be made:

(1) The shape of the gust is

$$U = \frac{U_{de}}{2} \left(1 - \cos \frac{2\pi s}{25\bar{c}} \right)$$

where

s = distance penetrated into gust (ft);

\bar{c} = mean geometric chord of wing (ft);

and

U_{de} = derived gust velocity referred to in paragraph (a) (fps)

(2) Gust load factors vary linearly between the specified conditions B' to G' , as shown on the gust envelope in Fig. 10-1.

(c) In the absence of a more rational analysis, the gust load factors

must be computed as follows:

$$n = 1 + \frac{K_g U_{de} V_a}{498 (W/S)}$$

where

$$K_g = \frac{0.88 \mu_g}{5.3 + \mu_g}$$

$$\mu_g = \frac{2(W/S)}{\rho \bar{c} a g} = \text{airplane mass ratio;}$$

U_{de} = derived gust velocities referred to in paragraph (a) (fps);

ρ = density of air (slugs/cu.ft.);

(W/S) = wing loading (psf);

\bar{c} = mean geometric chord (ft.);

g = acceleration due to gravity (ft/sec.²);

V_i = airplane equivalent speed (knots); and

a = slope of the airplane lift curve C_{L_a} per

radian if the gust loads are applied to the wings and horizontal tail surfaces simultaneously by a rational method. The wing lift curve slope C_{L_a} per radian may be used when the gust load is applied to the wings only and the horizontal tail gust loads are treated as a separate condition.

Note 1

V_B may not be less than the speed determined by the intersection of the line representing the maximum positive lift $C_{L_{a \max}}$ and the line representing the rough air gust velocity on the gust V-n diagram, or $(\sqrt{n_g}) V_S$, whichever is less, where -

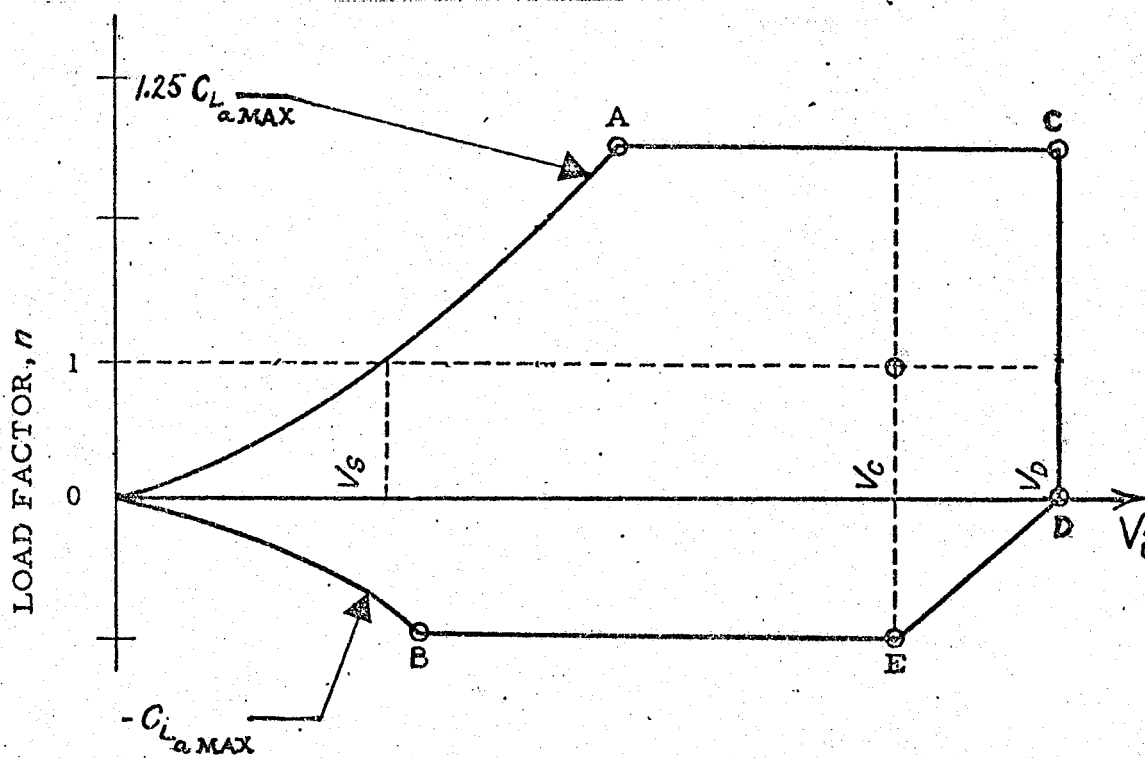


- (i) N_g is the positive airplane gust load factor due to gust, at speed V_C and at the particular weight under consideration; and
- (ii) V_s is the stalling speed with the flaps retracted at the particular weight under consideration.
- (2) V_B need not be greater than V_C .

Note 2

One factor that tends to reduce the gust load factor on swept back wings is the wing flexibility. A wing in flight tends to bend along its elastic axis. The spanwise flow parallel to the elastic axis of a swept wing has a vertical component which tends to reduce the angle of attack. This reduction in angle of attack decreases the C_L and therefore the effect of the gust loading. This reduction in gust load factor can be determined after the wing is designed, but it requires a lengthy and rigorous calculation. For preliminary design purposes a reduction in load factor of .15% is recommended for wings with 35° sweepback and aspect ratio of between 6 and 8. Hence for this wing.

$$n = .85 \left(1 + \frac{K_g U_{de} V_i a}{498(W/S)} \right)$$



Gust envelope.

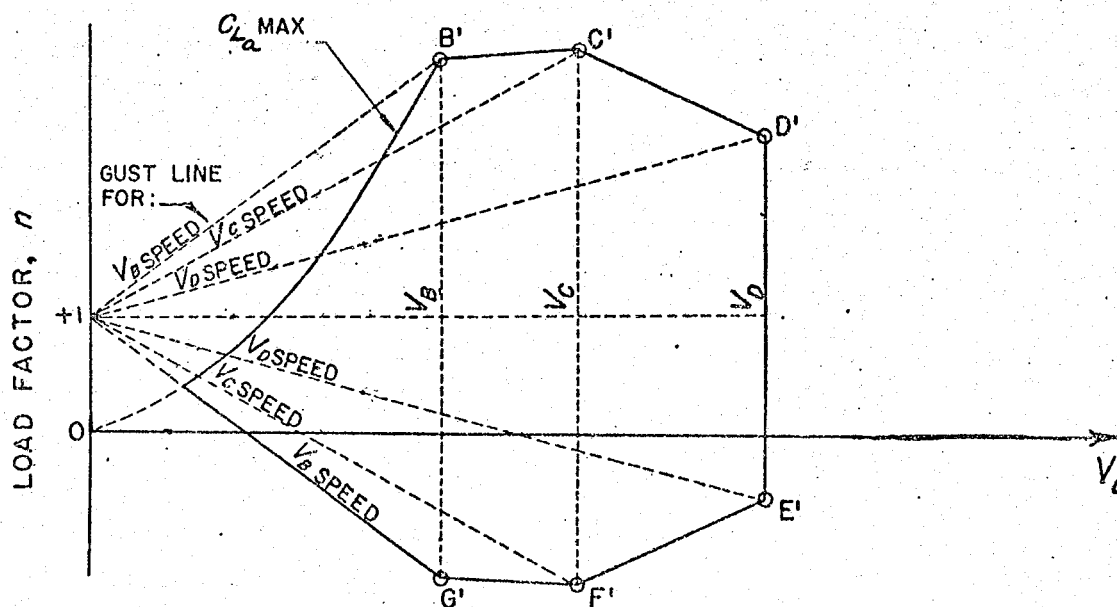


FIG. 10-1

23

○

○

1

○

APPENDIX I

'Load Calculation, Structural Design and
Analysis Techniques'

LOAD CALCULATION, STRUCTURAL DESIGN AND ANALYSIS

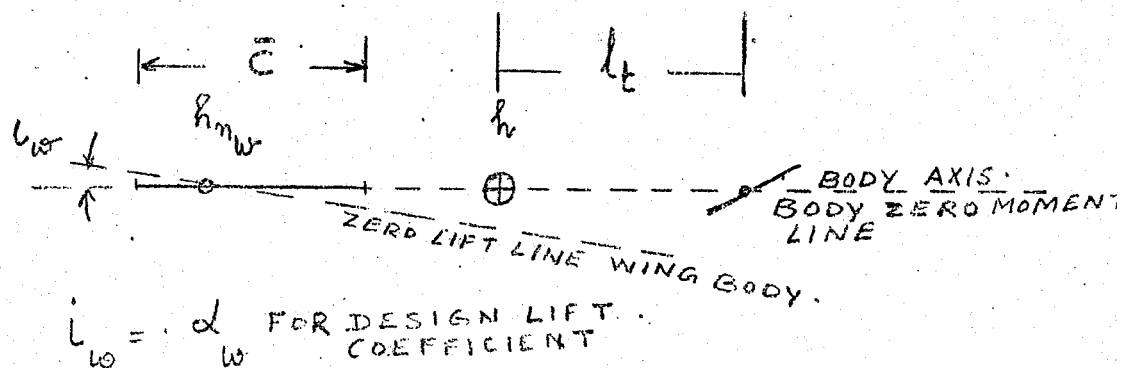
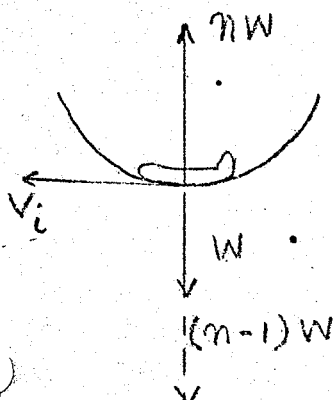
To be able to design a structure, such as the airplane wing, it is first necessary to study the various maneuvers the aircraft is likely to perform, and pick the most critical among these. A study of the V-n diagram, which has on it load factor limitations for maneuvers and gusts as required by Regulating agencies for the category of aircraft, yields boundary points, and the loads occurring at these critical boundary points would be the most severe, each producing a critical stress at different locations of the aircraft.

The F.A.A. Regulations are deemed sufficiently stringent and if met proves the airworthiness of the aircraft.

Considering such a point on the V-n diagram, one proceeds to evaluate the loads on the aircraft.

Consider a maneuver in the symmetric plane such as a pull out yielding a load factor n at a velocity V_i .

If the maneuver is a balanced maneuver such that the rate of pitch is constant, then the total lift is that occurring both on the wing and tail and the total moment about the C.G. is zero.



1. The first part of the paper is devoted to the study of the properties of the function $f(x)$ defined by the equation

$$f(x) = \int_0^x \frac{1}{1+t^2} dt$$

$$f(x) = \arctan x$$

$$f(x) = \arctan x$$

$$f(x) = \arctan x$$

$$f(x) = \arctan x$$

$$f(x) = \arctan x$$

$$f(x) = \arctan x$$

$$f(x) = \arctan x$$

$$f(x) = \arctan x$$

$$f(x) = \arctan x$$

$$f(x) = \arctan x$$

$$f(x) = \arctan x$$

$$f(x) = \arctan x$$

$$f(x) = \arctan x$$

$$M_{C.G.} = M_{wb} + M_t = 0$$

$$M_{wb} = M_{O_w} + C_{m_{\alpha_b}} \alpha_b q s \bar{c} + C_{L_w} q s \bar{c} (h - h_{n_w}) + C_T q s z$$

$$\begin{aligned} C_{m_{wb}} &= C_{m_{O_w}} + C_{m_{\alpha_b}} (\alpha_w - i_w) + a_w \alpha_w (h - h_{n_w}) + C_T \frac{z}{c} \\ &= C_{m_{O_w}} - C_{m_{\alpha_b}} i_w + \alpha_w [a_w (h - h_{n_w}) + C_{m_{\alpha_b}}] + C_T \frac{z}{c} \end{aligned}$$

$$C_{m_{\alpha_{wb}}} = a_w \left[h - (h_{n_w} - \frac{b_w}{a_w}) \right] = a_w [h - h_{n_{wb}}]$$

$$C_{m_{O_{wb}}} = C_{m_{O_w}} - C_{m_{\alpha_b}} i_w + \frac{z}{c} C_T$$

$$C_{m_{wb}} = C_{m_{O_{wb}}} + C_{L_w} [h - h_{n_{wb}}]$$

$$C_m = C_{m_{wb}} + C_{m_t} = 0$$

$$C_{m_t} = - \frac{\ell_t}{c} \frac{S_t}{S} C_{L_t}$$

$$C_{m_{O_w}} - C_{m_{\alpha_b}} i_w + C_T \frac{z}{c} + C_{L_w} (h - h_{n_{wb}}) - \frac{\ell_t S_t}{c S} C_{L_t} = 0$$

$$C_L = C_{L_w} + \frac{S_t}{S} C_{L_t}$$

$$C_L q s = n w$$

The incidence of the wing i_w is set equal to the angle of attack of wing at its design lift coefficient, and the lift coefficient required during cruise falls close to the design lift coefficient. One observes that the equations used above ignores drag moments and is valid for small angles of attack. One can however, proceed in exactly identical fashion if large

...the ... of ...
...the ... of ...
...the ... of ...

...the ... of ...
...the ... of ...
...the ... of ...
...the ... of ...
...the ... of ...
...the ... of ...

...the ... of ...
...the ... of ...
...the ... of ...
...the ... of ...
...the ... of ...
...the ... of ...
...the ... of ...
...the ... of ...
...the ... of ...
...the ... of ...

...the ... of ...
...the ... of ...
...the ... of ...
...the ... of ...
...the ... of ...
...the ... of ...

angles are involved and set down equations for total moment equalling to zero. The effect of damping on the wing during pitching would also be important. For a preliminary investigation, the above analysis is deemed sufficient.

From preceding analysis one isolates the lift acting on wing and tail, C_{L_w} and C_{L_t} . The spanwise lift distribution on the wing can then be estimated. (NACA: TR921 de Young & Harper). For a wing without twist the additional lift distribution along span is found (C_{l_a}). The loading due to lift is then $C_{l_a} C_q$ in lbs./ft. of span.

From the loading diagram the shear and bending moment distributions along span can be found.

In the same plane as the lift loading, are the inertial loading due to distributed weights and concentrated weights. These include wing structural weights, fuel weight and weight of engines.

Normal to this plane, in the direction of the relative wind is the drag plane. In the drag plane, along the span the profile drag, induced drag and compressibility drag are distributed. We have in addition concentrated thrust forces and inertial load distributions if load factors along this direction are involved.

The profile drag distribution may be estimated as $2 C_f K C q$ /ft. of span.

C_f - skin friction drag coefficient based on Reynolds Number

Corresponding to M.A.C. wing exposed

K - form factor

C - local chord

q - dynamic pressure.

The local induced drag coefficient can be estimated as $C_{l_a} \epsilon$, where ϵ is the downwash at the trailing edge in radians

That is, $C_{d_i} = C_{l_a} \epsilon$

and $\epsilon = \frac{C_{L_w}}{a_w} - \frac{C_{l_a}}{\frac{2\pi}{\beta} \cos \Lambda_\beta}$, the difference

in angles between angle of attack locally and the angle of attack of an infinite span yawed wing producing C_{l_a} at the Mach number in question

$$\Lambda_\beta = \tan^{-1} \left(\frac{\tan \Lambda}{\beta} \right)$$

The drag load distribution due to induced drag = $C_{d_i} C q/\text{ft. span}$.

Compressibility drag, if flight is at a Mach number beyond the drag divergent, depends on the local value of C_{l_a} .

Load distribution in the lift plane and drag plane being known along with concentrated forces in these planes, shear and bending movement distributions can be found. Integration of loading diagram would yield the shear distribution. Further integration would result in bending moment distribution along span.

Note must be taken of the fact that if V_i is to be constant (no load factor in drag plane) the drag must be matched by the thrust. If thrust is inadequate this would result in an inertial loading in the drag plane opposite to the direction of acceleration.

1990-1991

1990-1991

1990-1991

1990-1991

1990-1991

1990-1991

1990-1991

1990-1991

1990-1991

1990-1991

1990-1991

1990-1991

THEORITICAL SYMMETRIC SPAN LOADING AT SUBSONIC SPEEDS FOR WINGSHAVING ARBITRARY PLAN FORM

The span loading coefficient $\frac{C_{l_a} C}{C_L C_{av}}$ at any spanwise station $\eta = \frac{y}{b/2}$ may be read from the following charts.

- b - span
- y - semi span station
- C - chord at station y
- C_{av} - Average chord
- C_L - Wing lift coefft.
- C_{l_a} - lift coefft. at station y of the wing

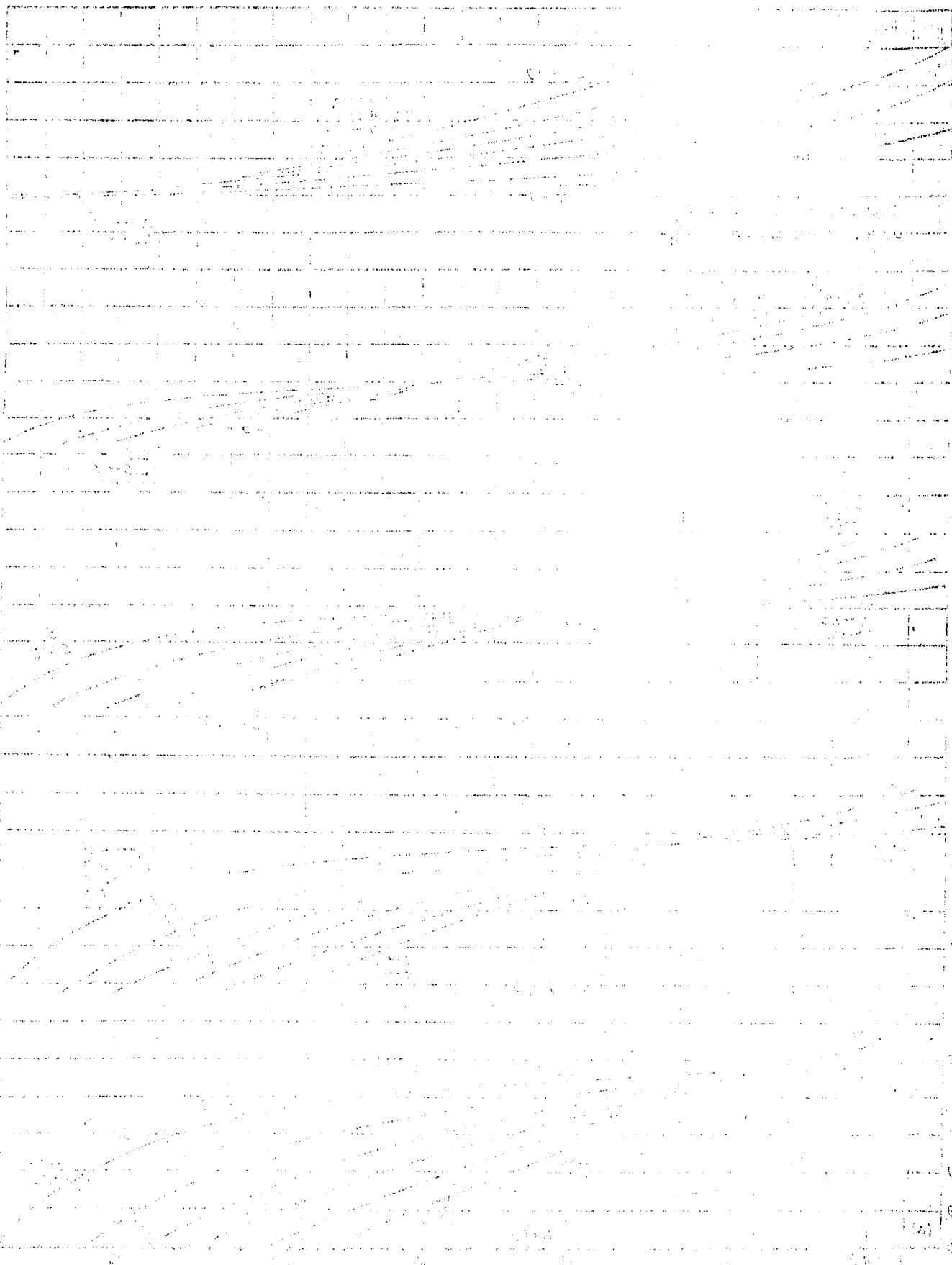
Charts are provided for values of $\eta = 0, 0.383, 0.707, \text{ and } 0.924$

For each value of η , for the taper ratio of the wing, read $\frac{C_{l_a} C}{C_L C_{av}}$ against values of Λ_β and $\beta A/k$

$$\Lambda_\beta = \tan^{-1} \left(\frac{\tan \Lambda}{\beta} \right), \text{ where } \Lambda = 35^\circ \text{ and } \beta = \sqrt{1-M^2}$$

A - Aspect ratio

$$k = \frac{C_{L_\alpha} (\text{wing section, per radian})}{\frac{2\pi}{\beta} \cos \Lambda_\beta}$$



Q

Q

Q

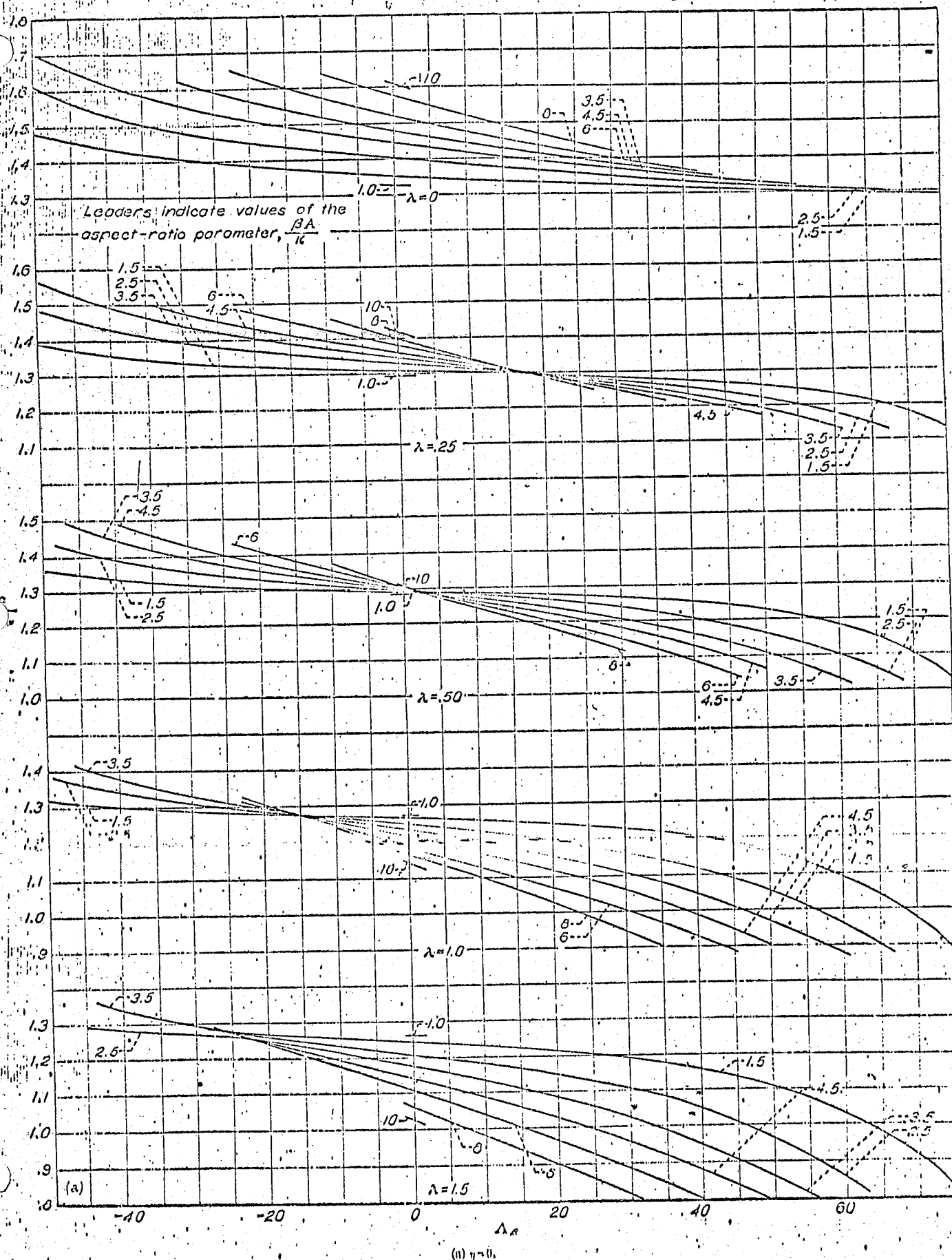


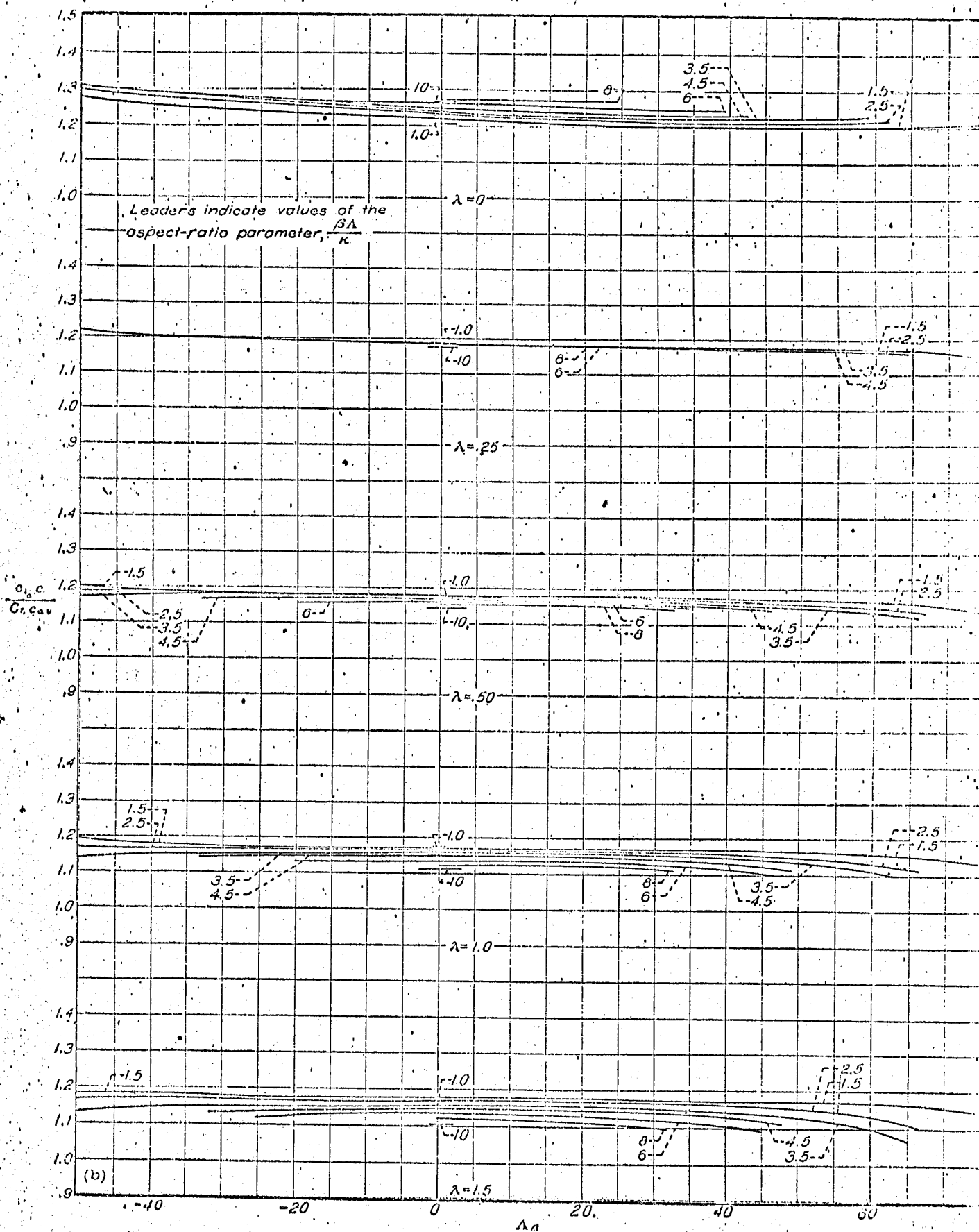
FIGURE 3. Variation of the spanwise loading coefficient $C_{l\alpha}$ with the compressibility sweep parameter Λ_α , degrees, for various values of the aspect-ratio parameter $\frac{\beta A}{\pi}$ and taper ratio λ .

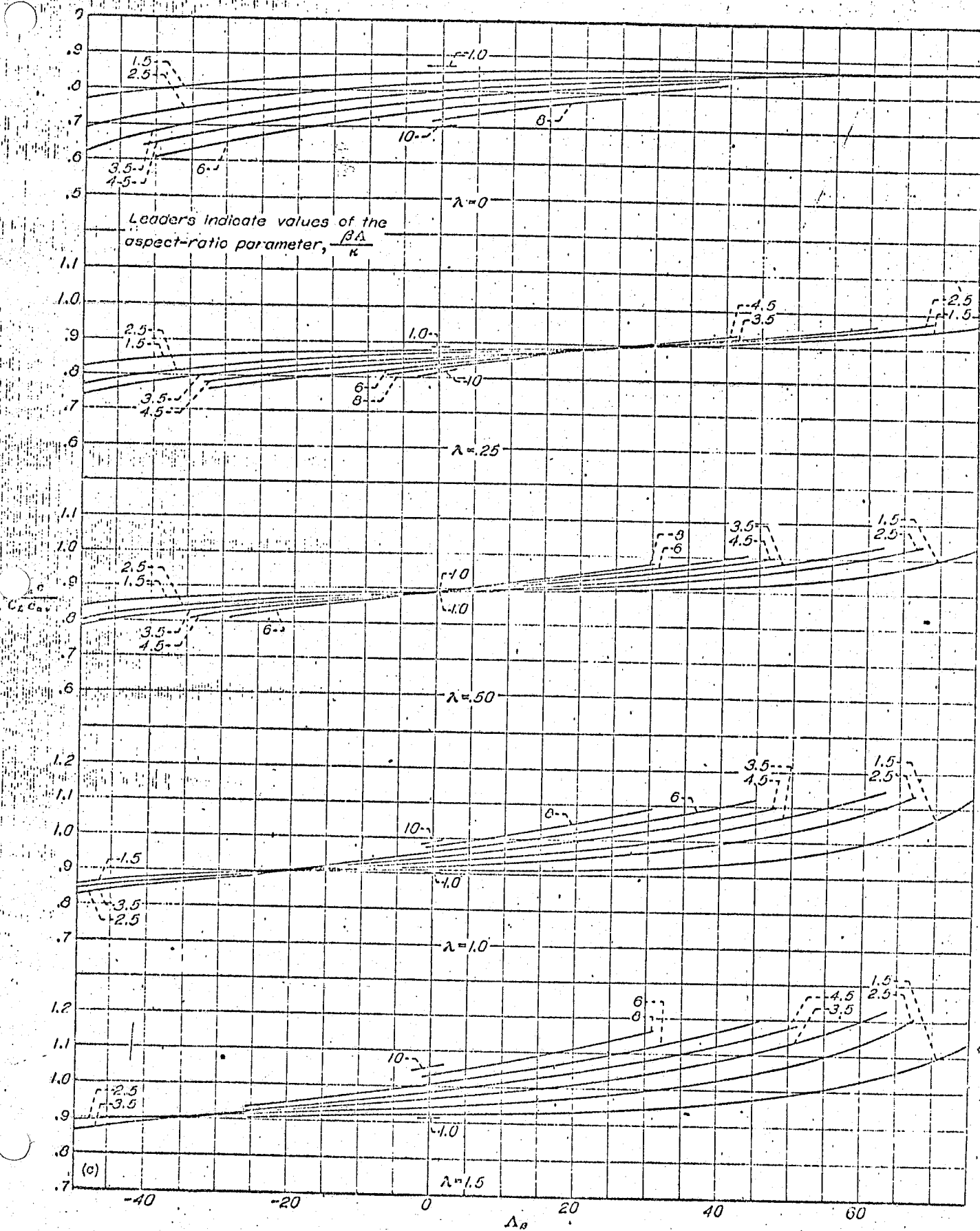
[illegible][illegible]

1. 2. 3. 4. 5. 6. 7. 8. 9. 10. 11. 12. 13. 14. 15. 16. 17. 18. 19. 20. 21. 22. 23. 24. 25. 26. 27. 28. 29. 30. 31. 32. 33. 34. 35. 36. 37. 38. 39. 40. 41. 42. 43. 44. 45. 46. 47. 48. 49. 50. 51. 52. 53. 54. 55. 56. 57. 58. 59. 60. 61. 62. 63. 64. 65. 66. 67. 68. 69. 70. 71. 72. 73. 74. 75. 76. 77. 78. 79. 80. 81. 82. 83. 84. 85. 86. 87. 88. 89. 90. 91. 92. 93. 94. 95. 96. 97. 98. 99. 100. 101. 102. 103. 104. 105. 106. 107. 108. 109. 110. 111. 112. 113. 114. 115. 116. 117. 118. 119. 120. 121. 122. 123. 124. 125. 126. 127. 128. 129. 130. 131. 132. 133. 134. 135. 136. 137. 138. 139. 140. 141. 142. 143. 144. 145. 146. 147. 148. 149. 150. 151. 152. 153. 154. 155. 156. 157. 158. 159. 160. 161. 162. 163. 164. 165. 166. 167. 168. 169. 170. 171. 172. 173. 174. 175. 176. 177. 178. 179. 180. 181. 182. 183. 184. 185. 186. 187. 188. 189. 190. 191. 192. 193. 194. 195. 196. 197. 198. 199. 200. 201. 202. 203. 204. 205. 206. 207. 208. 209. 210. 211. 212. 213. 214. 215. 216. 217. 218. 219. 220. 221. 222. 223. 224. 225. 226. 227. 228. 229. 230. 231. 232. 233. 234. 235. 236. 237. 238. 239. 240. 241. 242. 243. 244. 245. 246. 247. 248. 249. 250. 251. 252. 253. 254. 255. 256. 257. 258. 259. 260. 261. 262. 263. 264. 265. 266. 267. 268. 269. 270. 271. 272. 273. 274. 275. 276. 277. 278. 279. 280. 281. 282. 283. 284. 285. 286. 287. 288. 289. 290. 291. 292. 293. 294. 295. 296. 297. 298. 299. 300. 301. 302. 303. 304. 305. 306. 307. 308. 309. 310. 311. 312. 313. 314. 315. 316. 317. 318. 319. 320. 321. 322. 323. 324. 325. 326. 327. 328. 329. 330. 331. 332. 333. 334. 335. 336. 337. 338. 339. 340. 341. 342. 343. 344. 345. 346. 347. 348. 349. 350. 351. 352. 353. 354. 355. 356. 357. 358. 359. 360. 361. 362. 363. 364. 365. 366. 367. 368. 369. 370. 371. 372. 373. 374. 375. 376. 377. 378. 379. 380. 381. 382. 383. 384. 385. 386. 387. 388. 389. 390. 391. 392. 393. 394. 395. 396. 397. 398. 399. 400. 401. 402. 403. 404. 405. 406. 407. 408. 409. 410. 411. 412. 413. 414. 415. 416. 417. 418. 419. 420. 421. 422. 423. 424. 425. 426. 427. 428. 429. 430. 431. 432. 433. 434. 435. 436. 437. 438. 439. 440. 441. 442. 443. 444. 445. 446. 447. 448. 449. 450. 451. 452. 453. 454. 455. 456. 457. 458. 459. 460. 461. 462. 463. 464. 465. 466. 467. 468. 469. 470. 471. 472. 473. 474. 475. 476. 477. 478. 479. 480. 481. 482. 483. 484. 485. 486. 487. 488. 489. 490. 491. 492. 493. 494. 495. 496. 497. 498. 499. 500. 501. 502. 503. 504. 505. 506. 507. 508. 509. 510. 511. 512. 513. 514. 515. 516. 517. 518. 519. 520. 521. 522. 523. 524. 525. 526. 527. 528. 529. 530. 531. 532. 533. 534. 535. 536. 537. 538. 539. 540. 541. 542. 543. 544. 545. 546. 547. 548. 549. 550. 551. 552. 553. 554. 555. 556. 557. 558. 559. 560. 561. 562. 563. 564. 565. 566. 567. 568. 569. 570. 571. 572. 573. 574. 575. 576. 577. 578. 579. 580. 581. 582. 583. 584. 585. 586. 587. 588. 589. 590. 591. 592. 593. 594. 595. 596. 597. 598. 599. 600. 601. 602. 603. 604. 605. 606. 607. 608. 609. 610. 611. 612. 613. 614. 615. 616. 617. 618. 619. 620. 621. 622. 623. 624. 625. 626. 627. 628. 629. 630. 631. 632. 633. 634. 635. 636. 637. 638. 639. 640. 641. 642. 643. 644. 645. 646. 647. 648. 649. 650. 651. 652. 653. 654. 655. 656. 657. 658. 659. 660. 661. 662. 663. 664. 665. 666. 667. 668. 669. 670. 671. 672. 673. 674. 675. 676. 677. 678. 679. 680. 681. 682. 683. 684. 685. 686. 687. 688. 689. 690. 691. 692. 693. 694. 695. 696. 697. 698. 699. 700. 701. 702. 703. 704. 705. 706. 707. 708. 709. 710. 711. 712. 713. 714. 715. 716. 717. 718. 719. 720. 721. 722. 723. 724. 725. 726. 727. 728. 729. 730. 731. 732. 733. 734. 735. 736. 737. 738. 739. 740. 741. 742. 743. 744. 745. 746. 747. 748. 749. 750. 751. 752. 753. 754. 755. 756. 757. 758. 759. 760. 761. 762. 763. 764. 765. 766. 767. 768. 769. 770. 771. 772. 773. 774. 775. 776. 777. 778. 779. 780. 781. 782. 783. 784. 785. 786. 787. 788. 789. 790. 791. 792. 793. 794. 795. 796. 797. 798. 799. 800. 801. 802. 803. 804. 805. 806. 807. 808. 809. 810. 811. 812. 813. 814. 815. 816. 817. 818. 819. 820. 821. 822. 823. 824. 825. 826. 827. 828. 829. 830. 831. 832. 833. 834. 835. 836. 837. 838. 839. 840.

[illegible]

THEORETICAL SYMMETRIC SPAN LOADING AT SUBSONIC SPEEDS FOR WINGS HAVING ARBITRARY PLAN FORM





(c) $\eta = 0.707$.

FIGURE 3.—Continued.



THEORETICAL SYMMETRIC SPAN LOADING AT SUBSONIC SPEEDS FOR WINGS HAVING ARBITRARY PLAN FORM

